The Dissertation Committee for Matthew Brian Pomrenze Certifies that this is the approved version of the following Dissertation:

GENETIC DISSECTION OF AN AMYGDALA CRF CIRCUIT FOR FEAR AND ANXIETY

Committee:

Robert O. Messing, Supervisor

Michela Marinelli, Co-Supervisor

Michael R. Drew

R. Adron Harris

Boris V. Zemelman

Hiroshi Nishiyama

GENETIC DISSECTION OF AN AMYGDALA CRF CIRCUIT FOR FEAR AND ANXIETY

by

Matthew Brian Pomrenze

Dissertation

Presented to the Faculty of the Graduate School of

The University of Texas at Austin

in Partial Fulfillment

of the Requirements

for the Degree of

Doctor of Philosophy

The University of Texas at Austin

December 2018

Dedication

I dedicate this dissertation to the people in this world who mean the most to me. Those folks include my family, Allison, Bonnie, and Nat, and some of my closest friends and colleagues, Simone Giovanetti, Rajani Maiya, Natasha and Garrett Cornelison, Annie Park, Sam Dolzani, Michael Baratta, Micky Marinelli, and Bob Messing. And of course, I cannot forget two people who have provided unlimited and essential auditory inspiration from afar, Jerome John Garcia and William Smith Monroe.

Acknowledgements

If my words did glow, with the gold of sunshine… and my tunes were played on the harp unstrung… would you hear my voice…

No PhD dissertation could be complete without acknowledging the humans that played essential roles in its completion. First and foremost, I thank my family for lending unconditional support and enthusiasm for my scientific and intellectual endeavors. Allison, Bonnie, and Nat, I thank you for your interest and faith in my studies and giving me, directly and indirectly, the drive to understand the brain in both healthy and disease states.

My time in Austin Texas has been an unforgettable one, and that experience came with friendships that will last beyond a lifetime. Most prominently, I must mention Simone Mio Giovanetti, who has become one of my most indispensable friends on this Earth. Over the past couple years, Simone has become my closest confidant, comrade, companion, and partner. Her unconditional support and general interest in me and my studies has been and continues to be an omnipotent motivator and driving force for me to achieve. Words written here to do not come close to what she means to me. But it remains clear, at least to me, that this dissertation could not have been completed without her.

I must also acknowledge Rajani Maiya, who was a great friend and mentor to me through this entire process. My other close and essential friends in this voyage have been Annie Park, Natasha and Garrett Cornelison, Nitish Mittal, Joel Shillinglaw, Adam Gordon, Nathan Nocera, and Taylor Evans, graduate students (some not) undergoing the eternal struggle with me. I look forward to sharing a lifetime of experience with all of you. Additionally, I must mention my closest homies from Colorado, Sam Dolzani and Michael Baratta. These two have experienced some of the best and worst times with me, and it is

very likely that without our experiences back then I would not be in the position I am currently in. Let the struggles continue boys!

Aside from family and friends, Bob Messing and Micky Marinelli proved to be not only mentors and scientific role models, but also amazing friends whose dedication and support are matched by few. I want to also give a shout out to my committee, Michael Drew, Boris Zemelman, Adron Harris, and Hiroshi Nishiyama for putting up with my madness and allowing me to pursue a higher level of scientific intrigue in the future.

Outside of the scientific sector, I must acknowledge certain folks who have inspired me to achieve and continue this life with eternal happiness, from the great beyond. A huge trickle-down effect comes from these two (many, many musicians with enormous influence over my cognitive states), Jerry Garcia and Bill Monroe. Without the decades of recorded material from these two, whether grateful dead tunes or old timer traditional bluegrass 'goodins', the genius and mastery that has stemmed from their musical influence over the world has given me the inspiration and motive to not only achieve in science but in life (also in music). I thank you Jerry and Bill for everything you have done for me, and all of the rest in this world.

….If you should stand then who's to guide you? …..If I knew the way, I would take you home….

Abstract

Genetic Dissection of An Amygdala CRF Circuit for Fear and Anxiety

Matthew Brian Pomrenze, Ph.D.

The University of Texas at Austin, 2018

Supervisors: Robert O. Messing and Michela Marinelli

Fear and anxiety are ethological responses to threats and danger in the environment. The central amygdala (CeA) is a brain structure important for fear responses to discrete cues that predict threat. Recent findings indicate that the CeA also contributes to states of sustained apprehension in the absence of discrete cues that characterize anxiety, although less is known about the neural circuitry involved. The stress neuropeptide corticotropin releasing factor (CRF) is anxiogenic and produced by subpopulations of neurons in the CeA and the dorsolateral bed nucleus of the stria terminalis (dlBNST), a structure with strong connections to the CeA. Early models of the neurobiology of fear and anxiety proposed that the CeA promotes fear behaviors but not anxiety behaviors, and the BNST mediates anxiety but not fear. Furthermore, these models also hypothesized that a CRF pathway from the CeA to the dlBNST could be important for anxiety behavior, but this prediction remained untested. Here, the function of CeA CRF (CeA^{CRF}) neurons in fear and anxiety was investigated using Cre-dependent viral-genetic tools and male rats that express Cre recombinase from a *Crh* promoter. CeA^{CRF} neurons mediated both stress-induced anxiety and fear behaviors, both of which were dependent on CRF signaling. Additionally, the neuropeptide dynorphin, but not neurotensin, produced by CeA^{CRF} neurons was critical

for fear and anxiety behaviors. Neurotensin release had no effect on anxiety but dampened fear learning. GABA release from these neurons played a major role in setting the level of anxiety in the basal state. Finally, the CeA^{CRF} pathway to the dlBNST was tested for its role in anxiety and was found to be critical for these behaviors. This pathway also recruited CRF signaling and local CRF neurons in the dlBNST to engage anxiety-like behaviors. Collectively, these findings suggest that CeA^{CRF} neurons promote both fear and anxiety *via* the release of GABA and different neuropeptides and a projection to the dlBNST. The data presented here refine early neuroanatomical models of fear and anxiety and provide mechanistic support for recent human primate data suggesting that the CeA and BNST act together to generate negative emotional states.

Table of Contents

List of Tables

List of Figures

INTRODUCTION

Fear and anxiety

In nature, animals constantly assess their environments to ensure their own survival. Animals must identify and seek stimuli that promote survival, such as food, social interaction, and potential mates, which are perceived as rewarding and reinforcing. Additionally, animals must learn to avoid stimuli that threaten survival, such as predators, toxicities, and painful agents. When animals encounter aversive stimuli, they experience negative emotional states that energize behavioral processes that promote proper defensive action. If this does not happen, the probability of survival is greatly diminished.

When faced with a threat, animals typically experience negative emotional states characteristic of fear and anxiety. Fear is a subjective feeling of fright and apprehension precipitated by the detection of a real threat or imminent danger. The fear response is complex with many different components but is typically characterized by a short duration and a rapid induction by a discrete and threatening stimulus (Anderson and Adolphs, 2014; LeDoux, 2000, 2014; Tovote et al., 2015). In other words, fear is phasic and induced by a dangerous stimulus that is in close proximity and/or easily detected. In contrast, anxiety is apprehension and anticipation of danger that persists for extended periods of time and is present in environments where there is no direct evidence of danger or a threat is ambiguous or uneasily detected (Anderson and Adolphs, 2014; Davis and Shi, 2000; Grupe and Nitschke, 2013; LeDoux, 2000; Tovote et al., 2015). One useful analogy is to imagine riding a roller coaster. As one is climbing the track to the highest point, the anticipation of a scary drop could be considered anxiety, and the feeling during the actual drop is fear.

Both of these behavioral programs are essential to survival but may be engaged in different contexts. A direct encounter with a threat *should* precipitate a fear response because the animal must take behavioral action before it is harmed or killed. Anxiety is important so that animals avoid situations or environments in which safety could be threatened. Anxiety in a location where an animal was previously attacked is adaptive and healthy. This negative emotional state serves as a reminder of what happened in the past and that it could again, despite no direct evidence of a threat at the current time. Despite some behavioral and circumstantial differences, fear and anxiety evoke similar biological effects. They are both regarded as brain states caused by external or internal stimuli that underlie a specific set of measurable behavioral, physiological, hormonal, and autonomic actions (Tovote et al., 2015). Additionally, they both stimulate the hypothalamic-pituitary-adrenal (HPA) axis leading to the secretion of glucocorticoids and drive central limbic systems so emotional and behavioral action is properly executed. Therefore, fear and anxiety are conserved emotional and behavioral states that ensure animals' survival in nature.

Fear and anxiety disorders

Despite being adaptive states, fear and anxiety can persist and become maladaptive over time (Deisseroth, 2014). Fear responses should be short-lived and dissipate when fear-evoking stimuli have vanished. Anxiety should be experienced in places where threat or danger was previously detected or could be detected. When fear and anxiety become persistent, generalized, or exaggerated, well-being can be compromised and survival ability can be impaired. Unfortunately, anxiety disorders comprise some of the most prevalent neuropsychiatric disorders in humans (American Psychiatric Association., 2016;

Baxter et al., 2013). Anxiety disorders present with an estimated lifetime morbid risk (the proportion of people who will eventually develop the disorder at some time in their life whether or not they have a lifetime history at the time of assessment) of 41.7% and a lifetime prevalence of 33.4% with a 12-month prevalence of 22.2% (Kessler et al., 2012). The DSM-5 has divided these disorders into three categories, anxiety disorders, obsessive-compulsive disorders, and trauma and stress-related disorders (American Psychiatric Association. and American Psychiatric Association. DSM-5 Task Force., 2013). Anxiety disorders include generalized anxiety disorder, panic disorders, and phobias. Trauma and stress-related disorders include post-traumatic stress disorder (PTSD), acute stress disorder, and disinhibited social engagement disorder. It is well known that acute and chronic stress can lead to anxiety states in animals and humans. The class of "anxiety disorders" may have more heritable epidemiologies and thus possess genetic components. However, environmental stress can lead to their expression or exacerbation. Despite the sources of these disorders being different, the emotional and behavioral manifestations are similar. In addition, anxiety disorders are highly co-morbid with a host of other psychiatric states, including depression, schizophrenia, and substance use disorders.

Since anxiety phenotypes are so common, a substantial amount of work has gone into understanding and treating these disorders. Currently available pharmacotherapies, such as benzodiazepines or serotonin reuptake inhibitors are inconsistently effective or suffer from adverse side effects (Bystritsky, 2006; Griebel and Holmes, 2013; Insel, 2012). Cognitive behavioral therapies are also effective strategies for treating anxiety disorders. However, even with co-incident pharmaceutical administration many patients fail to achieve remission or relapse. Therefore, there is a clear need for a better understanding of brain circuits that control the experience and expression of fear and anxiety.

Neurobiology of fear and anxiety

Classic neuroscientific methods for understanding how specific brain regions contribute to behaviors in animal models include electrolytic lesions and pharmacological manipulation. Researchers used these methods to ablate a particular brain region and then test animal subjects for a behavior of interest. Studies evaluating the neurobiological basis of fear and anxiety relied on experimental designs that modeled fear and anxiety-like behaviors in animals. Since one cannot ask an animal if it is feeling fearful or anxious (subjective states), we must use models that produce measurable behaviors that represent manifestations of emotions like fear and anxiety that are objective in nature (Anderson and Adolphs, 2014). Perhaps the most important model for the study of fear and learning has been Pavlovian fear conditioning (Maren, 2001). In this procedure, a rodent is placed into a small chamber and presented with a neutral stimulus or cue, such as a discrete tone or light. As the cue terminates, the floor is briefly electrified and the rodent is footshocked, co-incident with termination of the cue (termed delay conditioning in the literature). Here, the animal learns to associate the aversive footshock (the unconditioned stimulus) with the previously neutral stimulus cue (which becomes the conditioned stimulus as the association is formed). After several pairings of the shock with the cue, the rodent learns to associate the cue with the 'fear' of experiencing the shock. If tested again later, the rodent will exhibit a fear response to the conditioned stimulus in the absence of any shocks. The behavior that is typically used as a readout of fear in rodents is freezing. It should be noted that in more naturalistic settings, imminent danger can also elicit other fear behaviors (e.g. attempts to flee and seek shelter, fighting, increased heartrate, respiration, etc.) (Blanchard et al., 1990), which can depend on sex (Jones and Monfils, 2016). Using these measurable behaviors as a proxy for

fear, the fear conditioning model has served as a fundamental tool for studying the neuroscience of aversive learning.

Anxiety is modeled differently in rodents. Some of the most reliable tests for anxiety in rodents rely on their natural behaviors and tendencies. Rodents are cautious animals and prefer to be active in environments that are dark and protected. Hence, they exhibit thigmotaxis, or a preference for staying near walls or enclosed spaces (Treit and Fundytus, 1988). A test called the elevated plus maze (EPM) test takes advantage of this phenomenon. This is an elevated platform in the shape of a "+" with two arms configured with high walls (closed arms) and two arms completely exposed (open arms). In this test, rodents spend most of their time in the closed arms and tend to avoid the open arms. Thus, time spent on the open arms is a measure of a rodent's anxiety levels. Another useful test is the open field (OF) test. This consists of an open topped arena in the shape of a square or circle with walls outlining the perimeter. Rodents will spend most of their time near the walls and tend to avoid exploring the center of the arena. These tests have excellent validities since drugs that decrease anxiety in humans, such as benzodiazepines, increase rodents' time on the open arms of the EPM and time spent in the center of the OF (Hazim et al., 2014). In addition, anxiogenic treatments (stress, yohimbine, etc.) reduce exploration of exposed areas (Cai et al., 2012; McCall et al., 2015). There are several other models for testing anxiety in rodents, such as social interaction time, novelty-induced suppression of feeding, light-dark box, and defensive burying (Bailey and Crawley, 2009). Altogether, fear conditioning and the aforementioned anxiety tests are reliable models for testing the neurobiology of fear and anxiety in animals.

Studies evaluating the neurobiology of fear was pioneered Joe Ledoux and colleagues. These researchers utilized brain site-specific lesions and pharmacological

silencing (*via* GABAergic agonists like muscimol and glutamatergic antagonists like CNQX and AP-5) in conjunction with fear conditioning procedures. It was soon clear that the acquisition and expression of fear behavior depends on activity in the amygdala complex, a small brain region in the temporal forebrain with a long-known role in emotion and aggression (LeDoux, 2003). Ledoux and colleagues demonstrated that synaptic plasticity within and across different subregions of the amygdala was critical to the learning and expression of fear behavior (Bauer et al., 2001; Clugnet and LeDoux, 1990). An anatomical model soon emerged where the lateral and basolateral amygdala (BLA) sends excitatory projections to the lateral central nucleus of the amygdala (CeA) which modulates activity of medial CeA neurons who send their axons to the midbrain periaqueductal gray (PAG) (Haubensak et al., 2010; Maren and Fanselow, 1996). Changes in neuronal activity in the PAG promotes defensive behaviors such as freezing, the main, but not sole, readout of fear in rodents (Tovote et al., 2016).

A massive amount of work went into the neurobiology of fear, but where in the brain anxiety was generated was less clear. Davis and colleagues were able to dissociate fear and anxiety by using fear and anxiety-like behavioral models (such as fear conditioning and acoustic startle reflex procedures) together and classic brain lesions and pharmacological inactivation. In rats, lesions of the amygdala reduced fear responses but had no effect on anxiety-like responses in the startle response test (Davis, 1992, 1997; Davis et al., 1994a). In contrast, lesioning of the bed nucleus of the stria terminalis (BNST), a forebrain structure nested between the striatum and septum and above the preoptic areas, significantly attenuated anxiety responses while leaving fear responses intact (Lee and Davis, 1997; Walker and Davis, 1997b, 2008; Walker et al., 2009b; Walker et al., 2003). From these data, Davis and colleagues developed an anatomical framework which

proposed that fear and anxiety were mediated by these two distinct brain structures, the amygdala and BNST, respectively (Davis et al., 2010). As these studies were replicated, it became an accepted principle in the neurobiology of fear and anxiety that the amygdala and BNST were dedicated to these two different aversive behaviors.

Fear, anxiety and CRF

In order to evoke anxiety in rats, investigators modified acoustic startle reflex procedures by shining a bright light. This generated enhanced startle responses that were characteristic of anxiety (since there was no real reason for the startle to be enhanced - brightly lit conditions only make the detection of predators more uncertain) (Walker and Davis, 1997a). This treatment also enhances anxiety-like behavior in the EPM and OF tests. In addition, administration of the stress-responsive neuropeptide corticotropin releasing factor (CRF) directly into the brain enhanced startle responses (Liang et al., 1992b). This peptide was infused because it was originally discovered as a critical gate of the HPA axis and thus played a major role in reactions to stress.

CRF is a 41 amino acid neuropeptide that has potent effects on behavior and physiology (Brown et al., 1982; Spiess et al., 1981). It is known to regulate both the neuroendocrine and emotional responses to stress, playing significant roles in behaviors of negative valence such as fear, anxiety, depression-like phenotypes, and stress-induced drug relapse (Heinrichs et al., 1995; Koob et al., 1990). A large population of neurons in the paraventricular nucleus of the hypothalamus express and release CRF into the anterior pituitary gland which stimulates corticotropic cells to release adrenocorticotropic hormone (ACTH) into circulation. ACTH then acts in the adrenal gland to stimulate the release of

glucocorticoids into the bloodstream. Thus, CRF serves as a critical component of the neuroendocrine stress response.

In addition to its expression in the hypothalamus, CRF is expressed at high levels across the brain in structures such as the CeA, the dorsal and ventral BNST, cortex, and many regions of the brainstem (Olschowka et al., 1982). CRF binds two receptors, the CRF 1 and 2 receptors (both G_s-coupled), that are widely expressed throughout the brain in many regions important for emotional and motivated behavior (Potter et al., 1994). CRF neurons, like all neuropeptide neurons, also secrete fast-acting neurotransmitters like glutamate or GABA (van den Pol, 2012). Furthermore, some CRF populations have been shown to co-express other neuropeptides. CRF neurons of the CeA (CeA^{CRF} neurons) also express neuropeptides like dynorphin, neurotensin, somatostatin, and neurokinin B (Kim et al., 2017; Marchant et al., 2007). Interestingly, some of these neuropeptides also regulate fear and anxiety-like states, but the precise roles of these neuropeptides sourced from CeA^{CRF} neurons have yet to be investigated.

With this functional anatomy in mind, it is easy to predict that CRF enhances behaviors associated with negative emotional states. Several subsequent studies determined that anxiety-like startle responses were suppressed with CRF antagonists (Walker et al., 2009a) and that inhibition of the BNST prevented CRF-induced anxiety behaviors (Lee and Davis, 1997). One study reported that CRF infusion into the dorsal BNST produces anxiety on the EPM and that this effect is blocked by co-administration of a CRF1 receptor, but not CRF2 receptor, antagonist into the dorsal BNST (Sahuque et al., 2006). This paper is also consistent with a study that found that intra-BNST infusion of CRF enhances startle responses (Lee and Davis, 1997). Data from these studies provided strong evidence that the BNST mediated anxiety-like behaviors that were generated by

stressful environments and CRF. In addition to a role in anxiety, other groups determined that CRF played critical roles in the acquisition of fear behaviors (Butler et al., 1990; Hikichi et al., 2000; Pitts et al., 2009; Sanford et al., 2017; Takahashi, 2001). Therefore, CRF plays critical roles in both fear and anxiety-like behavioral states.

In addition to behavior, CRF's effects on neurophysiology have been investigated. In the BNST, CRF enhances the frequency of spontaneous excitatory post-synaptic currents (EPSCs) *via* increasing presynaptic glutamate release (Kash et al., 2008; Nobis et al., 2011; Pliota et al., 2018; Silberman et al., 2013) and is primarily excitatory in the hippocampus (Blank et al., 2002). It has also been reported to enhance inhibitory post-synaptic currents (IPSCs) in some cells in the amygdala (Kash and Winder, 2006). Since few effects on EPSC or IPSC amplitudes are reported, it is thought that CRF typically exerts its effects by binding CRF receptors on presynaptic terminals. Therefore, in the BNST, it is predicted that CRF will enhance the release of glutamate to excite BNST cells and energize anxiety-like behaviors.

Gaps in knowledge

Despite the anatomical segregation of fear and anxiety, Davis and colleagues made another prediction. Since the CeA contains a large population of CRF neurons, and it was known that these neurons project strongly to the BNST (Sakanaka et al., 1986), it was hypothesized that a CeA^{CRF} neuron projection to the BNST was important for anxiety-like states (Davis et al., 2010). This hypothesis remained in the literature unproven. It was most likely never addressed because the tools to design the appropriate experiments were still in their infancy. The use of the classic neuroscience methods, such as lesions, were clearly invaluable for understanding the neurobiology of fear and anxiety. However, these methods

lack the spatial and temporal resolution to identify and functionally characterize individual circuit elements and their interactions with large brain-wide networks. As new genetic tools were produced, capitalizing on Cre recombinase activity and the Cre-lox system, discrete manipulation of genetically defined cells and pathways became possible. One achieves this specificity by injecting a Cre-dependent construct packaged into an adeno-associated virus (AAV) into a mutant animal that expresses Cre recombinase in a population of genetically-defined cells. Since Cre expression is controlled by the endogenous gene promoter, such as *Crh*, the AAV payload will only express in Cre^{+} cells. Tools of this kind were essential to testing the hypothesis proposed by Davis and colleagues.

As the use of these viral-genetic tools in Cre driver animals became widespread, many groups started studying the roles of genetically-defined CeA neurons in fear and anxiety. It became clear that not only does the CeA control fear, but it could also modulate anxiety (Ahrens et al., 2018; Botta et al., 2015; McCall et al., 2015; Pliota et al., 2018; Regev et al., 2012). Thus, the nuanced and finely tuned manipulations of specific neuronal cell-types demonstrated the anatomical segregation of fear and anxiety as inaccurate. As time moved on, several groups began to investigate the function of CeA^{CRF} neurons. These recent studies demonstrated that indeed these cells play important yet complex roles in fear (Fadok et al., 2017; Regev et al., 2012; Sanford et al., 2017). These results were not surprising considering manipulations of CRF itself, whether through pharmacology or genetic knockdown, also affected fear learning (Gafford et al., 2012; Pitts et al., 2009; Sanford et al., 2017). However, few studies on anxiety were conducted. One very recent paper showed that stimulating CeA^{CRF} neurons led to increased passive coping and anxiety responses on the EPM (Pliota et al., 2018), and another demonstrated that reducing GABA signaling in CeA^{CRF} neurons enhanced anxiety-like behavior (Gafford et al., 2012).

Additionally, since essentially all studies using genetic tools to manipulate CeA^{CRF} neurons were performed in mice, it begged the question of whether the same effects occurred in other species. This was particularly important since nearly all studies performed by Davis and colleagues and the early studies dissecting amygdala plasticity after fear conditioning were performed in rats. Therefore, several knowledge gaps in the literature were apparent. These gaps included whether rat CeA^{CRF} neurons modulate fear and anxiety, and whether the CeA^{CRF} projection to the BNST are important for anxiety states.

In addition to the complex roles these neurons most likely play in fear and anxiety behaviors, it was known for some time that these neurons were not only CRFergic (as mentioned above). The observation of co-expressed neuropeptides, especially some of which modulate fear and anxiety as well, suggests that these neurons release multiple neurotransmitters to promote specific behavioral states. However, similar to problems with pathway-specific manipulations, the tools to perform these types of studies did not exist. The notion of a neuron releasing multiple neurotransmitters and neuropeptides to control behavior has never been investigated to date.

In this dissertation, the gaps in knowledge described above have been addressed. Based on the previous data described in the literature, several important questions were generated: 1) do CeA^{CRF} neurons control fear and anxiety-like behaviors in rats? 2) if so, which neurotransmitters do they release to evoke any effects on fear and anxiety? and 3) does the CeA^{CRF} neuron projection to the dlBNST mediate anxiety-like behaviors? Discrete manipulations of the CeA^{CRF} neuron population in rats was achieved by using Cre-dependent AAV constructs in combination with transgenic *Crh*-Cre rats. These rats express Cre recombinase from a *Crh* promoter and thus Cre-dependent constructs will only express in Cre^{+} CRF neurons. The first chapter of this dissertation describes the generation and

utility of this rat, as well as some useful neuroanatomy that is consistent with previous literature while providing some new data. The subsequent chapters use the *Crh*-Cre rat with Cre-dependent viral-genetic tools to selectively manipulate CeA^{CRF} neurons and their projections to the dlBNST. In addition, Cre-dependent RNA interference tools were generated to disrupt the release of different neurotransmitters selectively in CeA^{CRF} neurons. The following data provide strong evidence that CeA^{CRF} neurons play versatile roles in fear and anxiety-like behaviors through the release of numerous neurotransmitters and the pathway to the dlBNST. These findings help confirm a previously untested, yet important hypothesis in the fear and anxiety literature, and provide novel information about how CeA^{CRF} neurons contribute to both fear and anxiety-like states.

CHAPTER 1: A TRANSGENIC RAT FOR INVESTIGATING THE ANATOMY AND FUNCTION OF CORTICOTROPIN RELEASING FACTOR CIRCUITS*

ABSTRACT

Corticotropin-releasing factor (CRF) is a 41 amino acid neuropeptide that coordinates adaptive responses to stress. CRF projections from neurons in the central nucleus of the amygdala (CeA) to the brainstem are of particular interest for their role in motivated behavior. To directly examine the anatomy and function of CRF neurons, we generated a BAC transgenic *Crh*-Cre rat in which bacterial Cre recombinase is expressed from the *Crh* promoter. Using Cre-dependent reporters, we found that Cre expressing neurons in these rats are immunoreactive for CRF and are clustered in the lateral CeA (CeL) and the oval nucleus of the BNST. We detected major projections from CeA CRF (CeA^{CRF}) neurons to parabrachial nuclei and the locus coeruleus, dorsal and ventral BNST, and more minor projections to lateral portions of the substantia nigra, ventral tegmental area, and lateral hypothalamus. Optogenetic stimulation of CeA^{CRF} neurons evoked GABAergic responses in 11% of non-CRF neurons in the medial CeA (CeM) and 44% of non-CRF neurons in the CeL. Chemogenetic stimulation of CeA^{CRF} neurons induced Fos in a similar proportion of non-CRF CeM neurons but a smaller proportion of non-CRF CeL neurons. The CRF1 receptor antagonist R121919 reduced this Fos induction by two thirds in these regions. These results indicate that CeA^{CRF} neurons provide both local inhibitory GABA and excitatory CRF signals to other CeA neurons and demonstrate the value of the *Crh*-Cre rat as a tool for studying circuit function and physiology of CRF neurons.

*Portions of this chapter have previously been published in *Frontiers in Neuroscience*. Pomrenze MB, Millan EZ, Hopf FW, Keiflin R, Maiya R, Blasio A, Dadgar J, Kharazia V, De Guglielmo G, Crawford E, Janak PH, George O, Rice KC, Messing RO. 2015. A transgenic rat for investigating the anatomy and function of corticotrophin releasing factor circuits. *Frontiers in Neuroscience*. 9:487. doi: 10.3389/fnins.2015.00487.

INTRODUCTION

Corticotropin-releasing factor (CRF) is a central regulator of endocrine, autonomic, and behavioral responses to stressors (Koob, 2009). Although CRF cell bodies are distributed in several brain regions, they are particularly concentrated in the central amygdala (CeA), the bed nucleus of the stria terminalis (BNST), and the paraventricular hypothalamic nucleus (PVN) (Wang et al., 2011). In the PVN CRF acts as a hormone to regulate the hypothalamic-pituitary-adrenal (HPA) axis and trigger the endocrine stress response (Rivier and Vale, 1983). Outside of the PVN CRF modulates synaptic transmission within specific circuits of the central nervous system (Gallagher et al., 2008). CRF neurons of the CeA are of particular interest, since they contribute to stress-related arousal, conditioned fear, and negative emotional states associated with drug withdrawal (Koob, 2009; Kravets et al., 2015; Walker et al., 2009b).

In the rat, the CeA subpopulation that expresses CRF resides in the lateral CeA (CeL) where another, mostly non-overlapping subpopulation expresses enkephalin (Day et al., 1999; Veinante et al., 1997). Approximately 60% of CeA^{CRF} neurons are also immunoreactive for dynorphin (Marchant et al., 2007). Anatomical studies have shown strong projections from the CeL as a whole to the medial CeA (CeM), the brainstem (parabrachial nucleus, reticular formation, locus coeruleus, nucleus of the solitary tract and dorsal vagal complex) and the BNST, with more modest projections to the lateral hypothalamus, lateral one-third of the substantia nigra pars compacta and an adjacent lateral part of the retrorubral field (Bourgeais et al., 2001; Dong et al., 2001; Petrovich and Swanson, 1997; Zahm et al., 1999). For CeA^{CRF} neurons in particular, tract-tracing studies have identified CRF projections from the rat CeA to the locus coeruleus (Reyes et al., 2011; Van Bockstaele et al., 1998), parabrachial nuclei (Moga and Gray, 1985), the midbrain

central gray (Gray and Magnuson, 1992), the dorsal vagal complex (including the nucleus tractus solitarius) (Gray and Magnuson, 1987), the pontine reticular nucleus (Fendt et al., 1997), the mesencephalic trigeminal nucleus (Sakanaka et al., 1986), and the BNST (Sakanaka et al., 1986). Whether CeA^{CRF} neurons also project locally within the CeA is not clear, and although some CRF immunoreactive fibers have been observed in the CeM (Veening et al., 1984), their source and functional significance are not known. Several recent studies have helped clarify CRF architectures and functions using *Crh*-Cre mouse lines (Gafford et al., 2014; Gafford et al., 2012; McCall et al., 2015; Wamsteeker Cusulin et al., 2013), but thorough characterization of CRF circuits across brain structures, and moreover across species, is still lacking.

Here, we describe a transgenic *Crh*-Cre rat that permits genetic access to CRF neurons, thereby allowing direct investigation of their anatomy and roles in physiology and behavior. To examine CRF cell localization and projection targets, we crossed *Crh*-Cre rats with a DsRed2/GFP-reporter rat, or infected the CeA with AAVs that express Cre-dependent mCherry, channelrhodopsin (ChR2)-eYFP, or hDM3q-mCherry. We found that Cre-expressing CeA neurons are immunoreactive for CRF and project to several brain regions in the brainstem and diencephalon. Using the *Crh*-Cre rat to investigate CeA circuitry, we provide new evidence that CeA^{CRF} neurons act as local interneurons to provide both inhibitory and excitatory signals to the CeL and CeM.

MATERIALS AND METHODS

Development of *Crh*-Cre rats

All animal studies were approved by the Institutional Animal Use and Care Committees of the Ernest Gallo Clinic and Research Center at the University of California San Francisco, the Scripps Research Institute and of The University of Texas at Austin, and were performed in adherence with the NIH Guide for Care and Use of Laboratory Animals. Studies utilized male and female *Crh*-Cre rats.

We identified the BAC clone CH230-206D8 from the CHORI-230 Rat (BN/SsNHsd/MCW) BAC library, which was derived from an inbred female brown Norway rat (Osoegawa et al., 2004), as containing the promoter region and exons 1 and 2 of the rat *Crh* gene on chromosome 2. The BAC clone has ~80 kb 3' of the *Crh* ATG and ~143 kb of DNA 5' of the ATG. BAC recombineering was performed as described (Cotta-de-Almeida et al., 2003) with vectors and bacterial host cell lines kindly provided by Dr. Scott Snapper (Harvard Medical School).

A ~2.7Kb modified/enhanced Cre metallothionein-1 polyadenaylation (CREM) fragment was PCR amplified from the plasmid p210 pCMV-CREM [Addgene # 8395; (Kaczmarczyk and Green, 2001)]. This fragment contains a modified human beta-globin intron within the Cre coding sequence to prevent expression of Cre recombinase in prokaryotes, thereby making it suitable for interim work in bacteria with plasmids containing loxP sites. The fragment was sub-cloned into the conditional replicon vector pBSB-171 and confirmed by sequencing. The plasmid pBSB-171 allows the cloning of the fragments of interest and contains a floxed aminoglycoside kinase (aph) gene cassette. A c-myc tag (EQKLISEEDL) was inserted (QuikChange II XL Site Directed Mutagenesis

kit, Agilent Technologies) immediately before the Cre "stop" codon, and confirmed by sequencing. The completed construct is referred to as CREM-myc pBSB-171.

We designed a forward PCR primer (P1) containing 58 bp homologous to the rat *Crh* sequence immediately adjacent to the ATG of CRF followed by 31 bp of CREM-myc pBSB-171 vector sequence, and a backward PCR primer (P2) containing 23 bp of CREM-pBSB-171 vector sequence followed by 64 bp homologous to the sequence immediately adjacent to the *Crh* stop codon. We then amplified a fragment containing the CREM-myc-floxed aph cassette with rat *Crh* homology ends by PCR with CREM-myc pBSB-171 and primers P1, P2. Lambda red-driven recombination between this PCR product and the BAC clone CH230-206D8 generated recombinants in which the endogenous *Crh* coding sequence was replaced with the CREM-myc-floxed aph fragment.

This recombineered CH230-206D8 BAC was transformed with the bacterial Cre expression plasmid 706-Cre;tet (Gene Bridges Gmbh, Heidelberg, Germany) to remove the floxed aph cassette. The recombineered circular BAC DNA without the aph cassette was purified (Bimboim and Doly, 1979) using a NucleoBond BAC 100 kit (Clontech # 740579). This DNA was sent to The University of Michigan Transgenic Animal Model Core for pronuclear injection into Hdr:W1 ES cells and implantation (Filipiak and Saunders, 2006). Rat-tail DNA from resulting progeny was purified using DNeasy (Qiagen # 69506), screened by PCR, and confirmed by sequencing to identify a total of 3 founder transgenic rats. Cre-expressing cells were identified by crossing *Crh*-Cre rats with the reporter rat line W-Tg(CAG-DsRed2/GFP) 15Jms (NBRP-Rat Number 0282), which was obtained from the National BioResource Project-Rat in Kyoto, Japan. The reporter rat has a DsRed coding region flanked by LoxP sites followed by a GFP sequence, all under

control of a CAG promoter. Cre recombination leads to excision of the DsRed coding region and expression of GFP.

Surgery and histology

We microinjected 0.8-1.2 μL/side (100 nL/min) of one of the following: AAV-Ef1α-DIO-eYFP, AAV-Ef1α-DIO-ChR2-eYFP (Zhang et al., 2010), AAV-hSyn-DIO-mCherry (UNC Vector Core, Chapel Hill, NC), AAV-hSyn-DIO-hM3Dq-mCherry, or AAV-hSyn-DIO-hM4Di-mCherry (Krashes et al., 2011). Coordinates for the CeA were AP 2.40, ML +/-4.85, DV -8.40 from the skull in adult rats, or AP -2.0, ML +/-4.3, DV -7.9 from the skull in adolescent rats weighing 200-220 g. Coordinates for the dlBNST were AP +0.00, ML +/-3.5, DV -6.8 with a 16-degree angle in adolescent rats weighing 200-220 g. After injection, we waited 10 min for virus to diffuse into the tissue before retracting the injector needle. We used adolescent rats in several experiments to facilitate transduction down axons for efficient labeling of neuronal projections. After 2-4 months, rats were deeply anaesthetized with sodium pentobarbital (100 mg/kg, *i.p.*) and perfused transcardially with phosphate buffered saline (PBS) followed by 4% paraformaldehyde in PBS. Brains were immediately removed, placed into the same fixative overnight, and then transferred to a 30% sucrose solution at 4°C before sectioning at 40 μm on a cryostat.

We detected co-localization of eYFP or mCherry fluorescence with CRF, prodynorphin, preproenkephalin, somatostatin, protein kinase C delta (PKCδ), or Fos immunoreactivity using immunofluorescent histochemistry. Sections were washed three times in PBS with 0.2% Triton X-100 (PBST) for 10 min at room temperature and then incubated in blocking solution made of PBST with 3% normal donkey serum (Jackson ImmunoResearch, number 017-000-121) or normal goat serum (Jackson ImmunoResearch,

number 005-000-121) for 1 hr. Sections were then incubated in one or more of the following primary antibodies: rabbit anti-cFos (1:2000, Santa Cruz Biotechnology, sc-52), goat anti-cFos (1:2000, Santa Cruz Biotechnology, sc-52-G), mouse anti-tyrosine hydroxylase (TH) (1:2000, Immunostar, 22941), mouse anti-tryptophan hydroxylase (TPH) (1:1000, Sigma Aldrich, T0678), goat anti-CRF (1:500-1000, Santa Cruz Biotechnology, sc-1761 Lot# B0315), rabbit anti-neurotensin (1:1000, ImmunoStar, Hudson, WI, Cat. No. 20072), guinea pig anti-prodynorphin (1:500, Neuromics, GP10110), rabbit preproenkephalin (1:100, Neuromics, RA14124), or rabbit anti-PKCδ (1:2000, Santa Cruz Biotechnology, sc-213) with or without mouse anti-NeuN (1:2000, Millipore, MAB377 clone A60) in blocking solution rotating at 4º C for 18-20 h. After three 10-min washes in PBST, sections were incubated in species-specific secondary antibodies Alexa Fluor 488, 568, or 647 (1:700, Thermo-Fisher Scientific, A-21206, A11067, A-11055, A-21202, A- 21208, A-11073, A-21447, A-31573) in blocking solution for 1 hr at room temperature. Finally, sections were washed four times in PBS, then mounted in 0.2% gelatin water onto SuperFrost Plus glass slides (Fisherbrand, 12-550-15) and coverslipped with Fluoromount-G (Southern Biotech, 0100-01). Slides were stored in the dark before microscopy and image acquisition.

For somatostatin staining, sections were pretreated with 50% ethanol twice for 10 minutes each and washed three times in PBS and then blocked in 10% normal donkey serum at room temperature for 10 minutes. The sections were then incubated with rat anti-somatostatin antibody (Millipore, MAB354) diluted 1:100 in PBS containing 0.05% Triton-X-100 and incubated for 20 hours at 4º C with shaking. Sections were washed for 10 minutes three times in PBS and then incubated with 2% NDS for 10 minutes. Primary antibody staining was visualized by incubating with Alexa Fluor 488-conjugated anti-rat

secondary antibody (1:700 dilution in PBS) for 2 hours. Sections were washed four times in PBS and prepared for imaging as described above.

Peroxidase immunohistochemistry was performed using 3,3'-diaminobenzidine tetrahydrochloride (DAB). Sections were first washed for 30 min each in 0.1 M sodium phosphate buffer, pH 7.2 (PB), followed sequentially by 50% ethanol, 50% ethanol with 3% H2O2, and then 5% normal donkey serum (NDS) in PB. Sections were then incubated in mouse antiserum against GFP (1:1500, Invitrogen or 1:1000, Abcam) in PB with 2% NDS and 0.2% Triton X-10 (PBTX; 48 h at 4°C). The sections were then washed with PB and incubated in PBTX containing biotinylated donkey anti-mouse IgG (1:1000, Jackson Immunoresearch Laboratories) for 24 hrs at 4°C. Finally, sections were washed in PB, incubated with peroxidase-conjugated avidin (ExtrAvidin, Sigma-Aldrich) in PB (1:2500; 2 hrs at RT), washed again, and then incubated in DAB (ImmPACT DAB, Vector Laboratories). Sections were then mounted with PB containing 1% gelatin, dehydrated, cleared in xylene and coverslipped with DEPEX mounting medium (Electron Microscopy Sciences).

Confocal acquisition & 3D analysis

Three-dimensional stacks of Images were acquired with a Zeiss 780 Laser Scanning Confocal microscope using either a 20x (1 µm image slice), 40x (0.6 µm image slice) or 63x (0.2 µm image slice) objective. The system is equipped with a stitching stage and Zen software to reintegrate the tiled image stacks. Stitched z series images of the entire CeA were imported into Imaris software (Bitplane-Andor, Inc.) for quantitation. The eYFP (green), and the CRF-A568 fluorescent labels (red) were first three dimensionally traced using the iso-surfacing module to obtain a clean outline of the neuronal cell body and

branches, which was then rendered solid using a control-based threshold. The isosurfaced eYFP signal was then used to create a new channel to determine how much red signal was present within green iso-surfaced regions. This assay was further corroborated using the colocalization module to confirm the extent and location of overlapping signals. The filament tracer module was used to identify the origin of disjointed axons and outline the neural branches of the same neuron. An alternative analysis of green fluorescent signals within red iso-surfaced neurons was performed for comparison. This use of multiple methods of analysis allowed us to quantify the location and extent of CRF-like immunoreactivity throughout eYFP positive cell bodies and axons. This approach was used on 1-3 sections per rat from 5 rats.

Cell counting

Immunostained sections were imaged on a Zeiss 710 LSM confocal microscope, Zeiss Imager M2 microscope or a Zeiss Axio Zoom stereomicroscope. Quantification of Fos and co-localization of mCherry or eYFP with neuropeptides in the CeA were performed on alternate sections from Bregma -1.90 to -3.00 (6-12 sections per rat) using Fiji (Schindelin et al., 2012).

Electrophysiology and optogenetics

To measure ChR2-evoked GABA IPSCs, we expressed ChR2-eYFP in Cre-expressing neurons and recorded light-evoked IPSCs as in recent work (Seif et al., 2013), with the following exceptions: rats were perfused intracardially with a glycerol-based aCSF (in mM: 252 glycerol, 2.5 KCl, 1.25 NaH_2PO_4, 1 $MgCl_2$, 2 $CaCl_2$, 25 $NaHCO_3$, 1 L-ascorbate, and 11 glucose), and then brain slices were cut in the same solution. A CsCl

internal solution (CsCl, 135; HEPES, 10; MgATP, 4; GTP, 0.3; MgCl2, 2; EGTA, 0.5 and QX-314, 5; pH 7.23, Maylor et al., 2010), with DNQX in the bath to block AMPARs, was used for measuring GABA IPSCs.

To distinguish small, evoked IPSCs from spontaneous IPSCs (sIPSCs), we recorded ~20 traces where a ChR2-eYFP+ terminal was stimulated once with blue light at 111 msec into a 1000 msec sweep. The sIPSC frequency was typically low (0.67 ± 0.13 Hz), and thus the likelihood of observing a spontaneous IPSC exactly at the time of ChR2 stimulation in more than a few of the 20 traces was very low. If an IPSC was observed at the time of ChR2 stimulation in only one or two of the 20 traces in a given cell, we did not consider this a cell responding to ChR2 stimulation. Of note, sIPSCs displayed variability in amplitude within the same cell as reported by others (Delaney and Sah, 2001), making the relative amplitude of evoked versus spontaneous IPSCs a less reliable measure. For spatial mapping, we used live visualization of the electrode tip and its exact location within the CeA instead of biocytin filling. Had we used biocytin in these experiments, there would have been many neurons filled within the same slice, including neurons where patch-clamping was attempted for several minutes but failed to achieve stable recording.

Chemogenetics and Fos mapping

Crh-Cre rats were microinjected bilaterally with AAV-hSyn-DIO-hM3Dq-mCherry, AAV-hSyn-DIO-hM4Di-mCherry, or AAV-hSyn-DIO-mCherry into the CeA. After 2-4 months, rats were administered intraperitoneally 2 mg/kg clozapine-N-oxide (CNO; NIMH Chemical Synthesis and Drug Supply Program) and perfused 120 min later for Fos immunohistochemistry. To inhibit CRF1 receptors, we administered 10 mg/kg R121919 (Chen et al., 2004) subcutaneously to rats 30 min before administration of CNO.

Data analysis

Data are shown as mean ± SEM values and were analyzed by two-tailed t-tests or by ANOVA with post-hoc Tukey's tests using GraphPad Prism v6.0.

RESULTS

Neurons that express Cre in *Crh*-Cre rats are immunoreactive for CRF

Cre-expressing cells in *Crh*-Cre rats were first identified by crossing *Crh*-Cre rats with W-Tg(AG-DsRed2/GFP)15Jms reporter rats and then immunostaining brain sections from bigenic progeny with anti-GFP antibody. There were clusters of immunoreactive neurons in the CeL and in the dorsolateral BNST (Figure 1.1A and 1.1B). We confirmed the presence of Cre activity in mature CeL and BNST neurons by microinjecting AAV-hSyn-DIO-mCherry into the CeA or the dorsal BNST of 6-week old rats and then examining brain slices for the presence of mCherry fluorescence 8 weeks later (Figure 1.1C and 1.1D). Surprisingly we did not detect Cre recombination in the ventral BNST or in the paraventricular hypothalamic nucleus, even following microinjection of a large volume (1.2µl) of Cre-dependent AAV into the hypothalamus.

To determine if Cre-expressing neurons also express CRF, we microinjected colchicine (4µg in 0.8µL) into the CeA 4 weeks after injection of AAV-Ef1α-DIO-eYFP and 72h prior to perfusion to allow CRF to accumulate in the cell soma (Merchenthaler, 1984). We found that 94.6 ± 1.2% $eYFP^+$ neurons were immunoreactive for CRF, while 77.1 ± 2.1% of CRF immunoreactive neurons expressed eYFP (Figure 1.1E; n = 3 rats, 12 amygdala sections/rat).

We also examined colocalization of ChR2-eYFP and CRF immunoreactivity in *Crh*-Cre rats microinjected with AAV-Ef1α-DIO-ChR2-eYFP and not treated with colchicine. ChR2-eYFP was present in the cell membrane of neuronal cell bodies and processes while CRF immunoreactivity was mainly scattered within neural processes. Because CRF is mainly localized in neural processes, quantification of colocalization in cell bodies using bright-field microscopy at 40x resulted in only a small percentage (16.5 ± 2.7%) of $eYFP^+$ neurons being colocalized with CRF. However, confocal analysis at 63x followed by 3D reconstruction of the neuronal cell bodies and branches using Imaris 3D software revealed that all $eYFP^+$ neurons contained CRF immunoreactivity in the cell soma or branches (Figure 1.1F). Out of 155 neurons analyzed, 100 ± 0% of $eYFP^+$ neurons were positive for CRF, while 99.4 ± 0.6% of CRF^+ neurons were positive for eYFP.

Using hSyn-DIO-mCherry to identify CRF neurons, we examined co-expression of other neuropeptides in the CeA (Figure 1.2). We found that about 63.4 ± 3.6% of CRF neurons expressed neurotensin. We also found that about 54.2 ± 2.8% of CRF neurons were immunoreactive for dynorphin while there was almost no colocalization with enkephalin, as described previously (Day et al., 1999; Marchant et al., 2007; Veinante et al., 1997). A population of neurons in the CeA expresses somatostatin (SOM), and recent studies demonstrate an active role for CeA SOM^+ neurons in conditioned fear in mice (Li et al., 2013; Penzo et al., 2015). We determined that approximately 44.2 ± 0.7% of CeA^{CRF} neurons co-localize with SOM^+ neurons. In addition to SOM^+ neurons, there is a distinct GABAergic subpopulation of CeA neurons in mice that expresses protein kinase C delta (PKCδ), but not CRF, and suppresses fear conditioning (Ciocchi et al., 2010; Haubensak et al., 2010). We similarly found that CRF and PKCδ are present in distinct populations in the rat amygdala with only approximately 9.2 ± 1.1% of CRF neurons co-expressing

PKCδ. Also, CRF-expressing cells were consistently more medial than PKCδ-expressing cells in the CeL (Figure 1.2A).

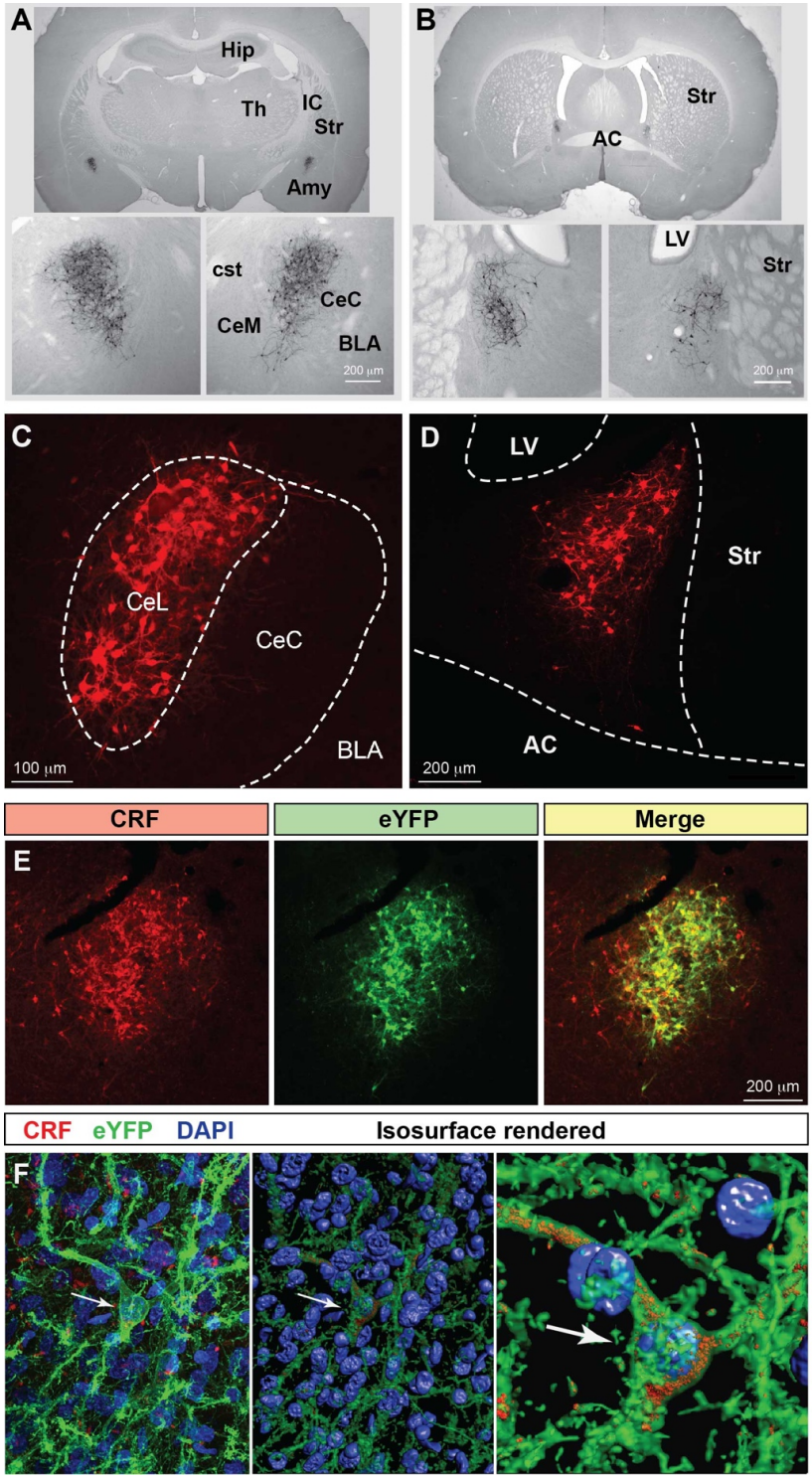

Figure 1.1. ***Crh*-Cre rats express Cre recombinase activity in the CeA and dlBNST**

(A-B) Bigenic progeny of a *Crh*-Cre X DsRed2/GFP cross display robust GFP labeling in the CeA and dlBNST. Scale bars, 200 μm. **(C-D)** Cre-dependent mCherry expression in Cre-expressing neurons of the CeA and dlBNST. Scale bars, 100 μm in **(C)**; 200 μm in **(D)**. (E) Cre-dependent eYFP co-localizes with CRF immunoreactivity in the CeL. Scale bar, 200 μm. **(F)** Rendered isosurface analysis demonstrates co-localization of CRF immunoreactivity within CeL neurons that also express Cre-dependent eYFP. AC = anterior commissure, AMY = amygdala, BLA = basolateral amygdala, CeC = capsular central amygdala, CeM = medial central amygdala, cst = commissural stria terminalis, Hip = Hippocampus, IC = internal capsule, LV = lateral ventricle, OT = optic tract, Str = Striatum, Th = Thalamus.

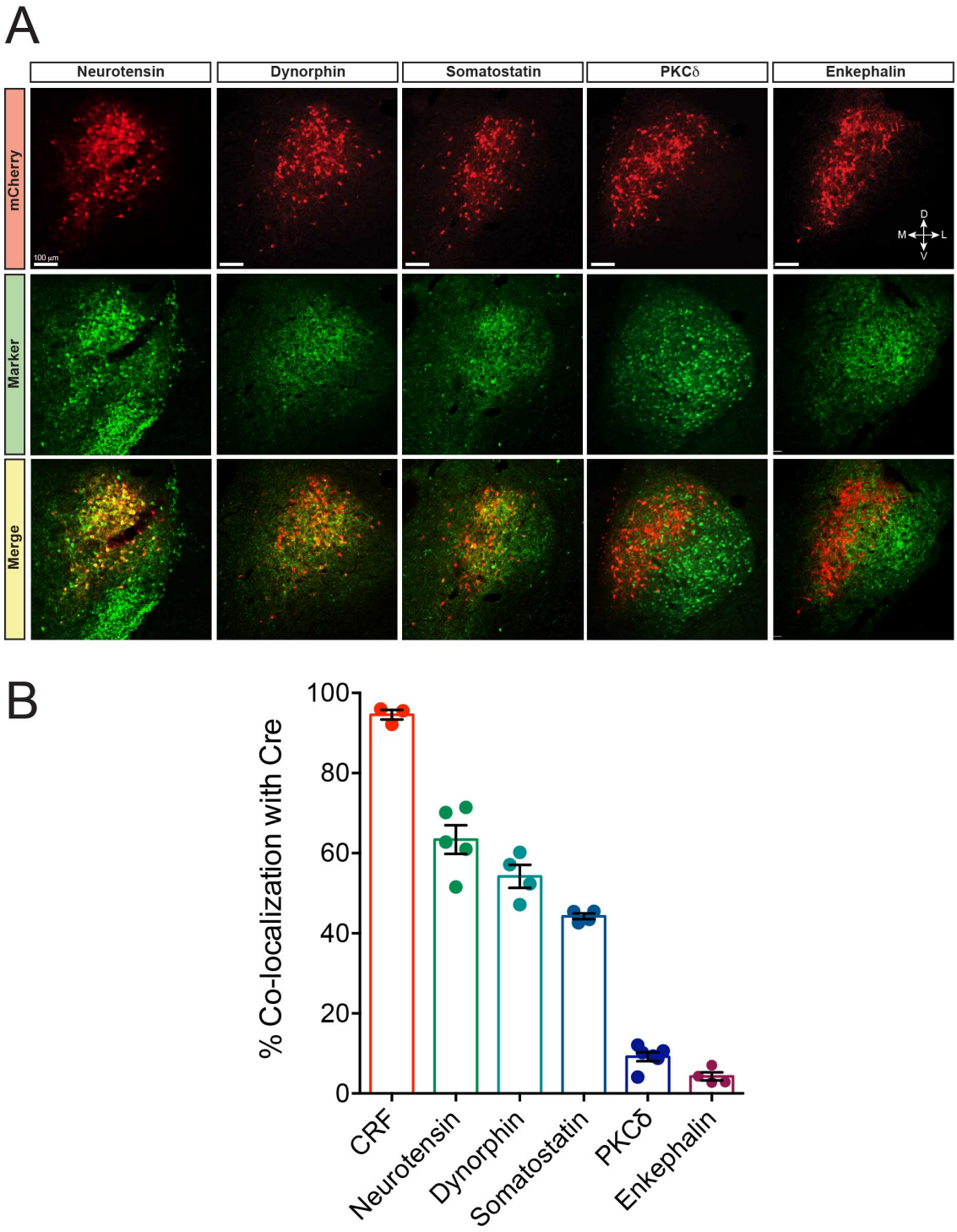

Figure 1.2. Co-expression of other neuropeptides in CeA^{CRF} neurons

(**A**) A large percentage of CRF neurons identified by expression of Cre-dependent mCherry are immunoreactive for neurotensin, dynorphin, and somatostatin, while few express enkephalin or PKCδ. Scale bars, 100 μm. Medial is to the left. (**B**) Quantification of mCherry expression with neuropeptide immunoreactivity; CRF n = 3 rats, 12 amygdala sections/rat; neurotensin n = 5 rats, 6-8 amygdala sections/rat; dynorphin n = 4 rats, 6 amygdala sections/rat; somatostatin n = 4 rats, 6 amygdala sections/rat; enkephalin n = 4 rats, 6 amygdala sections/rat; PKCδ, n = 6 rats, 10-12 amygdala sections/rat.

Projections from CeA^{CRF} neurons outside the CeA

We examined neuronal projections from CeA^{CRF} neurons using mCherry or ChR2-eYFP as a histological marker (Figures 1.3-1.6). We detected projections to several regions identified previously in nonselective tract tracing studies of the CeA (Bourgeais et al., 2001; Dong et al., 2001; Petrovich and Swanson, 1997; Veinante and Freund-Mercier, 1998; Zahm et al.). The largest and densest were to the PBN and the LC (Figure 1.3). Fibers were present in both the lateral and medial PBN and in the mesencephalic trigeminal nucleus and extended caudally within the medial PBN to the LC. CRF fibers there appeared to be interdigitated and orthogonal to the dorsolateral LC dendritic field (Figure 1.3D).

We also observed a substantial projection from the CeA to the dorsolateral and especially the ventral BNST (Figure 1.4A-1.4C). Dorsolateral CRF fibers appeared to cluster around the oval nucleus and also extend into the adjacent dorsal striatum. In addition, a small projection was detected slightly ventrolateral to the ventral BNST in the substantia innominata and ventral pallidum (Figure 1.4C). Caudal to the BNST, CRF projections were present in the most lateral portion of the lateral hypothalamus (LH) along its entire anterior-posterior axis traveling through the nigrostriatal bundle (Figure 1.4D). Most of these appeared to be fibers of passage with small projections extending laterally into the LH. Caudal to the hypothalamus, we observed CRF fibers coursing into the ventrolateral periaqueductal gray, and eventually into the caudal aspect of the serotonergic dorsal raphe nucleus (Figure 1.4E). Deep in the brainstem caudal to the LC, we detected a small projection to the nucleus tractus solitarius (NTS) throughout much of its anterior-posterior axis (Figure 1.4F-1.4I). At the most anterior aspect, CRF fibers were localized to the lateral NTS and overlapped with tyrosine hydroxylase positive processes

but not somata (Figure 1.4F). Further posterior, CRF fibers clustered within the medial NTS as it coursed towards the 4th ventricle (Figure 1.4G), and fibers eventually terminated in the caudal ventrolateral NTS around noradrenergic cell bodies (Figures 1.4H and 1.4I).

CRF signaling in the dopaminergic ventral tegmental area (VTA) has garnered much attention due to its significant role in relapse to drug seeking (Shalev et al., 2010). However, the source of CRF in the VTA has remained controversial (Grieder et al., 2014; Zhao-Shea et al., 2015). CRF fibers from the CeA were present traveling through the dorsolateral substantia nigra pars compacta, most likely as fibers of passage on their way to the brainstem (Figure 1.5A-1.5D). However, upon closer examination we detected minor collateral projections within the rostral VTA (Figure 1.5E).

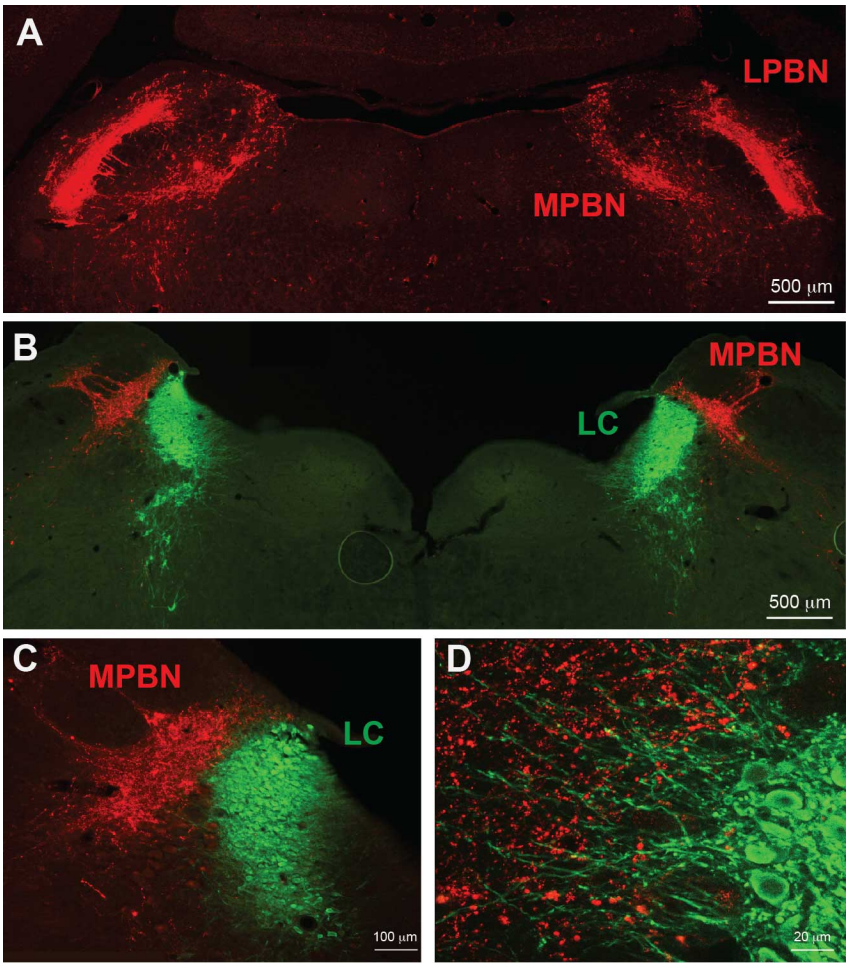

Figure 1.3. CeA^{CRF} neurons project strongly to brainstem nuclei

(**A**) After injection of AAV-hSyn-DIO-mCherry into the CeA, mCherry expressing fibers were detected in the lateral and medial parabrachial nuclei (Bregma -9.0). Scale bar, 500 µm. (**B**) mCherry expressing fibers were also detected in the medial parabrachial nucleus just lateral to the locus coeruleus (Bregma -9.6). Red = mCherry, Green = Tyrosine Hydroxylase. Scale bar, 500 µm. (**C-D**) High-magnification examples of mCherry fibers from the CeL and noradrenergic LC neurons. CeA^{CRF} fibers appear to run orthogonally to noradrenergic dendrites extending laterally from the LC core into the medial parabrachial

nucleus. Scale bars, 100 μm in (**C**); 20 μm in (**D**). MPBN = medial parabrachial nucleus, LPBN = lateral parabrachial nucleus, LC = locus coeruleus.

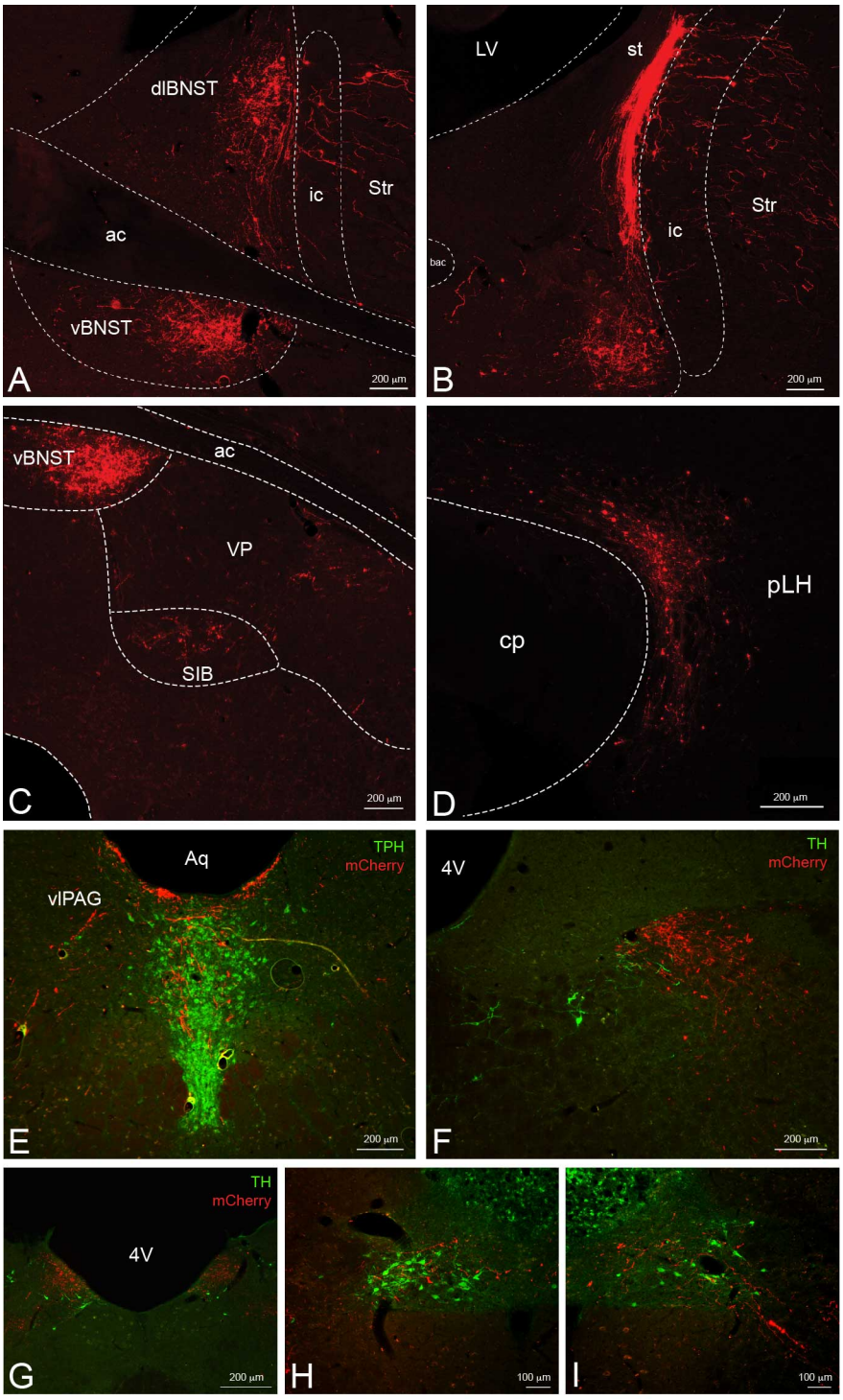

Figure 1.4. CeA^{CRF} neurons provide inputs to other limbic brain structures

(A-B) A dense bundle of mCherry expressing fibers from the CeA were observed in the dorsolateral and ventral BNST. (**A**) Rostrally, fibers clustered mainly in the oval nucleus of the dorsal bed nucleus and in the subcommisural zone of the ventral bed nucleus (Bregma -0.12). (**B**) Caudally, dense fibers of the stria terminalis were present in the dorsal region (Bregma -0.6). Scale bars, 200 μm. (**C**) Less dense projections were detected ventral and lateral to the ventral BNST in the substantia innominata and the ventral pallidum (Bregma -0.12). Scale bar, 200 μm. (**D**) Fibers were detected throughout the lateral hypothalamus (Bregma -4.20) within the nirgrostriatal bundle. Scale bar, 200 μm. (**E**) Fibers also projected dorsomedially into the caudal dorsal raphe nucleus and ventrolateral periaqueductal gray (Bregma -7.7). TPH = tryptophan hydroxylase. Scale bar, 200 μm. (**F-I**) Some fibers projected as far as the nucleus tractus solitarius where they came in close contact to noradrenergic processes and cell bodies in the most caudal regions. (Bregma (-12.9) – (-14.0). TH = tyrosine hydroxylase. Scale bars, 200 μm in (**F**); 200 μm in (**G**); 100 μm in (**H**); 100 μm in (**I**). ac = anterior commissure, ic = internal capsule, Str = striatum, st = stria terminalis, VP = ventral pallidum, SIB = substantia innominata, cp = cerebral peduncle, pLH = posterior lateral hypothalamus, Aq = central aqueduct, vlPAG = ventrolateral periaqueductal gray, DRL = lateral dorsal raphe nucleus, DRV = ventral dorsal raphe nucleus, 4V = fourth ventricle.

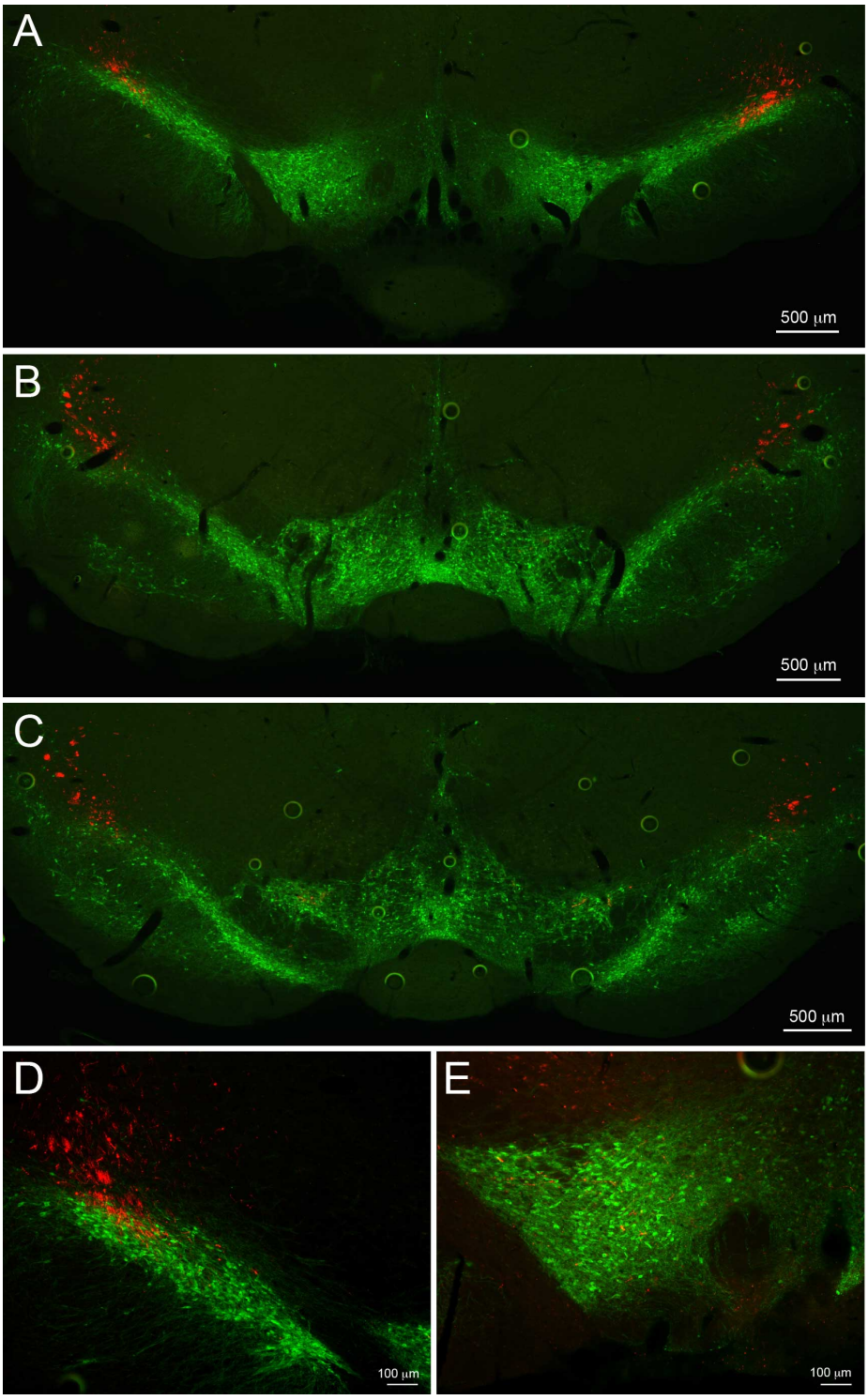

Figure 1.5. CeA^{CRF} projections to the substantia nigra and VTA

(**A**) Representative example of CeA^{CRF} fibers in the rostral VTA and substantia nigra pars compacta (SNc) (Bregma -5.0). Scale bar, 500 μm. (**B**) CeA^{CRF} fibers were observed projecting through the SNc, but not contacting the VTA slightly more caudally (Bregma -5.5). Scale bar, 500 μm. (**C**) CeA^{CRF} fibers were present at the most caudal aspects of the VTA and SNc (Bregma -6.1). Scale bar, 500 μm. (**D**) CeA^{CRF} fibers course through the most dorsolateral region of the SNc. Scale bar, 100 μm. (**E**) Low density collaterals were present in the rostral VTA surrounding dopamine neurons. Scale bar, 100 μm. Green = tyrosine hydroxylase.

Projections from CeA^{CRF} neurons within the CeA

Since the CeL sends dense projections to the CeM (Petrovich and Swanson, 1997), we investigated whether CeA^{CRF} neurons situated in the CeL contribute to these projections. Surprisingly, following microinjection of AAV-hSyn-DIO-mCherry into the CeA, we detected very few mCherry-expressing projections from the CeL to the adjacent CeM (Figure 1.1C and Figure 1.6A). We next used AAV-Ef1α-DIO-ChR2-eYFP to express ChR2-eYFP in CeA^{CRF} neurons (Figure 1.6B) and to detect light-evoked inhibitory postsynaptic currents (IPSCs) in CeA neurons that did not express ChR2-eYFP. To compare data across animals and brain slices, we mapped the spatial position of each recorded neuron to a common reference frame. First, we established a scale using the intermediate capsule between the BLA and CeA as a guide. We defined the distance between where the intermediate capsule meets the external capsule and the ventral border of the BLA as equal to 100 relative units (Figure 1.6A). We then mapped the position of each cell onto a common Cartesian coordinate system with the Y axis parallel to the intermediate capsule and the origin at the most ventral part of the ovoid cluster of CeA^{CRF} cell bodies (Figure 1.6A and 1.6E). The position of each neuron was expressed as relative units along both axes. To assess the accuracy of this method, we mapped the position and size of the CRF cell body cluster in slices from 12 rats. We found that the coordinates of points defined by the intersection of the oval border of the CeA^{CRF} cell body cluster with its maximal dorsal-ventral and medial-lateral diameters were consistent across slices (Figure 1.6E). The borders of the CeA^{CRF} cell body cluster were also consistent when expressed in relative units using the bottom of the intermediate capsule as the origin for the coordinate system (bottom X: 22.9 ± 2.2, Y: 19.7 ± 1.8; top X: 27.0 ± 2.0, Y: 55.0 ± 1.8; medial edge X: 35.5 ± 2.1, Y: 44.0 ± 1.5; lateral edge X: 13.7 ± 1.4, Y: 41.3 ± 1.3).

Stimulation of ChR2 evoked IPSCs in 8 of 18 (44.4%) non-CRF CeL neurons. In contrast only 8 of 71 (11.3 %) of CeM neurons demonstrated an IPSC, concurring with our histological findings of sparse mCherry fluorescence and eYFP immunoreactivity of fibers within the CeM (Figures 1.1C and 1.6A). Picrotoxin (100 μM) blocked light-evoked IPSCs more than 97.7 ± 0.9% ($n = 4$; Figure 1.6C), as well as blocking spontaneous IPSCs (Figure 1.6D), which is consistent with previous studies demonstrating that CeA^{CRF} neurons are GABAergic (Cassell et al., 1999; Day et al., 1999; Veinante and Freund-Mercier, 1998). The CeM neurons exhibiting light-evoked IPSCs were scattered rather than clustered in a subregion of the CeM (Figure 1.6E). The IPSC amplitudes were not different between CeM and CeL neurons at 2 versus 1 mW of LED illumination (Figure 1.6F), indicative of a weak input-output relationship for ChR2 as described (Stuber et al., 2011). Together, these results suggest that CeA^{CRF} neurons target a small subset of CeM neurons. Nearly all CeM neurons showed spontaneous ISPCs that were greatly inhibited by picrotoxin (Figure 1.6D), demonstrating that most CeM neurons can respond to synaptically released GABA. Many cells also exhibited electrically evoked IPSCs, with kinetics similar to those seen for spontaneous IPSCs and ChR2-evoked IPSCs (Table 1.1) and previously reported for CeA IPSCs (Delaney and Sah, 2001; Naylor et al., 2010). Thus, our optogenetic results indicate that CeA^{CRF} neurons send GABAergic projections to almost half of their neighboring non-CRF neurons in the CeL, but only to a small number of neurons in the CeM.

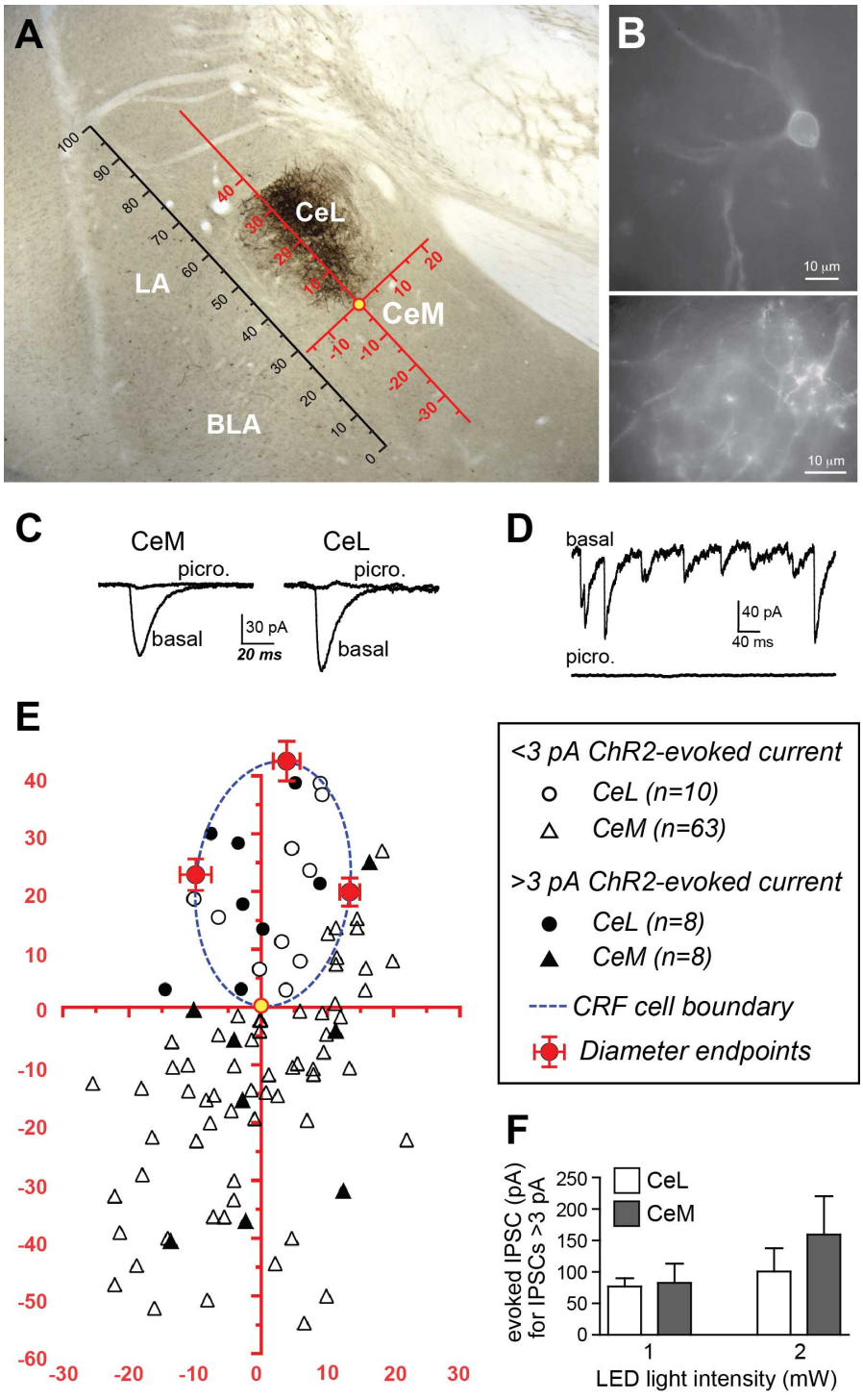

Figure 1.6. ChR2 stimulation of CeA^{CRF} terminals evokes IPSCs in a subset of CeA neurons

(**A**) Coronal section through the CeA with superimposed reference frame to identify the location of recorded neurons across slices. (**B**) Example of live CeL neurons (Scale bar, 10 μm) and fibers (Scale bar, 10 μm) expressing ChR2-eYFP. **C,** Examples of IPSCs evoked after stimulation of ChR2 in CeA^{CRF} neurons, which were blocked by picrotoxin. (**D**) Picrotoxin also blocked spontaneous IPSCs. (**E**) Diagram showing distribution of recorded cells relative to the cluster of CRF cell bodies and dendrites in the CeL (dotted blue circle). Filled symbols represent neurons with IPSC responses; open symbols are neurons without evoked IPSC responses. One CeL neuron with an IPSC response was found outside the cluster of CRF cell bodies and dendrites but within the confines of the CeL. (**F**) Similar magnitude of evoked IPSCs in CeL and CeM neurons and at two different LED intensities. BLA = basolateral amygdala, CeL = lateral central amygdala, CeM = medial central amygdala, LA = lateral amygdala.

	ChR2-evoked IPSC	Spontaneous IPSC	Electrically-evoked IPSC
Rise tau (msec)	0.79 ± 0.06	0.89 ± 0.06	0.97 ± 0.13
Decay tau (msec)	8.39 ± 1.25	10.01 ± 0.98	10.79 ± 1.34
Half-width (msec)	9.22 ± 0.60	9.77 ± 0.84	11.31 ± 1.16
Peak amplitude (pA)	159.6 ± 65.0	78.3 ± 11.3	196.1 ± 39.0
Area under the curve	1787 ± 425	885 ± 136	2433 ± 514

Table 1.1. IPSC kinetics for spontaneous and evoked IPSCs in CeM neurons

The kinetic values for each IPSC event in a given cell were determined and then all events for that cell were averaged. No significant differences were observed between the three classes of IPSCs for any measure (one-way ANOVA). Data shown are from 8 CeM cells with ChR2-evoked currents and 10 additional cells with electrically evoked IPSCs <200 pA (peak amplitude approximately matching those of ChR2-evoked currents, since larger IPSCs exhibit longer half-widths), with spontaneous IPSCs determined from IPSC events in the same traces except at the time of evoked IPSCs (at 111 msec into the 1 sec sweep).

Chemogenetic activation of CeA^{CRF} neurons induces CRF1 receptor-dependent c-Fos expression in the CeA

Since the *Fos* promoter is rapidly induced in strongly activated neurons, *Fos* mRNA and Fos protein are commonly used as surrogate markers of recent neuronal activation (Kaczmarek and Chaudhuri, 1997). To identify patterns of activation downstream of CeA^{CRF} neurons, we examined Fos immunoreactivity following activation of Designer Receptors Exclusively Activated by Designer Drugs (DREADDs) expressed in CeA^{CRF} neurons. Systemic administration of clozapine-N-oxide (CNO; 2 mg/kg, *i.p.*) induced Fos expression (Figure 1.7A and 1.7B) in CeA^{CRF} neurons expressing hM3Dq-mCherry, but not in CeA^{CRF} neurons expressing hM4Di-mCherry or mCherry alone [$F(2,10) = 351$, $P < 0.0001$]. These results suggest that CeA^{CRF} neurons are relatively inactive at baseline. We also found substantial induction of Fos in non-CRF neurons (Figure 1.7C and 1.7D) throughout the CeL [$F(2,10) = 27$, $P < 0.0001$] and in some cells of the CeM [$F(2,10) = 43$, $P < 0.0001$]. In the CeL, the proportion that expressed Fos was less than the proportion that exhibited IPSCs after ChR2 stimulation, while in the CeM these proportions were similar (compare Figures 1.7F and 1.6E).

Since CeA^{CRF} neurons are GABAergic, we were surprised to find that DREADD stimulation excited subpopulations of CeA neurons. We hypothesized that CRF released onto local CRF1 receptors was responsible, since CRF1 receptors are expressed in the CeA (Van Pett et al., 2000), and in the mouse CeA CRF1 receptor activation enhances spontaneous glutamate release (Silberman and Winder, 2013). To test this hypothesis, we treated rats with 10 mg/kg of the selective CRF1 receptor antagonist R121919 (Chen et al., 2004) prior to activation of hM3Dq. This treatment reduced Fos expression in non-CRF neurons in both CeL and CeM [$F_{drug}(1,14) = 40.13$, $P < 0.0001$] (Figure 1.7E and 1.7F). Importantly, the proportion of hM3Dq-mCherry positive CRF neurons expressing Fos was

similar between R121919 and vehicle-treated groups, indicating that the hM3Dq-driven activity of CeA^{CRF} neurons was not impaired by CRF1 receptor blockade [$t(7) = 0.282$, $P = 0.786$, unpaired t-test, Figure 1.7H]. These results demonstrate that stimulation of CeA^{CRF} neurons with hM3Dq excites a subpopulation of non-CRF neurons in the CeL and CeM in a CRF1 receptor-dependent manner, presumably through local release of CRF.

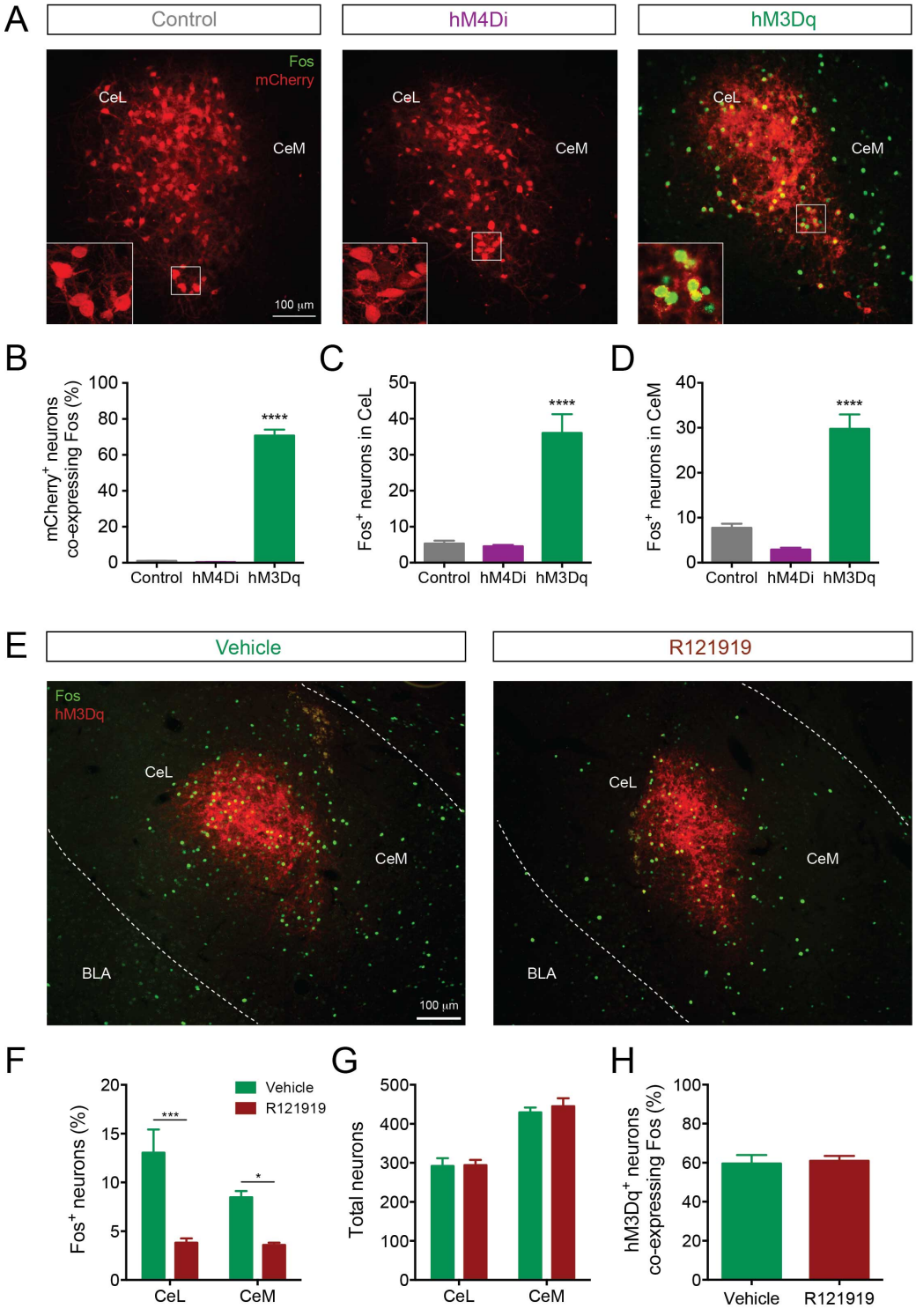

Figure 1.7. CeA^{CRF} neurons activate non-CRF neurons in the CeL and CeM

(A) Representative overlay images of Fos immunoreactivity and mCherry fluorescence in control, hM4Di, and hM3Dq-expressing CeL neurons. Scale bar, 100 μm. Insets show high-magnification examples of mCherry expressing neurons immunostained for Fos. **(B)** Percentage of $mCherry^+$ neurons co-expressing Fos following administration of CNO. **(C-D)** Fos induction in non-CRF neurons of the CeL **(C)** and the CeM **(D)** after administration of CNO. $^{****}P < 0.001$ compared with Control or hM4Di, n = 4-5 rats, 10 sections/rat, Tukey's multiple comparisons test. **(E)** Representative overlay images of Fos immunoreactivity and native mCherry fluorescence in hM3Dq-expressing cells from vehicle- or R121919-treated rats. Scale bar, 100 μm. **(F)** Percentage of Fos^+ neurons in the CeL and CeM after administration of R121919. **(G)** Total neuron counts per amygdala section are equivalent between groups. **(H)** Percentage of hM3Dq neurons expressing Fos after administration of CNO is equivalent between groups. $^{***}P < 0.001$, $^{*}P < 0.05$, n = 4-5 rats, 10-12 sections/rat, Tukey's multiple comparisons test.

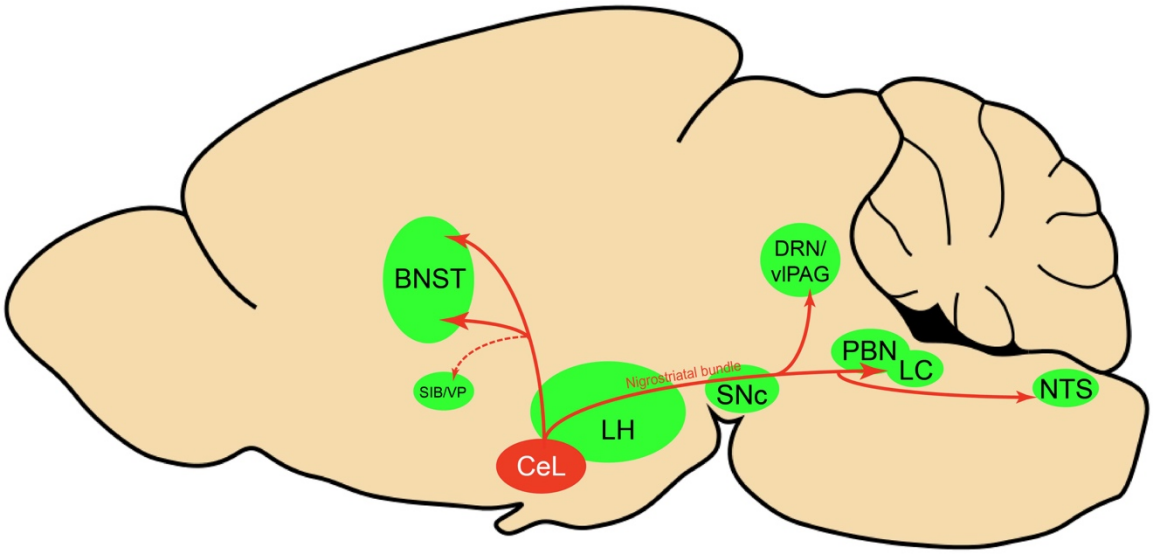

Figure 1.8. Sagittal rat brain schematic of CeA^{CRF} neuron projections

BNST = bed nucleus of the stria terminalis, CeL = lateral central amygdala, DRN = dorsal raphe nuclei, LC = locus coeruleus, LH = lateral hypothalamus, NTS = nucleus tractus solitarius, PBN = parabrachial nucleus, SIB = Substantia innominata, SNc = substantia nigra pars compacta, vlPAG = ventrolateral periaqueductal gray, VP = ventral pallidum.

DISCUSSION

Until recently our knowledge about the anatomy of CRF systems has rested on traditional neuroanatomical methods and inferences about CRF function through administration of drugs that act at CRF receptors. To gain more direct access to CRF neurons to study their functional neuroanatomy we generated a novel BAC transgenic *Crh*-Cre rat. Using Cre-dependent reporters we found Cre recombinase expression in neurons of the lateral CeA and the dorsolateral BNST. There was strong concordance of Cre-dependent transgene expression and CRF immunoreactivity in the CeL, indicating lack of ectopic expression of Cre recombinase in this area. CeA^{CRF} projections were similar to targets of CRF cells identified in previous neuroanatomical studies. However, little is known about their local projections within the CeA, and we found that CeA^{CRF} neurons projected to other non-CRF CeL cells, and also to a smaller number of CeM neurons. These intra-CeA^{CRF} projections exhibited both inhibitory effects, indicated by evoked GABA currents, and excitatory effects, indicated by increased Fos expression, which were prevented by blocking CRF1 receptors. These findings indicate that CeA^{CRF} neurons are a mixed population of interneurons and projection neurons that encode both inhibitory and excitatory information.

Although we found CRF neurons in the CeL and dorsal BNST, CRF cells were absent from the ventral BNST, PVN, and other brainstem and forebrain regions where CRF neurons have been reported (Merchenthaler, 1984; Wang et al., 2011). Thus, despite the size of our BAC vector (~224 kb), Cre expression was limited to two major CRF cell populations, possibly due to incomplete capture of all regulatory elements in the integrated BAC transgene. Although we do not know the precise reason for restricted CRF expression in our animals, it is notable that CRF neurons of the dorsolateral BNST and the CeL share

several common features, including medium spiny neuron morphology (Cassell and Gray, 1989; Phelix and Paull, 1990; Sun and Cassell, 1993), expression of the phosphatase STEP (Dabrowska et al., 2013b), and production of GABA (Cassell et al., 1999; Dabrowska et al., 2013b; Day et al., 1999). In contrast, PVN CRF neurons produce glutamate (Dabrowska et al., 2013a) and ventral BNST CRF neurons may also be glutamatergic (Dabrowska et al., 2013a). The *Crh* gene also is regulated differently in these populations of neurons. For example, while corticosterone suppresses CRF expression in the PVN, it up-regulates expression in the CeA and dorsolateral BNST (Makino et al., 1994; Swanson and Simmons, 1989). This differential regulation could involve PKC signaling since we previously found that production of pro-CRF mRNA and protein in the CeA, but not in the PVN, is impaired in PKC epsilon knockout mice (Lesscher et al., 2008). Additionally, a recent study identified novel CRF expressing neurons in the VTA, but this expression was only detectable in animals undergoing nicotine withdrawal (Grieder et al., 2014). The detailed mechanisms responsible for heterogeneity in phenotypic characteristics and control of CRF expression among subpopulations of CRF neurons remain to be explored, but the present findings suggest our *Crh*-Cre rats may prove useful for selective study of one major subtype of CRF neurons.

Using viral delivery of Cre-dependent reporters to identify CeA^{CRF} neurons, we found robust CRF projections from CeA to the brainstem, terminating in the medial and lateral PBN and the LC. There were also extensive projections to the diencephalon, terminating in the dorsal and ventral BNST and the LH. This pattern of connectivity concurs with previously reported CeA^{CRF} projections in the rat (Moga and Gray, 1985; Reyes et al., 2011; Sakanaka et al., 1986; Van Bockstaele et al., 1998). We did not, however, observe projections to the pontine reticular nuclei, as reported in earlier

neuroanatomical tracing studies (Fendt et al., 1997; Gray and Magnuson, 1992). A previous study of neuropeptide afferents from the CeA found CRF neurons in the CeL that contained retrograde tracer after injections into the dorsal vagal complex (Gray and Magnuson, 1987). Our results refine this finding by demonstrating that CeA^{CRF} fibers specifically innervate the NTS. Since the NTS provides noradrenergic input to the extended amygdala that plays a role in drug withdrawal and anxiety (Smith and Aston-Jones, 2008), it will be interesting to determine whether a reciprocal connection between CeA^{CRF} neurons and the NTS exists, and whether this circuit is recruited during withdrawal states.

Within the CeA, despite extensive CeL innervation of the CeM (Petrovich and Swanson, 1997), we surprisingly found few CeA^{CRF} projections to the CeM. Instead, we found that CeA^{CRF} neurons preferentially innervate other CeL neurons. Given the sparseness of projections to CeM, we speculate that CeA^{CRF} projection neurons act in parallel with CeM projection neurons to regulate behavior, and that the small number of direct CeA^{CRF} projections to the CeM, and potentially more extensive indirect projections *via* non-CRF neurons in the CeL, coordinate the actions of CeL and CeM systems on behavior. Interesting questions for the future are whether individual CeA^{CRF} neurons project to many or a restricted set of targets and whether the same or different CeA^{CRF} neurons serve as interneurons and projection neurons. Future studies using *Crh*-Cre rats and Cre-dependent tracing tools and actuators should allow us to unravel this circuitry in greater detail.

Despite CeA^{CRF} neurons being GABAergic, activation of the excitatory DREADD hM3Dq in these neurons induced expression of Fos in several non-CRF neurons of the CeL and CeM. Thus, CeA^{CRF} neurons can generate both excitatory (Fos) and inhibitory (GABA IPSCs) responses in CeL and CeM neurons. Fos induction following activation of CeA^{CRF}

neurons involved CRF release since it was substantially reduced by administration of a CRF1 receptor antagonist. Depending on the synapse, activation of CRF1 receptors can activate neurons by enhancing glutamatergic transmission. For example, in the rat lateral capsular CeA, CRF acting at CRF1 receptors enhances glutamatergic transmission from parabrachial efferents (Ji et al., 2013), and CRF increases the frequency of spontaneous EPSCs in the mouse CeL through actions at CRF1 and CRF2 receptors (Silberman and Winder, 2013). The actions of CRF on excitatory neurotransmission in the rat CeL have yet to be determined.

Given our limited knowledge of intra-CeA circuitry, we can envision several mechanisms by which activating CeA^{CRF} neurons could generate both inhibitory and excitatory responses. First, GABA and CRF may affect different target neurons, with GABA released at synapses and CRF released non-synaptically to signal via local volume transmission that results in excitation of CeA neurons through convergent disinhibition and CRF signaling. A somewhat similar situation has been recently described for innervation of the cerebral cortex and striatum by histaminergic neurons of the hypothalamus that also release GABA (Yu et al., 2015). Alternatively, excitatory effects of CRF may be partly suppressed by concurrent GABA release, for example where CRF acting at CRF1 receptors enhances GABA release, as has been demonstrated in the rat CeM (Herman et al., 2013). On the other hand, in cells having a depolarized Cl^- reversal potential, activation of $GABA_A$ receptors could synergize with CRF to directly activate postsynaptic neurons (Staley and Proctor, 1999), although this may be more speculative for adult neurons. Finally, stimulus intensity and duration may affect GABA and CRF release differently, leading to a range of inhibitory and excitatory responses on the same target neuron population. Future optogenetic and chemogenetic studies using *Crh*-Cre rats could help to determine if the

actions of GABA and CRF occur at the same or at different neurons and to elucidate mechanisms by which these transmitters act.

The generation of several *Crh*-Cre mouse lines has facilitated our understanding of CRF circuits and their roles in several behavioral states. At least three *Crh*-Cre mouse lines have been reported, and have been used to demonstrate roles for CRF neurons in fear conditioning (Gafford et al., 2014), fear extinction (Gafford et al., 2012), anxiety and avoidance behaviors (Gafford et al., 2012; McCall et al., 2015), and binge-like alcohol consumption (Pleil et al., 2015). However, a recent review (Chen et al., 2015) indicates that two of these lines, the *Crh*-BAC transgenic (Alon et al., 2009) and CRFp3.0Cre (Martin et al., 2010) exhibit ectopic Cre transgene expression, whereas *Crh*-IRES-Cre mice (Taniguchi et al., 2011) express Cre with high fidelity to endogenous CRF across the brain. Since our current rat line is a BAC transgenic, our determination of Cre and CRF fidelity in the amygdala (Figure 1.1) was critically important. Although our rat shows limited expression of Cre, it provides a tool to study the role of GABAergic CRF neurons of the amygdala and dorsolateral BNST to not only complement work done with *Crh*-Cre mice, but to permit investigation of more complex behaviors such as operant conditioning and sophisticated learning tasks that cannot easily be studied using mice.

The anatomy of projections from CeL to CeM has been examined recently in mouse models of fear conditioning (Ciocchi et al., 2010; Haubensak et al., 2010; Li et al., 2013), although without a focus on CeA^{CRF} neurons or employing *Crh*-Cre mice. An anatomical framework has emerged in which fear-related cues excite BLA neurons, which in turn enhance firing in a CeL cell subpopulation termed 'On-cells' that inhibit a separate CeL subpopulation termed 'Off-cells', the net result of which is to disinhibit CeM neurons. The subsequent increase in CeM activity mediates conditioned fear *via* projections downstream

to somatic and autonomic brainstem nuclei. In mice the PKCδ neuron subpopulation in the CeL represents 'Off-cells' (Haubensak et al., 2010), which tonically suppress CeM neurons to inhibit fear responses. 'On-cells' in mice are at least partially SOM^+ (Li et al., 2013). In contrast, the role of CeA^{CRF} neurons in this fear control circuit has been largely overlooked. Here we provide evidence consistent with rat CRF neurons being mostly a subpopulation of 'On-cells' based on co-expression of SOM in about 40% of CRF neurons and sparse projections to the CeM. Future challenges will be to dissect the relative contribution of CeA^{CRF} neurons (SOM^+ and SOM^-) to fear-related circuitry and behavior, and to determine whether CRF neurons with unique neuropeptide co-expression profiles provide distinct inputs to local and distant projection targets.

In summary, we present a novel transgenic Cre driver rat line that permits selective targeting of CRF-expressing GABAergic neurons of the extended amygdala. The *Crh*-Cre rat will be an important tool for dissecting extended amygdala CRF systems in the control of fear and anxiety, as well as stress-sensitive behaviors, such as feeding and drug seeking. Furthermore, species-specific phenotypic differences can be evaluated by comparing *Crh*-Cre rats with *Crh*-Cre mice, which should help unify conclusions about CRF circuits across rodent species.

ACKNOWLEDGMENTS

The W-Tg(CAG-DsRed2/GFP) 15Jms rat line was provided by NBRP-Rat with support in part by the National BioResource Project of MEXT, Japan. We acknowledge Wanda Filipiak and the Transgenic Animal Model Core of the University of Michigan's Biomedical Research Core Facilities for the preparation of transgenic rats.

CHAPTER 2: CENTRAL AMYGDALA CRF NEURONS REGULATE FEAR AND ANXIETY BEHAVIORS

ABSTRACT

The central amygdala (CeA) and the stress-related neuropeptide CRF have well-established roles in fear and anxiety. The CeA contains a large population of CRF neurons, yet the role of these neurons in fear and anxiety has only recently begun to be addressed using mouse models. We directly investigated the contribution of CeA CRF (CeA^{CRF}) neurons to fear and anxiety-like behaviors using *Crh*-Cre rats and chemogenetic tools. We find that acute immobilization stress produces an anxiety-like state which is prevented by chemogenetic inhibition or genetic ablation of CeA^{CRF} neurons. In a non-stressed state, inhibition of these cells did not alter anxiety behavior but excitation generated an anxiety state similar to stress that was normalized by administration of the CRF1 receptor antagonist R121919. Chemogenetic silencing of CeA^{CRF} neurons during fear conditioning did not affect shock-induced freezing but disrupted contextual and cued freezing during retrieval testing. Silencing immediately after conditioning or prior to fear expression trials had no effect, demonstrating that CeA^{CRF} neurons contribute selectively to fear learning. Finally, excitation of CeA^{CRF} neurons prevented fear extinction, an effect that was also dependent on CRF1 receptor signaling. These findings indicate that CeA^{CRF} neurons contribute to both fear and anxiety behaviors, most likely through the release of CRF acting at CRF1 receptors.

INTRODUCTION

Fear and anxiety are evolutionarily conserved emotional and behavioral states. When faced with a threat, animals experience fear and anxiety to help ensure survival in dangerous environments. Fear responses are transient and occur when an animal is in close proximity to a threat or a discrete cue stimulus that predicts danger. Anxiety responses are characterized by more persistent states of apprehension in ambiguous environments when the threat of danger is uncertain or uneasily detectable. The differences in fear and anxiety phenotypes has led to the hypothesis that the underlying neurobiology is also different. However, recent studies have challenged this notion by demonstrating overlapping roles of brain structures that mediate behaviors associated with these two emotional states.

Early lesion and pharmacological inactivation studies quickly suggested the central amygdala (CeA) as a structure critical to the induction and expression of fear behaviors, but not those associated with anxiety (Davis et al., 2010; Walker and Davis, 1997b, 2008; Walker et al., 2003). In contrast, lesion studies proposed the bed nucleus of the stria terminalis (BNST) as the anatomical substrate for persistent anxiety states, but not those characteristic of phasic fear (Davis et al., 2010; Walker and Davis, 2008; Walker et al., 2009b; Walker et al., 2003). Thus, an anatomical framework was developed that segregated the neurobiology of fear and anxiety. However, the ability to target discrete populations of neurons with genetic tools has led to new data that opposes this framework. Manipulation of different CeA neuron populations can affect both fear and anxiety-like behaviors in mice (Ahrens et al., 2018; Botta et al., 2015; McCall et al., 2015; Pliota et al., 2018; Regev et al., 2012; Sanford et al., 2017). Hence, the CeA, depending on the specific neurons within, can contribute to both fear and anxiety.

Along these same lines, it was discovered that the stress-responsive neuropeptide CRF is anxiogenic when delivered into the brain (Lee and Davis, 1997; Liang et al., 1992b; Swerdlow et al., 1986) and is a potent modulator of fear learning (Gafford et al., 2012; Pitts et al., 2009; Sanford et al., 2017). The CeA contains a large population of CRF neurons (Pomrenze et al., 2015, Chapter 1), and thus it is possible that this population controls both fear and anxiety behaviors. In mice, these neurons are essential to fear learning and passive coping behaviors in unfamiliar environments (Pliota et al., 2018; Sanford et al., 2017), and are important for stress-induced anxiety (Regev et al., 2012). However, it is not known whether CeA^{CRF} neurons control fear and anxiety behaviors in rats. This represents an important step forward since essentially all early lesion and inactivation studies demonstrating the anatomical segregation of fear and anxiety were performed in rats.

In this study, we utilized *Crh*-Cre rats to gain genetic access to the CeA^{CRF} neuron population and test its causal contributions to fear and anxiety. We find that inhibition of CeA^{CRF} neurons with Cre-dependent viral-genetic tools prevents anxiety produced by stress and that stimulation generates an anxiety state that is dependent on CRF1 receptor activation. Inhibition of these cells prevents fear learning, but not fear expression, and stimulation blocks the development of fear extinction that is also dependent on CRF1 receptors. Together these data demonstrate that the rat CeA does indeed contribute to both fear and anxiety-like behavioral states, and these effects can at least in part be attributed to the local CRF neuron population.

MATERIALS AND METHODS

Subjects

All experiments and procedures were approved by the University of Texas at Austin Institutional Animal Care and Use Committee and were performed in accordance with the guidelines described in the US National Institutes of Health Guide for the Care and Use of Laboratory Animals. We used male heterozygous *Crh*-Cre rats (Pomrenze et al., 2015) outcrossed to wild-type Wistar rats (Envigo, Houston, TX), aged 5-6 weeks at the start of the surgical procedures and 10-14 weeks at the start of experimental procedures. Rats were group housed and maintained on a 12-h light:dark cycle (lights on 4AM to 4PM) with food and water available ad libitum. Rats prepared with guide cannulas were singly housed. All experiments were done between 9AM and 3PM. Rats were randomly assigned to either experimental or control groups within each litter.

Drugs and viral vectors

Clozapine-N-oxide (CNO) was supplied through the NIMH Chemical Synthesis and Drug Supply Program. CNO (2 mg/kg body weight) was dissolved in 5% dimethyl sulfoxide (DMSO) and then diluted to 2 mg/mL with 0.9% saline. The selective CRF1 receptor antagonist R121919 (3-[6-(dimethylamino)-4-methyl-pyrid-3-yl]-2,5-dimethyl-N,N-dipropyl-pyrazolo[2,3-a]pyrimidin-7-amine, NBI 30775, was a gift from Dr. Kenner Rice (Chemical Biology Research Branch, Drug Design and Synthesis Section, National Institute on Drug Abuse and National Institute on Alcohol Abuse and Alcoholism, Rockville, MD) and dissolved in a 1:1 solution of 0.9% saline and 1N HCl before adding 25% hydroxypropyl-β-cyclodextrin (HBC) to yield a final concentration of 10mg/mL

R121919 in 20% HBC, pH 4.5. All systemic injections were administered at 1 mL/kg, except for R121919 which was administered at 2 mL/kg.

Cre-dependent adeno-associated viral vectors AAV8-hSyn-DIO-hM3Dq-mCherry, AAV8-hSyn-DIO-hM4Di-mCherry, AAV8-hSyn-DIO-mCherry, AAV5-EF1α-DIO-eYFP, and AAV2-Ef1α-flex-taCaspase3-TEVp were obtained from the University of North Carolina Viral Vector Core and were injected at 4-6 × 10^{12} infectious units per mL.

Stereotaxic surgery

At the start of surgical procedures, rats were anesthetized with isoflurane (5% v/v) and placed in a stereotaxic frame (David Kopf Instruments, Tujunga, CA, USA). Viruses were injected into the CeA (AP: -2.1; ML: ± 4.5; DV: -8.0 from skull) or dlBNST (AP: -0.0; ML: ± 3.5; DV: -6.8 from skull, 16° angle) at a rate of 150nL min^{-1} over 5 min (750-800nL total volume per hemisphere) with a custom 32-gauge injector cannula coupled to a pump-mounted 2μL Hamilton syringe. Injectors were slowly retracted after a 5 min diffusion period. Rats were 190-220 g at the time of viral injection. Virus-injected rats were group housed to recovery for 1-2 months before behavioral or histological examination.

Immobilization stress (IMS)

Rats were transferred to an experimental room distinct from the behavioral testing room and placed in ventilated plastic Decapicone bags (Braintree Scientific, Braintree, MA, USA) for 30 min. Each rat was monitored every 5 min to ensure sufficient immobilization and respiration rate. Rats were tested for anxiety-like behavior 10 min later. Some rats received injections of the CRF1 receptor antagonist R121919 (20mg/kg, *s.c.*) 60 min prior to stress. Separate groups of rats received CNO (2mg/kg, *i.p.*) 60 min prior to stress.

Behavior

Anxiety

We used three assays to evaluate anxiety-like behavior: the elevated plus maze (EPM), the open field test (OF) and the social interaction test. Anxiety testing occurred in a room that was different than the one used to immobilize and administer drugs. The elevated plus maze consisted of two open arms (50 x 10 cm) and two enclosed arms (50 x 10 x 40 cm) connected by a central area measuring 10 x 10 cm, 50 cm above the floor. At the beginning of each trial, rats were placed in the center facing one open arm. Trials lasted for 6 min and were performed under red lighting to promote exploration. The open field consisted of an open topped arena (100 x 100 x 50 cm) situated on the floor. The center area was designated as a central zone measuring 55 x 55 cm. Rats were placed into a corner of the arena at the beginning of each trial. Each test lasted for 10 min and was performed under red lighting to promote exploration of the center. Social interaction was measured by placing a novel juvenile rat (4-5 weeks) into a 70 x 70 cm arena and then placing an experimental adult rat into the arena. The adult rat was allowed to interact with the juvenile rat for 5 min under red lighting. Exploratory behaviors such as allogrooming, sniffing, and pinning initiated by the adult rat were considered interactions (Christianson et al., 2010). All testing equipment was cleaned with 70% ethanol between trials. Behaviors were tracked with EthoVision (Noldus Information Technology, Leesburg, VA, USA).

Fear conditioning

Rats were subjected to a typical fear conditioning protocol with 3 CS-US (tone-shock) pairings (75 dB, 5 kHz, 20 s tones co-terminating with 0.7 mA, 500 ms shocks, variable ITI (average 180 s)) for delay conditioning (Monfils et al., 2009; Schafe et al., 1999).

Twenty-four hrs later rats were tested for contextual fear retrieval by being placed back into the original context for 5 min. Twenty-four hrs later rats were tested for cued fear retrieval in a distinct context with the presentation of 4 CS tones. The distinct context consisted of pinstripe and checkered walls, smooth tactile floors, and the presence of 1% acetic acid. For fear extinction testing, rats were fear conditioned and then subjected to 18 tone cues within the same trial on the same variable ITI schedule for mass extinction. In this experiment, rats were injected with CNO (2 mg/kg, *i.p.*) 1 hr prior to extinction trials. Other groups of rats (expressing hM3Dq) were administered R121919 (20 mg/kg, *s.c.*) 30 min prior to a CNO injection.

Chemogenetic manipulations

Crh-Cre rats were microinjected bilaterally in the CeA with AAV8-hSyn-DIO-hM3Dq-mCherry, AAV8-hSyn-DIO-hM4Di-mCherry, or AAV8-hSyn-DIO-mCherry. After 4-6 weeks of recovery, rats were injected with CNO (2 mg/kg, *i.p.*) and subjected to immobilization stress or behavioral tests 60 min later. Rats tested for fear learning were administered the same dose of CNO and fear conditioned 60 min later. Separate rats were fear conditioned and then administered the same dose of CNO either immediately after conditioning or 60 min prior to fear expression tests. Finally, rats tested during fear extinction were administered the same dose of CNO 60 min prior to extinction training.

Brain slice electrophysiology

Rats were injected with AAV-hSyn-DIO-hM4Di-mCherry or AAV-hSyn-DIO-hM3Dq-mCherry into the CeA. After 2-3 months, rats were anesthetized with pentobarbital (100 mg/kg, *i.p.*) and decapitated, and brain slices containing the CeA were cut in an ice-cold

glycerol-based solution (in mM: 252 glycerol, 2.5 KCl, 1.25 NaH_2PO_4, 1 $MgCl_2$, 2 $CaCl_2$, 25 $NaHCO_3$, 1 L-ascorbate, and 11 glucose, bubbled with carbogen). Slices recovered at 32°C in carbogen-bubbled aCSF (containing, in mM: 126 NaCl, 2.5 KCl, 1.2 NaH_2PO_4, 1.2 $MgCl_2$, 2.4 $CaCl_2$, 18 $NaHCO_3$, 11 glucose, pH 7.2–7.4, mOsm 302–305) for at least 30 min before experiments, with 1mM ascorbic acid added just before the first slice. During experiments, slices were submerged and perfused (2 mL/min) with aCSF at 31–32°C. CNO-related changes in firing or membrane potential were recorded in current-clamp mode using Clampex 10.1 and an Axon Multiclamp 700A patch amplifier (Molecular Devices, Sunnyvale, CA). All experiments used whole-cell recording with infrared-DIC visualization and 2.5–3.5 MΩ electrodes that were filled with a potassium-methanesulfonate-based internal solution (in mM: 130 KOH, 105 methanesulfonic acid, 17 HCl, 20 HEPES, 0.2 EGTA, 2.8 NaCl, 2.5 mg/ml Mg-ATP, 0.25 mg/ml GTP, pH 7.2–7.4, 278–287 mOsm).

Corticosterone measurement

Rats were microinjected with AAV8-hSyn-DIO-hM4Di-mCherry into the CeA. After recovery rats were injected with CNO (2 mg/kg, *i.p.*) or vehicle and 60 min later immobilized for 30 min. Rats were then immediately euthanized for trunk blood collection. Blood corticosterone concentrations were measured using an enzyme immunoassay kit (900-097, Enzo Life Sciences).

Histology

All rats were checked for virus expression and implanted cannula locations after behavioral studies were completed. For immunofluorescence, rats were anesthetized with isoflurane

and perfused transcardially with 1X PBS followed by 4% paraformaldehyde in PBS, pH 7.4. Brains were extracted, allowed to postfix overnight in the same fixative and cryoprotected in 30% sucrose in PBS at 4º C. Each brain was sectioned at 40 μm on a cryostat (Thermo Scientific) and collected in PBS. Staining for injected viruses was omitted due to strong native fluorescence.

For immunohistochemistry, free-floating sections were washed three times in PBS with 0.2% Triton X-100 (PBST) for 10 min at room temperature. Sections were then incubated in blocking solution made of PBST with 3% normal donkey serum (Jackson ImmunoResearch, number 017-000-121) for 1 hr. Sections were next incubated in primary antibodies goat anti-CRF (1:1000, Santa Cruz Biotechnology, sc1761, Lot #B0315) in blocking solution rotating at 4º C for 18-20 h. After three 10 min washes in PBST, sections were incubated in species-specific secondary antibodies Alexa Fluor 488, 594, or 647 (1:700, Life Technologies, A-21206, A-11055, A-21208, A11073, A-21447, A-31573) in blocking solution for 1 hr at room temperature. Finally, sections were washed three times for 10 min in 1X PBS. Sections were then mounted in 0.2% gelatin water onto SuperFrost Plus glass slides (Fisherbrand, 12-550-15), coverslipped with Fluoromount-G with DAPI (Southern Biotech, 0100-20), and stored in the dark. Fluorescent images were collected on a Zeiss 710 LSM confocal microscope or a Zeiss Axio Zoom stereo microscope. Quantification of fluorescence was performed on 3-6 sections per rat from 5 rats spanning the rostral-caudal axis of the CeA (from approximately Bregma -1.90 to -3.00) using the cell-counter plugin in Fiji (Schindelin et al., 2012).

Statistical analyses

We calculated sample sizes of n = 8-12 animals per condition using SD values measured in pilot studies of IMS-induced anxiety-like behavior, $\alpha = 0.05$, and power = 0.80, with the goal of detecting a 25-35% difference in mean values for treated and control samples, using the program G*Power (Faul et al., 2007). Studies were performed with the experimenter blind to the identity of the drugs that were administered. All results were expressed as mean ± S.E.M. values and analyzed using Prism (GraphPad Software, San Diego, CA). Data distribution and variance were tested using Shapiro-Wilk normality tests. Normally distributed data were analyzed by unpaired, two-tailed t-tests, or one or two factor ANOVA with post-hoc Tukey's multiple comparisons tests. In one case, where only one direction of change was expected, we used a one-tailed t-test (Figure 2.2B, percentage of total distance in the center of the OF). Data that were not normally distributed were analyzed by Mann-Whitney U tests when comparing two conditions. Differences were considered significant when $P < 0.05$.

RESULTS

CeA^{CRF} neurons regulate anxiety-like behavior

To evoke anxiety, we subjected Wistar rats to 30 min of immobilization stress (IMS), which is a commonly used procedure that reliably increases anxiety-like behavior (Buynitsky and Mostofsky, 2009; Pare and Glavin, 1986) through a process mediated by CRF (Regev et al., 2012). We measured subsequent behavior in the elevated plus maze (EPM) and open field (OF), which are commonly used to assess anxiety-like behavior in rodents. IMS reduced the percentage of time spent on the open arms and percentage of open arm entries on the EPM without affecting closed arm entries (Figures 2.1A and 2.2A).

IMS also reduced the time spent in the center of the OF (Figure 2.1A). Although IMS also reduced the total distance traveled in the OF (Figure 2.2A), the percentage of total distance traveled in the center of the OF was significantly lower in stressed rats (Figure 2.2A). Consistent with a role for CRF in stress-induced anxiety, systemic administration of a selective CRF1 receptor antagonist, R121919 (Chen et al., 2004) (20 mg/kg, *s.c.*, administered 1 hr before IMS), prevented the IMS-induced reduction in percentages of open arm time and entries without affecting the number of closed arm entries on the EPM (Figures 2.1B and 2.2B). R121919 also prevented IMS-induced reductions in the time spent and distance traveled in the center of the OF without altering the total distance traveled (Figures 2.1B and 2.2B).

One central question is whether CRF neurons in the CeA (CeA^{CRF} neurons) mediate anxiety-like behavior in the rat like they do in the mouse (McCall et al., 2015; Pliota et al., 2018; Regev et al., 2012). To manipulate neuronal activity, we used BAC transgenic *Crh*-Cre Wistar rats, which express Cre recombinase in the CeA under control of the *Crh* promoter (Pomrenze et al., 2015). We bilaterally transduced CeA^{CRF} neurons with an AAV encoding a Cre-dependent inhibitory hM4Di designer receptor with an mCherry reporter (Sternson and Roth, 2014). In *Crh*-Cre rats, nearly all CeA neurons expressing Cre recombinase produce CRF (Pomrenze et al., 2015). In acute brain slices, cells expressing hM4Di displayed hyperpolarization when treated with the designer receptor agonist clozapine-N-oxide (CNO) (Figure 2.1D). CNO (2 mg/kg, *i.p.*, 1 hr before IMS) also reduced anxiety-like behavior in rats expressing hM4Di when compared with control animals expressing mCherry. CNO increased the percentage of open arm time and the percentage of open arm entries on the EPM without changing the number of closed arm entries (Figures 2.1E and 2.2C). CNO also increased the time spent and distance traveled

in the center of the OF without altering the total distance traveled (Figures 2.1E and 2.2C). In addition, CNO increased social interaction time in rats that expressed hM4Di compared with control rats that expressed mCherry (mCh) in CeA^{CRF} neurons (Figure 2.1E).

To further explore the role of CeA^{CRF} neurons in anxiety-like behavior, we used a different approach in which we genetically ablated neurons with a Cre-dependent Caspase3 (Yang et al., 2013) instead of inhibiting them with hM4Di. Bilateral Caspase3-mediated ablation of CeA^{CRF} neurons increased the percentage of open arm time and the percentage of open arm entries in the EPM without affecting the number of closed arm entries (Figure 2.3A). Caspase3-mediated ablation also increased the time spent and the percentage of total distance traveled in the center of the OF without altering the total distance traveled (Figure 2.3B). These results indicate that genetic ablation of CeA^{CRF} neurons, like DREADD inhibition, reduces IMS-induced anxiety-like behavior.

The CeA regulates hypothalamic-pituitary-adrenal (HPA) axis activity *via* its projections to the brainstem (Schwaber et al., 1982; van der Kooy et al., 1984). To determine whether CeA^{CRF} neurons affect stress-induced activation of the HPA axis, we examined circulating corticosterone levels. Inhibiting hM4Di-expressing CeA^{CRF} neurons with CNO did not affect circulating corticosterone levels in stressed rats [Veh: 766.9 ± 46.9 ng/mL, CNO: 849.5 ± 84.4 ng/mL: $t(7) = 0.9061$, $P = 0.395$, $n = 5$ Control, 4 CNO, unpaired t-test, data not shown). This result indicates that CeA^{CRF} neurons mediated stress-induced anxiety-like behavior independent of the HPA axis.

Since activity of CeA^{CRF} neurons was required for stress-induced anxiety, we next investigated whether activating CeA^{CRF} neurons is sufficient to induce anxiety-like behavior, and whether inhibiting CeA^{CRF} neurons reduces baseline anxiety-like behavior in the absence of stress. We injected the CeA of *Crh*-Cre rats with AAVs encoding Cre-

dependent excitatory (hM3Dq) or inhibitory (hM4Di) designer receptors fused to an mCherry reporter, or an mCherry control (Figures 2.1C and 2.1F). CNO (2 mg/kg, *i.p.*) evoked anxiety-like behavior in rats expressing hM3Dq in CeA^{CRF} cells but had no effect in rats that expressed hM4Di or mCherry alone. In rats that expressed hM3Dq, CNO reduced the percentage of time spent on the open arms and the percentage of open arm entries on the EPM without affecting the number of closed arm entries (Figures 2.1F and 2.2D). Activation of hM3Dq with CNO reduced the time spent in the center of the open field and the number of entries into the center (Figures 2.1F and 2.2D). The total distance traveled in the OF was unaffected by hM3Dq activation [$F(2,23) = 0.4411$, $P = 0.6487$, one-way ANOVA, data not shown].

An important question is how CeA^{CRF} neurons promote anxiety. One parsimonious explanation is through the release of CRF. To evaluate whether CRF signaling is critical, we performed a similar anxiety experiment in which groups of rats were injected with Cre-dependent hM3Dq into the CeA but some received a systemic injection of the CRF1 receptor antagonist R121919 (20 mg/kg, *s.c.*) just prior to a CNO injection (2 mg/kg, *i.p.*). We observed that rats treated with CNO exhibited anxiety in both assays, but those pretreated with R121919 showed less anxiety in the EPM test but not in the OF test (Figure 2.4). Importantly, rats without hM3Dq stimulation of CeA^{CRF} neurons that were injected with R121919 showed minimal changes in baseline anxiety, aside from a modest increase in OF center entries, confirming the absence of CRF signaling effects on anxiety in a non-stressed state. These data suggest that CRF release promotes anxiety on the EPM but not in the OF.

These findings demonstrate that activation of CeA^{CRF} neurons was sufficient to increase anxiety-like behavior in non-stressed rats through activation of CRF1 receptors,

but inhibition of these neurons did not alter baseline anxiety-like behavior, suggesting that CeA^{CRF} neurons act specifically under conditions of stress. These findings also indicate that CNO induction of anxiety-like behavior in rats expressing hM3Dq was specific for activation of the hM3Dq DREADD and not due to an off-target effect of CNO or its metabolite clozapine (Gomez et al., 2017).

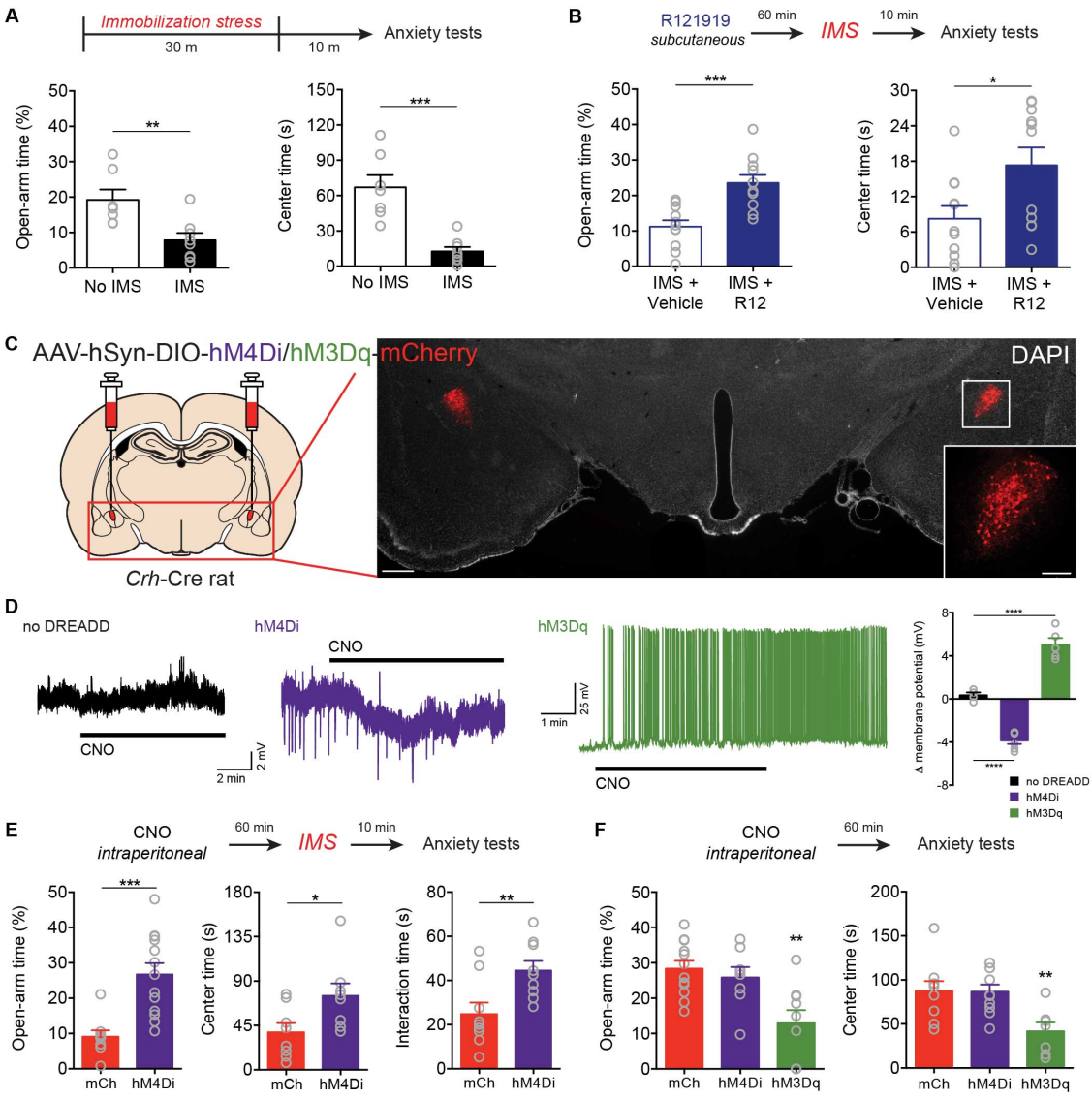

Figure 2.1. CeA^{CRF} neurons promote anxiety

(A) Top, protocol for immobilization stress (IMS)-induced anxiety. Bottom, 30 min of IMS reduced the percentage of time spent on the open arms of the EPM [t(13) = 3.28, $^{**}P$ = 0.006, unpaired t-test] and time spent in the center of the OF [t(13) = 5.19, $^{***}P$ = 0.0002;

$n = 7$ control, 8 IMS, unpaired t-test]. **(B)** Top, experimental protocol for administration of R121919 before IMS. Bottom, blockade of CRF1 receptors with R121919 (20 mg/kg, *s.c.*) prevented IMS-induced reduction in percentage of time spent on open arms of the EPM [$t(20) = 4.324$, $^{***}P = 0.0003$, unpaired t-test] and in the center of the OF [$U = 29$, $^{*}P = 0.04$, Mann-Whitney test]. **(C)** Injection schematic and image of AAV-DREADD-mCherry expression in CeA^{CRF} neurons. Scale bar, 500 μm. Boxed region is enlarged in inset (scale bar, 200 μm). **(D)** Representative traces showing that bath application of CNO (2 μM) had no effect in a neuron not expressing a DREADD (Left), induced hyperpolarization of a neuron expressing DIO-hM4Di (Center), and promoted depolarization and spontaneous firing in a neuron expressing DIO-hM3Dq (Right). Quantification of changes in resting membrane potential in CeA neurons during CNO application [$F(2,12) = 111.9$, $P < 0.0001$, one-way ANOVA; $n = 4$-6 cells per condition 10 rats total; $^{****}P < 0.0001$ compared with control (no-DREADD) cells by Dunnett's test]. **(E)** Top, experimental protocol for administration of CNO before IMS. Bottom, CNO (2 mg/kg, *i.p.*) increased the percentage of time spent in the open arms of the EPM [$t(20) = 4.273$, $^{***}P = 0.004$, unpaired t-test], time spent in the center of the OF [$t(14) = 2.354$, $^{*}P = 0.037$, unpaired t-test], and social interaction time [$t(14) = 2.923$, $^{**}P = 0.01$, $n = 9$ each group, unpaired t-test] in rats that expressed hM4Di compared with control rats that expressed mCherry (mCh) in CeA^{CRF} neurons. **(F)** Top, Protocol for anxiety testing. Bottom, in rats that expressed hM3Dq in CeA^{CRF} neurons, CNO (2 mg/kg, *i.p.*) reduced the percentage of time spent on the open arms of the elevated plus maze [$F(2,26) = 8.061$, $P = 0.0019$, one-way ANOVA, $^{**}P = 0.0013$ compared with mCherry (mCh) by Dunnett's test], and reduced the time spent in the center of the open field [$F(2,23) = 6.205$, $P = 0.007$, one-way ANOVA, $^{**}P = 0.0091$ compared with mCherry by Dunnett's test]. In contrast, activation of hM4Di had no effect

on anxiety-like behavior when compared with mCherry control animals. Data are represented as mean ± SEM.

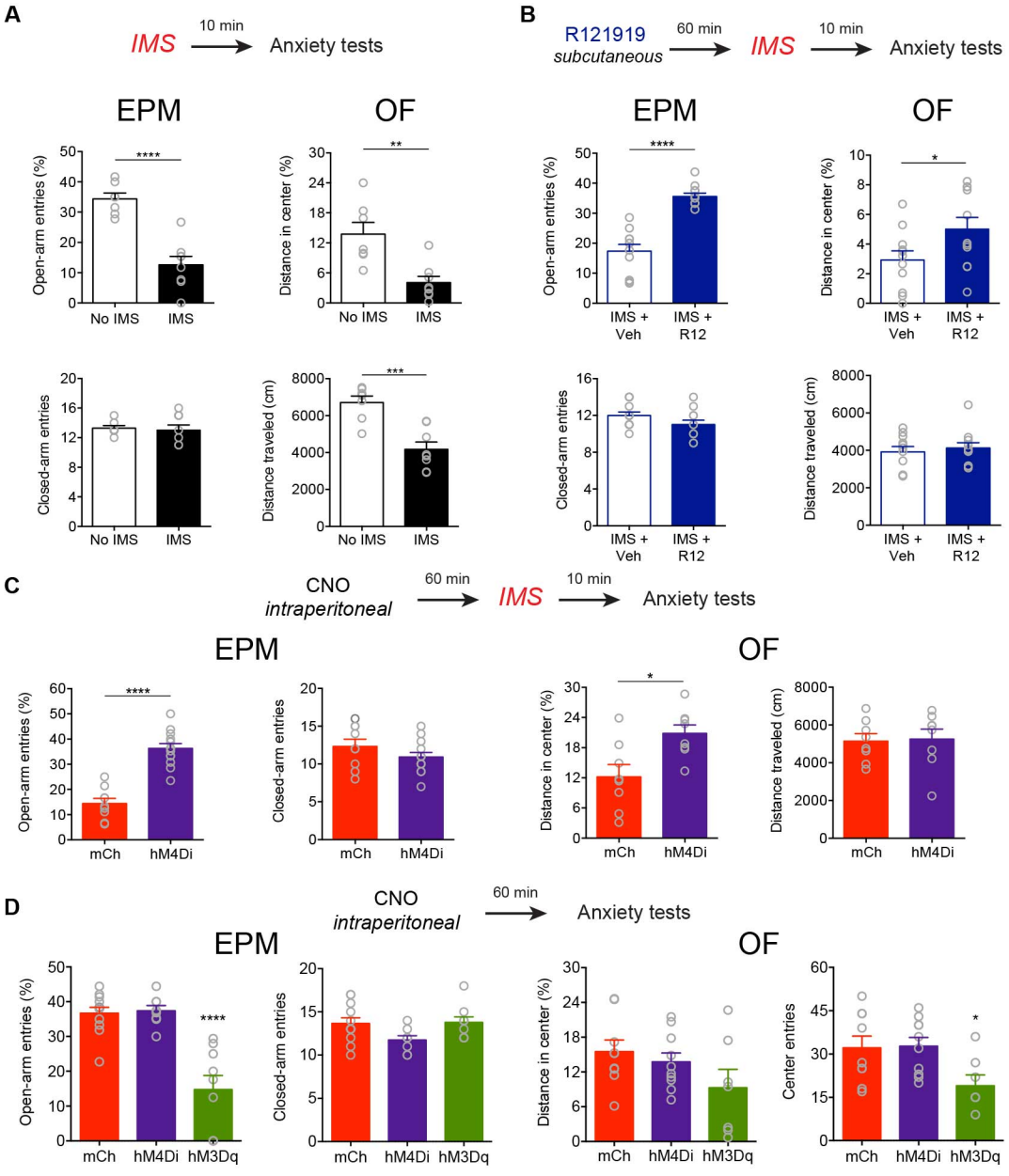

Figure 2.2. Effects of immobilization stress and DREADDs on other measures of anxiety-like behavior

(A) IMS reduced the percentage of open arm entries on the EPM [t(13) = 6.164, ****P < 0.0001, n = 7 no IMS, 8 IMS, unpaired t-test] without affecting closed arm entries [t(13) =

0.3344, $P = 0.7434$, $n = 7$ no IMS, 8 IMS, unpaired t-test]. Although IMS reduced the total distance traveled in the OF [t(13) = 4.749, ***$P = 0.0004$, $n = 7$ no IMS, 8 IMS, unpaired t-test], the percentage of total distance traveled in the center of the OF was significantly lower in stressed rats [t(13) = 3.791, **$P = 0.0022$, $n = 7$ no IMS, 8 IMS, unpaired t-test]. **(B)** Systemic administration of the CRF1 receptor antagonist R121919 prevented IMS-induced reductions in the percentage of open arm entries [t(20) = 7.280, ****$P < 0.0001$, $n = 11$ both groups, unpaired t-test] without affecting the number of closed arm entries on the EPM [t(20) = 1.618, $P = 0.1213$, $n = 11$ both groups, unpaired t-test]. R121919 also prevented IMS-induced reductions in the distance traveled in the center of the OF [t(20) = 2.072, P = *0.0275, $n = 11$ both groups, unpaired t-test] without altering the total distance traveled [t(20) = 0.5164, $P = 0.6112$, $n = 11$ both groups, unpaired t-test]. **(C)** Top, experimental protocol. Bottom, activation of hM4Di with CNO (2 mg/kg, *i.p.*) during IMS increased the percentage of open arm entries on the EPM [t(20) = 7.610, ****$P < 0.0001$, $n = 9$ mCherry (mCh), 13 hM4Di, unpaired t-test] without changing the number of closed arm entries [t(20) = 1.312, $P = 0.2044$, $n = 9$ mCh, 13 hM4Di, unpaired t-test] . Activation of hM4Di during IMS increased distance traveled in the center of the OF [t(14) = 2.923, *$P = 0.0111$; $n = 8$ both groups, unpaired t-test] but did not alter the total distance traveled [t(14) = 0.1652, $P = 0.8711$, $n = 8$ both groups, unpaired t-test]. **(D)** Activation of CeA^{CRF} neurons with hM3Dq reduced the percentage of open arm entries on the EPM [F(2,26) = 23.75, $P < 0.0001$, $n = 12$ mCh, 8 hM4Di, 9 hM3Dq, one-way ANOVA; ****$P < 0.0001$ compared with mCh by Dunnett's test] without affecting the number of closed arm entries [F(2,26) = 2.982, $P = 0.0682$, $n = 12$ mCh, 8 hM4Di, 9 hM3Dq, one-way ANOVA]. hM3Dq tended to reduce the distance traveled in the center of the OF [F(2,23) = 1.973, $P = 0.1618$, $n = 9$ mCh, 10 hM4Di, 7 hM3Dq, one-way ANOVA] but significantly reduced

the number of entries into the center OF [F(2,23) = 4.038, P = 0.0314, n = 9 mCh, 10 hM4Di, 7 hM3Dq, one-way ANOVA; *P = 0.0424 compared with mCh by Dunnett's test]. The total distance traveled in the OF was unaffected by hM3Dq activation [F(2,23) = 0.4411, P = 0.6487, n = 9 mCh, 10 hM4Di, 7 hM3Dq, one-way ANOVA] (data not shown). Data are represented as mean ± SEM.

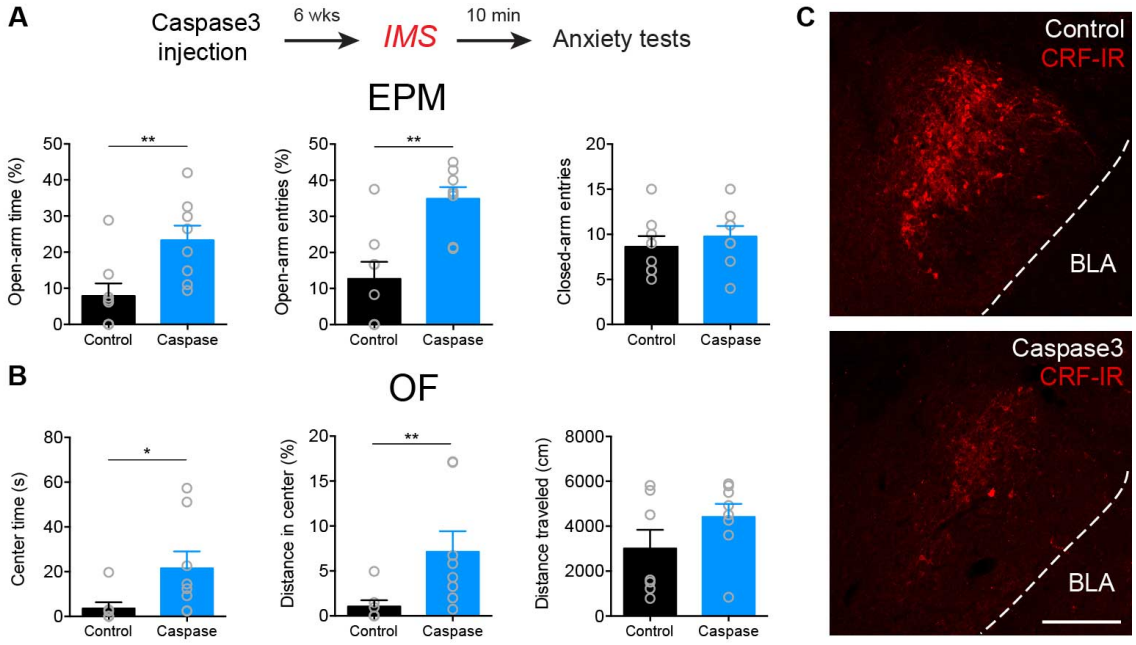

Figure 2.3. Genetic ablation of CeA^{CRF} neurons prevents stress-induced anxiety

(A) Top, experimental protocol. Bottom, bilateral caspase3-mediated ablation of CeA^{CRF} neurons increased the percentage of time spent on the open arm [U = 7, $^{**}P$ = 0.0070, Mann-Whitney test] and percentage of open arm entries [t(14) = 3.909, $^{**}P$ = 0.0016, unpaired t-test] during the EPM test without affecting the number of closed arm entries [t(14) = 0.6754, P = 0.5104, n = 8 both groups, unpaired t-test]. **(B)** Time spent [U = 7, $^{*}P$ = 0.0126, n = 7 eYFP, 8 Caspase, Mann-Whitney test] and the percentage of total distance traveled in the center of the OF [U = 6, $^{**}P$ = 0.0084, n = 7 eYFP, 8 Caspase, Mann-Whitney test] were also increased without altering the total distance traveled [t(13) = 1.415, P = 0.1807, n = 7 eYFP, 8 Caspase, unpaired t-test]. **(C)** Example of CRF immunoreactivity in the CeA of control animal microinjected with eYFP+PBS (top) versus animal microinjected with eYFP+Caspase3 (bottom). Scale bar, 200 µm. Data are represented as mean ± SEM.

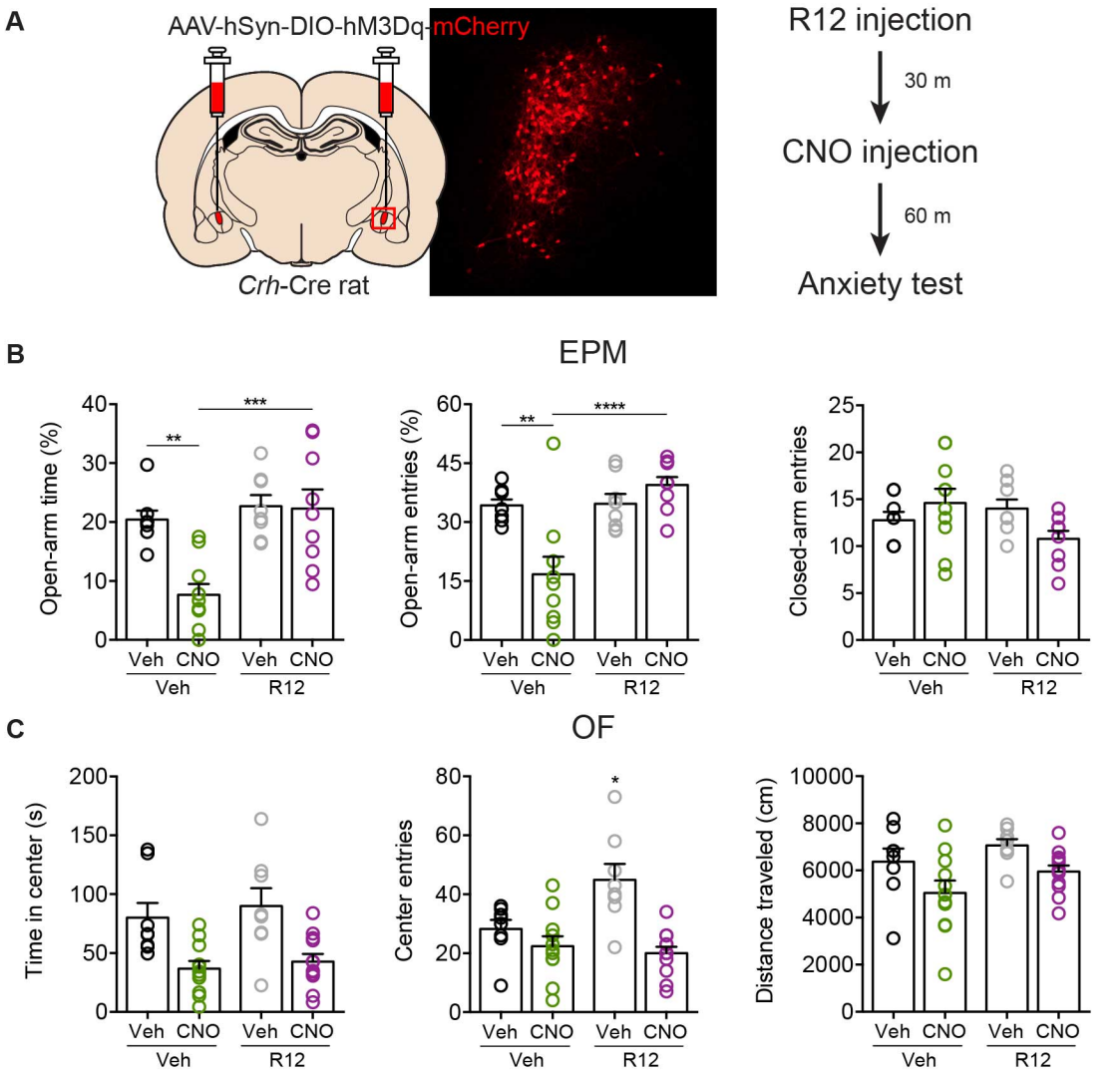

Figure 2.4. Systemic blockade of CRF1 receptors prevents EPM but not OF anxiety after hM3Dq stimulation of CeA^{CRF} neurons

(A) Left, example of image of hM3Dq-mCherry expression in CeA^{CRF} neurons. Right, experimental design. **(B)** CNO activation of hM3Dq reduced open arm time [$F_{CNO \times R12}$ (1,31) = 7.292, **P* = 0.0111, two-way ANOVA, *n* = 8-10; ***P* = 0.002 for Veh:Veh compared with CNO:Veh and ****P* = 0.0003 for CNO:Veh compared with CNO:R12 by Tukey's tests] and open arm entries [$F_{CNO \times R12}$ (1,31) = 12.92, ***P* = 0.0011, two-way

ANOVA, n = 8-10; $^{**}P$ = 0.0017 for Veh:Veh compared with CNO:Veh and $^{****}P$ < 0.0001 for CNO:Veh compared with CNO:R12 by Tukey's tests] on the EPM in a CRF1 receptor-dependent manner. Marginal effects on closed arm entries were detected [$F_{CNO \times R12}(1,31) = 4.812$, $^{*}P = 0.0359$, two-way ANOVA, n = 8-10; no significant comparisons by Tukey's tests]. **(C)** CNO activation of hM3Dq also reduced time spent in [$F_{CNO \times R12}(1,35) = 0.0395$, $P = 0.8437$; $F_{CNO}(1,35) = 21.29$, $^{****}P < 0.0001$; $F_{R12}(1,35) = 0.6647$, $P = 0.4204$, two-way ANOVA, n = 8-12] and entries into the center [$F_{CNO \times R12}(1,35) = 7.329$, $^{*}P = 0.0104$, two-way ANOVA, n = 8-12; $P = 0.6455$ for Veh:Veh compared with CNO:Veh and $P = 0.9523$ for CNO:Veh compared with CNO:R12 by Tukey's tests] of the open field, but these effects were not affected by CRF1 receptor blockade. R121919 however did increase entries into the center in rats without hM3Dq activation *via* CNO. No effects on locomotion were detected [$F_{CNO \times R12}(1,35) = 0.06212$, $P = 0.8046$, two-way ANOVA, n = 8-12]. Data are presented as mean ± SEM.

CeA^{CRF} neurons regulate fear learning

CRF neurons of the CeA mediate fear learning in mice (Sanford et al., 2017). We confirmed this effect in rats by injecting the inhibitory designer receptor hM4Di into the CeA of *Crh*-Cre to silence the activity of CeA^{CRF} neurons. Rats were injected with CNO (2 mg/kg, *i.p.*) either prior to fear conditioning, immediately after fear conditioning, or prior to retrieval trials (Figures 2.5). All rats exhibited shock-induced freezing, however only those whose neurons were silenced during conditioning showed reduced freezing during both contextual and cued retrieval trials (Figure 2.5B). Rats with CeA^{CRF} neuron inhibition immediately after conditioning or prior to retrieval trials exhibited no differences in contextual or cued freezing (Figure 2.5C and 2.5D). These data help confirm the hypothesis that CeA^{CRF} neurons contribute to fear learning, and are relatively dispensable during expression tests once fear associations have been formed.

Since CeA^{CRF} neurons promoted fear learning, we next asked whether stimulation these neurons could have an opposite effect on fear behavior. To do so, we decided to evaluate fear extinction during CeA^{CRF} neuron stimulation since freezing to cues decreases as more cues are presented in the absence of shock. Rats were injected with hM4Di, hM3Dq, or mCherry into the CeA and fear conditioned. Twenty-four hrs after conditioning, rats were presented with 18 tone cues for massed extinction. Rats expressing hM4Di or mCherry extinguished freezing, yet rats expressing hM3Dq failed to exhibit reductions in freezing, indicative of minimal extinction learning (Figure 2.6A). In a retrieval trial 24 hrs after extinction training, hM3Dq rats froze more to the tone cues (Figure 2.6B). This result shows that stimulation of CeA^{CRF} neurons can disrupt normal fear extinction, and further indicates that these neurons promote fear behavior. To determine whether CRF release is an important factor for disrupting extinction learning, we repeated the same hM3Dq

experiment but administered some rats the CRF1 receptor antagonist R121919 (20 mg/kg, *s.c.*). Blockade of CRF1 receptors prevented the CeA^{CRF} neuron-induced disruption in extinction learning (Figures 2.6C and 2.6D). Altogether, these data demonstrate that CeA^{CRF} neurons promote fear learning and can oppose fear extinction, most likely through the release of CRF acting at central CRF1 receptors.

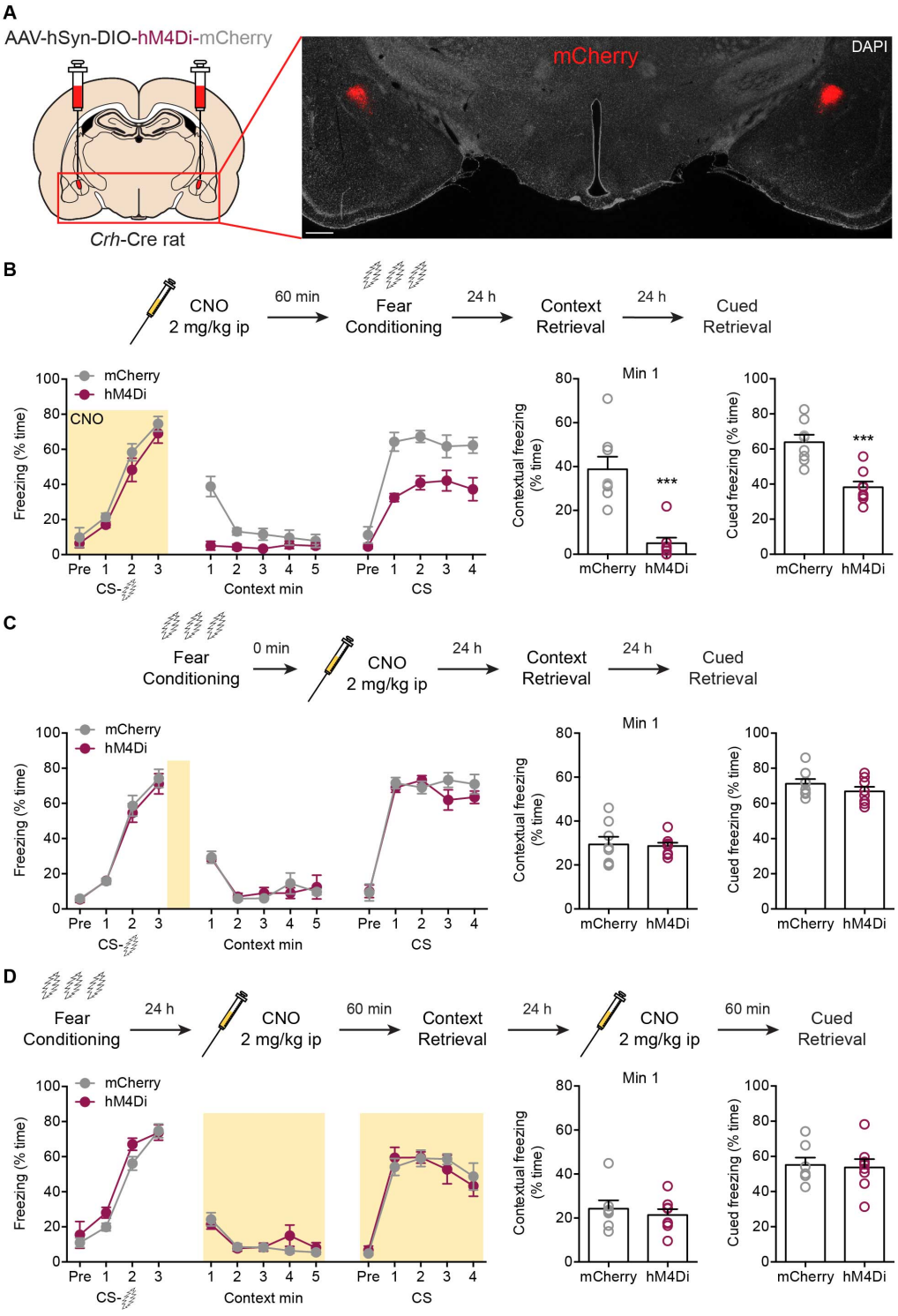

Figure 2.5. CeA^{CRF} neurons mediate fear learning, but not fear expression

(A) Injection schematics and example of viral expression in CeA^{CRF} neurons for hM4Di DREADD inhibition (left) and shRNA knockdown (right). Scale bar, 200 μm. **(B)** Top, experimental protocol for fear conditioning. Bottom, chemogenetic inhibition of CeA^{CRF} neurons with hM4Di and CNO (2 mg/kg, *i.p.*) did not affect shock-induced freezing during fear conditioning but disrupted contextual fear retrieval during the first minute [U = 1, $***P = 0.0003$, $n = 8$ for both groups, Mann-Whitney test] as well as cued fear retrieval [t(14) = 4.846, $***P = 0.0003$, $n = 8$ for both groups, unpaired t-test]. **(C)** Top, experimental protocol. Bottom, inhibition of CeA^{CRF} neurons immediately after conditioning did not affect contextual [t(14) = 0.2019, $P = 0.8429$, $n = 8$ for both groups, unpaired t-test] or cued fear retrieval [t(14) = 1.165, $P = 0.2636$, $n = 8$ for both groups, unpaired t-test]. **(D)**. Top, experimental protocol. Bottom, inhibition of CeA^{CRF} neurons before retrieval trials did not affect contextual [t(13) = 0.6246, $P = 0.5431$, $n = 7$ mCherry, 8 hM4Di, unpaired t-test] or cued [t(13) = 0.2142, $P = 0.8337$, $n = 7$ mCherry, 8 hM4Di, unpaired t-test] freezing. Yellow shading indicates times when CNO is on board. Data are presented as mean ± SEM.

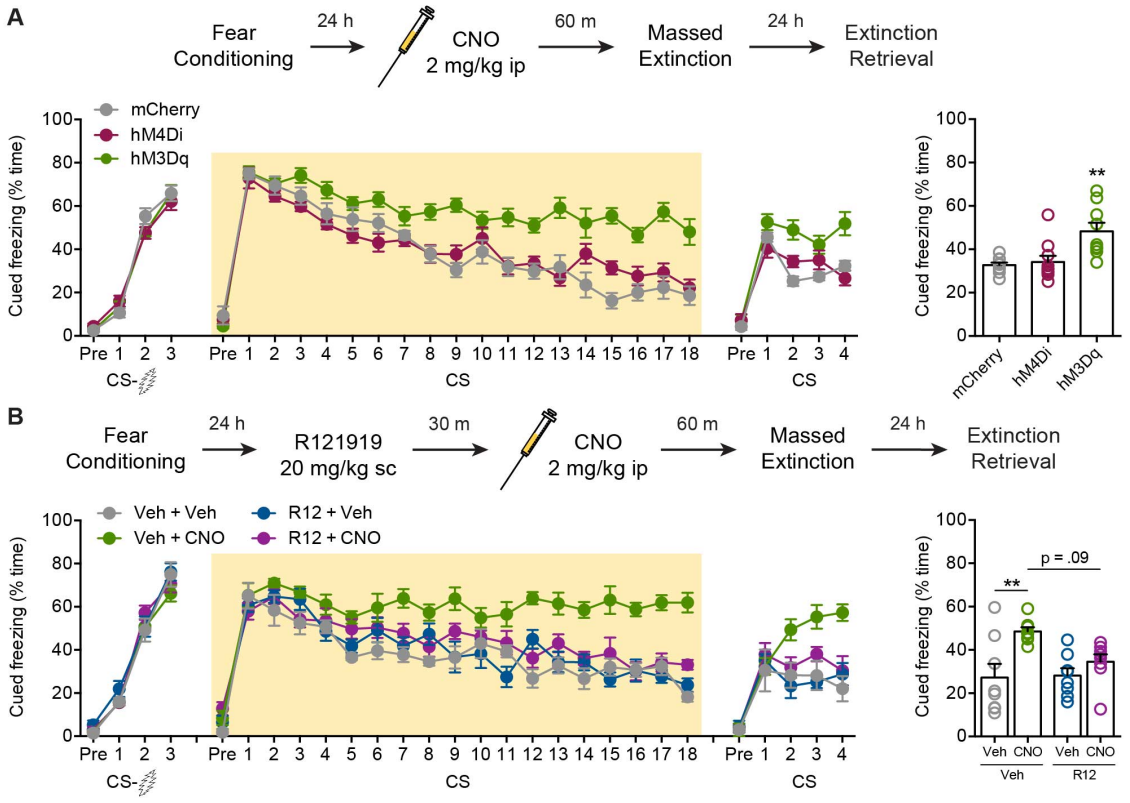

Figure 2.6. Stimulation of CeA^{CRF} neurons interferes with fear extinction

(A) Top, experimental protocol for fear conditioning and extinction. Bottom left, chemogenetic stimulation of CeA^{CRF} neurons with hM3Dq and CNO (2 mg/kg, *i.p.*) disrupted cued fear extinction [$F_{Time \times Virus}(36,450) = 3.586$, $^{****}P < 0.0001$, two-way RM ANOVA, n = 9-10; $^{*}P < 0.05$ for hM3Dq compared with hM4Di starting at the 3rd tone and hM3Dq compared with mCherry starting at the 8th tone by Tukey's tests]. Bottom right, extinction memory 24 hrs later is reduced in rats expressing hM3Dq, reflected as increased freezing during the extinction retrieval test [$F(2,25) = 8.781$, $P = 0.0013$, one-way ANOVA; n = 9-10; $^{**}P = 0.0017$ hM3Dq compared with mCherry by Dunnett's test]. **(B)** Top, experimental protocol. Bottom left, blockade of CRF1 receptors with R121919 (20 mg/kg, *s.c.*) prevented hM3Dq-induced disruptions in extinction performance [$F_{Time \times Virus}$

(54,504) = 2.152, ****$P < 0.0001$, two-way RM ANOVA, $n = 8$; *$P < 0.05$ for Veh + CNO compared with Veh + Veh starting at the 5th tone and Veh + CNO compared with R12 + Veh and R12 + CNO at the 12th tone by Tukey's tests]. Bottom right, blockade of CRF1 receptors marginally prevented deficits in extinction memory 24 hrs later [$F_{CNO \times R12}$ (1,28) = 3.340, $P = 0.0783$, two-way ANOVA, $n = 8$; **$P = .0049$ for Veh + CNO compared with Veh + Veh, and $P = .0935$ for Veh + CNO compared with R12 + CNO, by Tukey's tests]. Yellow shading indicates times when CNO is on board. Data are presented as mean ± SEM.

DISCUSSION

Canonical models of fear and anxiety circuitry propose that the CeA is a critical structure for fear-like behaviors but not those related to anxiety (Davis, 1992, 1997; Davis et al., 2010; Liang et al., 1992a). Since these were done with crude inactivation methods such as lesions and pharmacology (infusions of GABA receptor agonists like muscimol), the precise roles of different co-existing neuronal populations were not addressed. In this study, we demonstrate overlapping roles for a discrete population of CeA neurons, those expressing and releasing CRF, in both fear and anxiety behaviors in rats. CeA^{CRF} neurons mediated immobilization stress-induced anxiety and were capable of generating an anxiogenic state when stimulated with hM3Dq designer receptors. These neurons also mediated fear learning to both contexts and cues and disrupted fear extinction when stimulated. These effects were most likely due to the release of CRF acting at CRF1 receptors since blockade with R121919 prevented evoked fear and anxiety when CeA^{CRF} neurons were stimulated. Therefore, these data challenge early models of fear and anxiety circuitry by showing that CeA^{CRF} neurons contribute to both of these behaviors.

Acute immobilization stress produces anxiety in rodents (Buynitsky and Mostofsky, 2009; Pare and Glavin, 1986). We were able to prevent this anxiety by suppressing the activity of CeA^{CRF} neurons either by hM4Di-mediated silencing or Caspase3-medaited ablation. These data suggest that these neurons are engaged by stress and help orchestrate anxiety responses that stress produces. Stimulation with hM3Dq recapitulated stress effects on anxiety, and this effect was blocked by CRF1 receptor antagonism. Since CRF1 receptors also blocked stress-induced anxiety in wild-type rats, it is likely that a critical source of CRF released by stress is the CeA. This is consistent with a previous report (Regev et al., 2012) and is similar to the effects we observed during fear

conditioning. It is likely that CRF release is involved with the induction of fear learning and can interrupt extinction of fear associations (Gafford et al., 2012; Pitts et al., 2009; Sanford et al., 2017). Based on these findings, CeA^{CRF} neurons likely exert their influences over fear and anxiety states through the release of CRF. However, this is most likely not the full story.

CeA^{CRF} neurons are heterogenous. They express several other neuropeptides aside from CRF (neurotensin, dynorphin, somatostatin, etc.) and at least some are projection neurons that send axons to many brain structures implicated in fear and anxiety states (Kim et al., 2017; Marchant et al., 2007; Pomrenze et al., 2015). These features suggest that CeA^{CRF} neurons can promote fear and anxiety through several mechanisms. For instance, these neurons could co-release multiple peptides when stimulated by stress, footshocks, or hM3Dq, leading to complex neurophysiology effects downstream and a fine-tuning of behavioral outputs. Dynorphin is involved in aversive features of stress and drug withdrawal (Ahrens et al., 2018; Anderson and Becker, 2017; Koob, 2008) and neurotensin mediates chronic stress-induced plasticity in the BNST (Normandeau et al., 2018b) but is rewarding when signaling in the CeA (Laszlo et al., 2010). Thus, a mixture of peptides was most likely released in our experiments, all with presumably different effects that led to a net effect of pro-fear and pro-anxiety. However, the effects of these peptides in isolation will need to be tested in the future.

Among all the brain regions that CeA^{CRF} neurons project to, the BNST stands out as a promising candidate for mediating anxiety. The dorsal BNST has been implicated in anxiety states (Crowley et al., 2016; Davis et al., 2010; Kim et al., 2013; Normandeau et al., 2018b), has strong connectivity with the CeA (Li et al., 2012; Chapter 1), and exhibits strong physiological responses to CRF, dynorphin, and neurotensin (Crowley et al., 2016;

Kash et al., 2008; Kash et al., 2015; Normandeau et al., 2018a; Normandeau et al., 2018b). Thus, it is possible that CeA^{CRF} neurons target the dorsal BNST to mediate acute stress-induced anxiety behaviors. The role of the different neuropeptides CeA^{CRF} neurons express, and the role of their projection targets should be the focus of future investigations.

Why do lesions and pharmacological inactivation of the CeA have no effects on anxiety? It is becoming increasingly clear that intermingled subpopulations of genetically-defined neurons can exhibit opposing functions (Daniel and Rainnie, 2016; Fadok et al., 2017; Fadok et al., 2018; Kim et al., 2017). The ability to target a given brain region with cellular precision has helped generate a new understanding of how the brain controls behavior. As such, global inactivation of the CeA could inhibit the function of pro-anxiety and anti-anxiety cells that antagonize each other, leading to a null net effect. By manipulating discrete cell-types, we can begin to understand 1) what brain structures are capable of doing and 2) how they carry out these functions on the circuit and systems levels. Thus, despite this not being the first example of this methodology, manipulating CeA^{CRF} neurons here has provided insight into how the CeA contributes to both fear and anxiety. Our data demonstrate that the CeA has a role in fear and anxiety states, and that there are most likely counter-circuits within the CeA that oppose or modulate these states.

In summary, we have demonstrated how CeA^{CRF} neurons can control fear and anxiety behaviors in rats using viral-genetic tools and pharmacology. Our data identify this cell population as critical to both aversive states through the release of the primary neuropeptide CRF. In addition, we challenge the anatomical segregation of fear and anxiety and suggest a more versatile role for the CeA, and most likely other brain regions as well. These data will hopefully also be informative to the development of new therapeutic strategies for treating human fear and anxiety disorders.

ACKNOWLEDGMENTS

The experiments in this study were conducted by a team of researchers. I thank Dr. Rajani Maiya for her assistance gathering data and her intellectual contributions, Dr. Angelo Blasio for data collection and stereotaxic surgeries, Simone Giovanetti for her help with experiments, collecting data, acquiring critical reagents, and her intellectual contribution, and Dr. Woody Hopf and Kell Lei for generating electrophysiology data for validating DREADDs in CeA^{CRF} neurons (a critical part of the study). Importantly, I thank Dr. Robert Messing for providing space and funding for the project. And finally, the National Science Foundation for my funding (NSF fellowship DGE-1110007).

CHAPTER 3: GABA AND NEUROPEPTIDES FROM CENTRAL AMYGDALA CRF NEURONS PLAY DISTINCT ROLES IN FEAR AND ANXIETY

ABSTRACT

Central amygdala CRF neurons regulate fear and anxiety-like behaviors in rats and mice. These neurons release GABA and co-express several neuropeptides other than CRF that play important roles in a variety of behaviors. Genetic tools have allowed for precise manipulations of these CRF cells, but few studies have determined which neurotransmitters or neuropeptides are released to control behavior. Here we dissect the relative roles GABA, CRF, dynorphin, and neurotensin play in fear and anxiety-like behaviors by disrupting their expression and release potential with Cre-dependent RNA interference tools in *Crh*-Cre rats. We find that GABA release, but not neuropeptide release, regulates baseline anxiety-like behavior. We also observed that chemogenetic stimulation of central amygdala CRF neurons evokes anxiety-like behavior that is dependent on expression of CRF and dynorphin, but not neurotensin. Finally, expression of CRF and dynorphin promote fear learning whereas neurotensin expression dampens fear. These results demonstrate differential roles of different neuropeptides released from the same neurons in fear and anxiety-like behaviors.

INTRODUCTION

The field of neuroscience has been transformed by the advent of genetic tools that permit access to specific neuronal cell types (Roth, 2016; Yizhar et al., 2011). Cell-type and pathway-specific targeting of fluorescent tracers and effector proteins has provided unprecedented insight into how neural circuits control behavior. Cre-driver mouse lines and viral genetic tools are typically used to manipulate the activity of neuronal subpopulations (Daigle et al., 2018; Harris et al., 2014; Madisen et al., 2015; Taniguchi et al., 2011). However, a pitfall in this approach lies in the temptation to attribute the actions of the subpopulation to the peptide or neurotransmitter whose promoter was used to drive Cre recombinase expression, thereby overlooking the contributions of other signaling molecules released by the targeted neurons.

Neuropeptides are interesting and elusive signaling molecules with unique properties. Essentially all neurons that express neuropeptides express more than one, and also release a fast-acting amino acid neurotransmitter such as glutamate or GABA (van den Pol, 2012). Compared with fast-acting neurotransmitters, neuropeptides may require higher frequency stimulation and larger increases in intracellular calcium for release. Neuropeptides can also signal over longer distances due to extrasynaptic release, local diffusion, and the requirement of extracellular proteolytic cleavage as opposed to local reuptake for signal termination. A particularly interesting question is how multiple peptides released by a single neuron interact, particularly when they evoke initially opposing responses. Are they released from different dense-core vesicles that respond to different patterns of stimulation, or if co-released do they bind to receptors with different latencies or durations of action? Or do they bind receptors expressed on different target neurons within a circuit that generates a synergistic effect?

One brain structure rich with neuropeptides is the central amygdala (CeA). The CeA contains a large population of cells that express the stress-responsive neuropeptide corticotropin releasing factor (CRF). CeA CRF (CeA^{CRF}) neurons release GABA and co-express numerous neuropeptides, including dynorphin and neurotensin, and have been found to promote anxiety-like behavior and fear learning (Asok et al., 2018; McCall et al., 2015; Pliota et al., 2018; Sanford et al., 2017). Interestingly, some of the neuropeptides expressed in CeA^{CRF} neurons have been shown to play distinct roles in fear and anxiety-like phenotypes. CRF and dynorphin promote fear and anxiety-like behaviors, whereas neurotensin has been reported to play a minimal role in anxiety and dampens fear learning (Asok et al., 2018; Crowley et al., 2016; Knoll et al., 2007; Knoll et al., 2011; Laszlo et al., 2010; McCall et al., 2015; Pitts et al., 2009; Prus et al., 2014; Regev et al., 2012; Sanford et al., 2017; Steele et al., 2017; Toda et al., 2014; Yamada et al., 2010). Despite having established roles in fear and anxiety, the contribution of other neurotransmitters released from CeA^{CRF} neurons to fear and anxiety-like behaviors has never been explored.

In this study, we examined the question of how neurons control and fine-tune behavior through the release of diverse signaling molecules predicted to have opposing actions. Here we used a rat line that expresses Cre recombinase under control of the corticotropin releasing factor (CRF) promoter (Pomrenze et al., 2015). Using RNA interference, we dissected the roles of CRF, GABA, and the co-expressed neuropeptides dynorphin and neurotensin in modulating anxiety-like behavior and fear learning. Our results demonstrate that this subpopulation of amygdala neurons plays a multimodal role in regulating different behaviors through the coordinate actions of different neurotransmitters and neuromodulators. These findings highlight the importance of

considering the spectrum of signaling molecules expressed by a subpopulation of neurons when studying brain physiology and behavior.

MATERIALS AND METHODS

Subjects

All procedures were approved by the University of Texas at Austin Institutional Animal Care and Use Committee. We used male hemizygous *Crh*-Cre rats (Pomrenze et al., 2015) outcrossed to wild-type Wistar rats (Envigo, Houston, TX), aged 5-6 weeks at the start of the surgical procedures and 10-14 weeks at the start of experimental procedures. Rats were group housed and maintained on a 12-h light:dark cycle with food and water available *ad libitum*. Cre^+ rats were randomly assigned to either experimental or control groups within each litter.

Drugs and viral vectors

Clozapine-N-oxide (CNO) was supplied through the NIMH Chemical Synthesis and Drug Supply Program. CNO (2 mg/kg body weight) was dissolved in 5% dimethyl sulfoxide (DMSO) and then diluted to 2 mg/mL with 0.9% saline. Systemic injections were administered at 1 mL/kg. The selective CRF1 receptor antagonist 3-[6-(dimethylamino)-4-methyl-pyrid-3-yl]-2,5-dimethyl-*N*,*N*-dipropyl-pyrazolo[2,3-a]pyrimidin-7-amine (R121919) was provided by Dr. Kenner Rice (Drug Design and Synthesis Section, NIDA, Bethesda, MD) and dissolved in a 1:1 solution of 0.9% saline and 1N HCl before adding 25% hydroxypropyl-β-cyclodextrin (HBC; Sigma Aldrich, St. Louis, MO) to yield a final concentration of 10 mg/mL R121919 in 20% HBC, pH 4.5.

The Cre-dependent viral vector AAV8-hSyn-DIO-hM3Dq-mCherry was obtained from Addgene (Cambridge, MA). AAV constructs containing shRNAs targeting *proCrh*, *proDynorphin*, *Neurotensin*, and a scrambled control were packaged by the University of North Carolina Chapel Hill viral vector core. All AAVs were injected at 4-6 × 10^{12}

infectious units per mL. Canine adeno virus 2 (CAV2) carrying a flex-ZsGreen reporter expressed from the CAG promoter (CAV2-CAG-flex-ZsGreen) was a gift from Dr. Larry Zweifel (University of Washington, Seattle, WA) and was injected at 2×10^{12} infectious units per mL.

Stereotaxic surgery

Rats weighing 200-250 g were anesthetized with isoflurane (5% v/v) and secured in a stereotaxic frame (David Kopf Instruments, Tujunga, CA). Viruses were injected bilaterally into the CeA (AP: -2.2; ML: ± 4.5; DV: -8.0 from skull) at a rate of 150 nL min^{-1} for 5 min (750-800nL total volume per hemisphere) with a custom 32-gauge injector cannula coupled to a pump-mounted 2µL Hamilton syringe. Injectors were slowly retracted after a 5-min diffusion period. Rats were group housed to recover for 4-6 weeks before experiments began.

Generation of shRNAs

Three shRNA oligonucleotides targeting the 3'-untranslated region (UTR) of *proCrh*, *proDynorphin*, or *Neurotensin* were generated and subcloned into a pPRIME lentiviral transfer vector (Addgene #11663). Constructs containing shRNAS along with a cDNA encoding each peptide with the respective 3'-UTR were transfected into HEK293 cells. Seventy-two hrs after transfection, cells were harvested, lysed and assayed by western blot (*in vitro* validation of sh*Crh* and sh*Dyn*) or qPCR (*in vitro* validation of sh*Nts*). The shRNA for each peptide with the greatest and most consistent knockdown was chosen and subcloned into a pAAV vector containing a previously validated Cre-dependent (*flex*) shRNA targeting the 3'-UTR of the vesicular GABA transporter (*Vgat*) within a modified

microRNA (*miR30*) cassette (a gift from Dr. William Wisden - Imperial College, London, UK; Yu et al., 2015), replacing the sh*Vgat* sequence. Thess constructs and a control hairpin construct were packaged into AAV8 by the UNC Viral Vector Core. AAV8-hSyn-*flex*-eGFP-sh*Crh* (sh*Crh*), AAV8-hSyn-*flex*-eGFP-sh*Dynorphin* (sh*Dyn*), AAV8-hSyn-*flex*-eGFP-sh*Neurotensin* (sh*Nts*), and AAV8-hSyn-*flex*-eGFP-sh*Control* (sh*Con* - sequence targeting luciferase) were injected at 2-3 × 10^{12} particles per mL into the CeA. Knockdown *in vivo* was verified using RT-qPCR from AAV-infected CeA tissue punches.

RT-qPCR

Crh-Cre rats were bilaterally injected into the CeA with AAVs carrying sh*Crh*, sh*Dyn*, sh*Nts*, or sh*Con*. After 4 weeks rats were euthanized and their brains flash frozen in isopentane on dry ice and stored at -80°C. Brains were then equilibrated to -20°C in a cryostat for 1 hr and the CeA sectioned coronally at 250 μm and mounted onto cold Superfrost Plus slides (Fisher Scientific). Tissue punches (2 mm diameter) spanning the CeA from both hemispheres were collected onto dry ice and snap frozen in liquid nitrogen. RNA was extracted immediately using RNeasy Lipid Tissue Mini Kit (Qiagen, Hilden, Germany). Purified RNA samples were reverse transcribed by using the High Capacity cDNA Synthesis Kit (Invitrogen, Carlsbad, CA). Quantitative real-time PCR was performed using a TaqMan Gene Expression Assay Kit (Applied Biosystems, Foster City, CA). All TaqMan probes were purchased from Applied Biosystems: *Crh*, *Dynorphin*, *Neurotensin*, *GusB* and *Hprt1*. Target amplification was performed by using ViiA 7 Real-Time PCR System (Applied Biosystems). Relative mRNA expression levels were calculated via a comparative threshold cycle (Ct) method using *GusB* as an internal control:

ΔCt = Ct (gene of interest) – Ct (*GusB*). The gene expression fold change was normalized to the control sample and then was calculated as $2^{-\Delta\Delta Ct}$.

Western blotting

shRNA-mediated knockdown was tested in vitro using HEK293T cells. Cells were plated at a density of 3 x 105 cells/well in 12-well plates. Twenty-four hours after plating, cells were co-transfected with the pPRIME vector plus a transgene encoding CRF or DYN (including their 3'-UTRs) using Lipofectamine 2000 (Life Technologies). 60 hrs after transfection, media was aspirated and cells were lysed by incubating with 200 µl of ice-cold RIPA buffer at 4ºC for 30 min. The lysate was then centrifuged at 10,000 x g for 15 min at 4ºC. Supernatant was collected and protein concentrations were measured using the bicinchonnic assay method (Life Technologies). 40 µg of protein was resolved on a 10% SDS Polyacrylamide gel and transferred on to a nitrocellulose membrane. After transfer, the membrane was blocked with 5% milk in Tris-buffered saline containing 0.01% Tween-20 (TBST). The blot was probed with 1:200 dilution of goat anti-CRF antibody (Santa Cruz Biotechnology, sc-1761) or 1:1000 dilution of guinea pig anti-DYN antibody (Neuromics, GP10110) in 5% milk overnight at 4ºC with shaking. Blots were washed three times in 1X TBST and probed with 1:2500 dilution (in 5% milk) of horseradish peroxidase conjugated anti-goat or anti-guinea pig secondary antibodies (Jackson Immunoresearch) for 1 hr at room temperature followed by chemiluminescent detection (Super-signal West, Life Technologies). Blots were stripped (Restore buffer, Life Technologies) and probed with anti-rabbit GAPDH (1:10,000 dilution in 5% milk, Cell Signaling Technologies, 5174S). Immunoreactive bands were quantified using Image J. CRF and DYN levels were normalized to GAPDH and percent knockdown was calculated.

Behavior

Anxiety

We used two assays to evaluate anxiety-like behavior: the elevated plus maze (EPM) and the open field test (OF). The EPM consisted of two open arms (50 x 10 cm) and two enclosed arms (50 x 10 x 40 cm) connected by a central area measuring 10 x 10 cm, 50 cm above the floor. At the beginning of each trial, rats were placed in the center facing one open arm. Trials lasted for 5 min and were performed under red lighting. The OF consisted of an open topped arena (100 x 100 x 50 cm) situated on the floor. The center zone measured 55 x 55 cm. Rats were placed into a corner of the arena at the beginning of each trial. Each trial lasted 10 min and was performed under red lighting. All testing equipment was cleaned with 70% ethanol between trials. Behaviors were tracked with EthoVision (Noldus Information Technology, Leesburg, VA, USA).

Fear conditioning

Rats were subjected to a typical fear conditioning protocol with 3 CS-US (tone-shock) pairings (75 dB, 5 kHz, 20 s tones co-terminating with 0.7 mA, 500 ms shocks, variable ITI (average 180 s)) for delay conditioning (Monfils et al., 2009; Schafe et al., 1999). Twenty-four hrs later rats were tested for contextual fear retrieval by being placed back into the original context for 5 min. Twenty-four hrs later rats were tested for cued fear retrieval in a distinct context with the presentation of 4 CS tones. The distinct context consisted of pinstripe and checkered walls, smooth tactile floors, and the presence of 1% acetic acid.

Histology

Rats were anesthetized with isoflurane and perfused transcardially with PBS followed by 4% paraformaldehyde in PBS, pH 7.4. Brains were extracted, postfixed overnight in the same fixative and cryoprotected in 30% sucrose in PBS at 4º C. Brains were sectioned at 40 μm on a cryostat and collected in PBS. Free-floating sections were washed three times in PBS with 0.2% Triton X-100 (PBST) for 10 min and then incubated in PBST with 3% normal donkey serum (Jackson ImmunoResearch, West Grove, PA, Cat. No. 017-000-121) for 1 hr. Sections were next incubated in goat anti-cFos (1:2000, Santa Cruz Biotechnology, Dallas, TX, Cat. No. sc-52-G), guinea pig anti-proDynorphin (1:500, Neuromics, Edina, MV, Cat. No. GP10110), rabbit anti-neurotensin (1:1000, ImmunoStar, Hudson, WI, Cat. No. 20072), and/or rabbit anti-PKCδ (1:2000, Santa Cruz Biotechnology, Cat. No. sc-213) in blocking solution rotating at 4ºC for 18-20 hr. After three 10 min washes in PBST, sections were incubated in species-specific secondary antibodies Alexa Fluor 488, 594, or 647 (1:700, Life Technologies, Carlsbad, CA, Cat. Nos. A-21206, A-11055, A-21208, A11073, A-21447, A-31573) in blocking solution for 1hr at room temperature. Finally, sections were washed three times for 10 min in 1X PBS, mounted in 0.2% gelatin onto SuperFrost Plus glass slides, and coverslipped with Fluoromount-G with DAPI (Southern Biotech, Birmingham, AL, Cat. No. 0100-20). Fluorescent images were collected on a Zeiss 710 confocal microscope or a Zeiss AxioZoom stereo microscope. Quantification of fluorescence was performed on 3-6 sections per rat from 5 rats from approximately Bregma -1.90 to -3.00 in the CeA and Bregma +0.2 to -0.2 in the BNST using the cell-counter plugin in Fiji (Schindelin et al., 2012).

Fluorescence *in situ* hybridization

Coronal sections were processed for fluorescent *in situ* hybridization by RNAscope according to manufacturer's guidelines. Genes examined in the CeA were *Crh* (ACDBio cat# 318931) and *egfp* (ACDBio cat# 409971) and hybridization was performed using RNAscope Fluorescent Multiplex Kit (Advanced Cell Diagnostics). Slides were coverslipped with Fluoromount-G with DAPI (Southern Biotech, 0100-20) and stored at 4°C in the dark before imaging.

Statistical Analyses

We calculated sample sizes of n = 8-12 animals per condition using SD values measured in pilot studies of IMS-induced anxiety-like behavior, $\alpha = 0.05$, and power = 0.80, with the goal of detecting a 25-35% difference in mean values for treated and control samples, using G*Power (Faul et al., 2007). All results were expressed as mean ± S.E.M. values and analyzed using Prism 7.0 (GraphPad Software, San Diego, CA). Data distribution and variance were tested using Shapiro-Wilk normality tests. Normally distributed data were analyzed by unpaired, two-tailed t-tests, or one or two factor ANOVA with *post-hoc* Tukey's or Bonferroni's tests. Data that were not normally distributed were analyzed by Mann-Whitney U tests when comparing two conditions or were transformed to square root values before performing a two-factor ANOVA. Differences were considered significant when $P < 0.05$.

RESULTS

CeA^{CRF} neuron neuropeptides and baseline anxiety

We have shown previously that rat CeA^{CRF} neurons co-localize with several other neuropeptides (Pomrenze et al., 2015), consistent with previous reports in rats and mice (Kim et al., 2017; Marchant et al., 2007). Pharmacological studies suggest that CRF and dynorphin are anxiogenic (Ahrens et al., 2018; Arborelius et al., 1999; Bruchas et al., 2009; Crowley et al., 2016), raising the question of how these co-expressed signaling molecules interact to set the level of baseline anxiety-like behavior. To examine this question, we designed Cre-dependent short hairpin RNAs (shRNAs) targeting the 3'-UTRs of the pro-peptides for CRF, dynorphin, and neurotensin. These sequences were cloned into the vector pPRIME-GFP and transfected into HEK-293 cells together with cDNAs encoding open reading frames plus 3'-UTRs for these peptides. Three days later, we measured the abundance of CRF and dynorphin by western blot analysis and neurotensin mRNA by qPCR (Figures 3.1A and 3.1B). The most effective shRNA sequences were packaged into AAV8 vectors and injected bilaterally into the CeA of *Crh*-Cre rats. After 4 weeks we verified *in vivo* knockdown of respective mRNAs by qPCR (Figures 3.2C and 3.2D).

We then injected a new cohort of rats and after 4-6 weeks tested them for baseline anxiety-like behavior in elevated plus maze (EPM) and open field (OF) assays. Compared with rats expressing a control construct, knockdown of each peptide modestly increased the percentage of open arm entries, but did not alter the percentage of time in the open arms (Figure 3.2B) or the number of closed arm entries (Figure 3.6A). Knockdown also did not alter the time spent in the center or the number of entries into the center of the OF (Figure 3.2C). Locomotion in the OF was not affected (Figure 3.6B). These findings suggest that

CRF, dynorphin, and neurotensin from CeA^{CRF} neurons play a minor role in setting the level of baseline anxiety-like behavior.

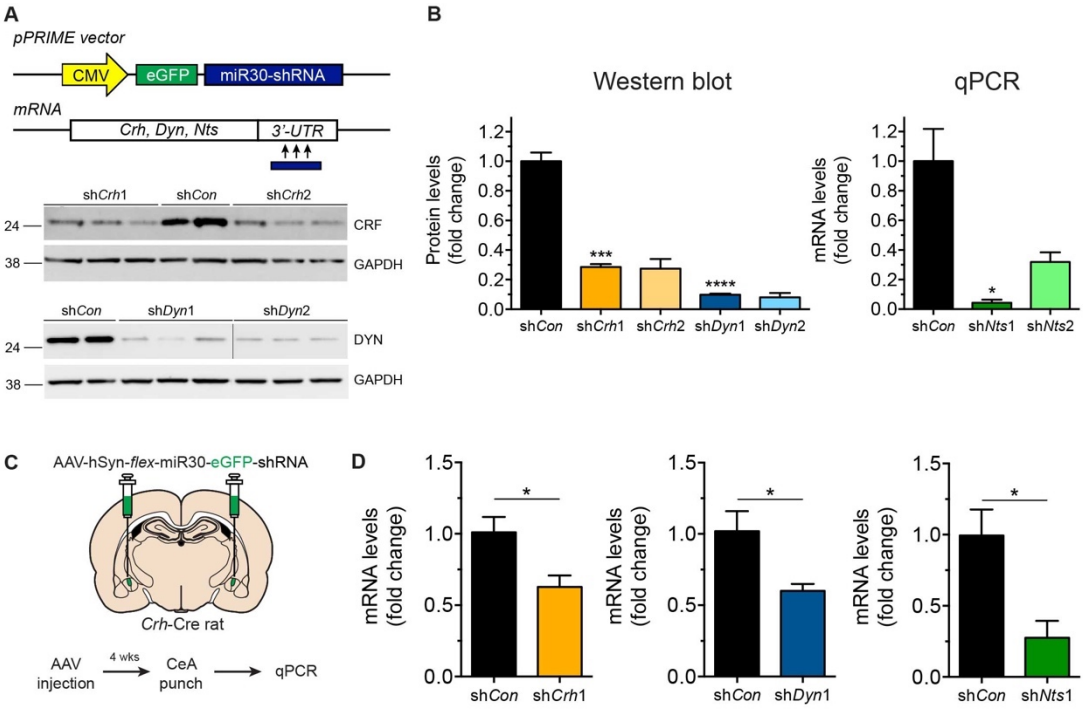

Figure 3.1. Validation of shRNAs targeting *Crh*, *Dyn*, or *Nts*

(A) Top, schematic of initial lentiviral vector containing shRNAs and interaction with mRNA transcripts of interest. Bottom, western blots demonstrating shRNA knockdown of *Crh* or *Dyn* in HEK293 cells. **(B)** Western blot and qPCR results for *in vitro* knockdown. shRNAs targeting *Crh* or *Dyn* were validated by western blot [sh*Con* compared with sh*Crh*1: t(5) = 9.965, ***P = 0.0002; sh*Con* compared with sh*Dyn*1: t(5) = 12.86, ****P < 0.0001, unpaired t-tests; n = 3-4] and shRNAs targeting *Nts* were validated using qPCR (due to lack of validated antibodies for neurotensin) [sh*Con* compared with sh*Nts*1: t(4) = 4.373, *P = 0.0119]. **(C)** Injection schematic and experimental design of *in vivo* validation of shRNAs after packaging into AAV. **(D)** qPCR validation of sh*Crh* [t(4) = 2.855, *P = 0.0462; n = 3], sh*Dyn* [t(4) = 2.804, *P = 0.0486; n = 3], and sh*Nts* [t(8) = 3.286, *P =

0.011; $n = 5$] after bilateral tissue punches of AAV-infected CeA in *Crh*-Cre rats. Data are presented as mean ± SEM.

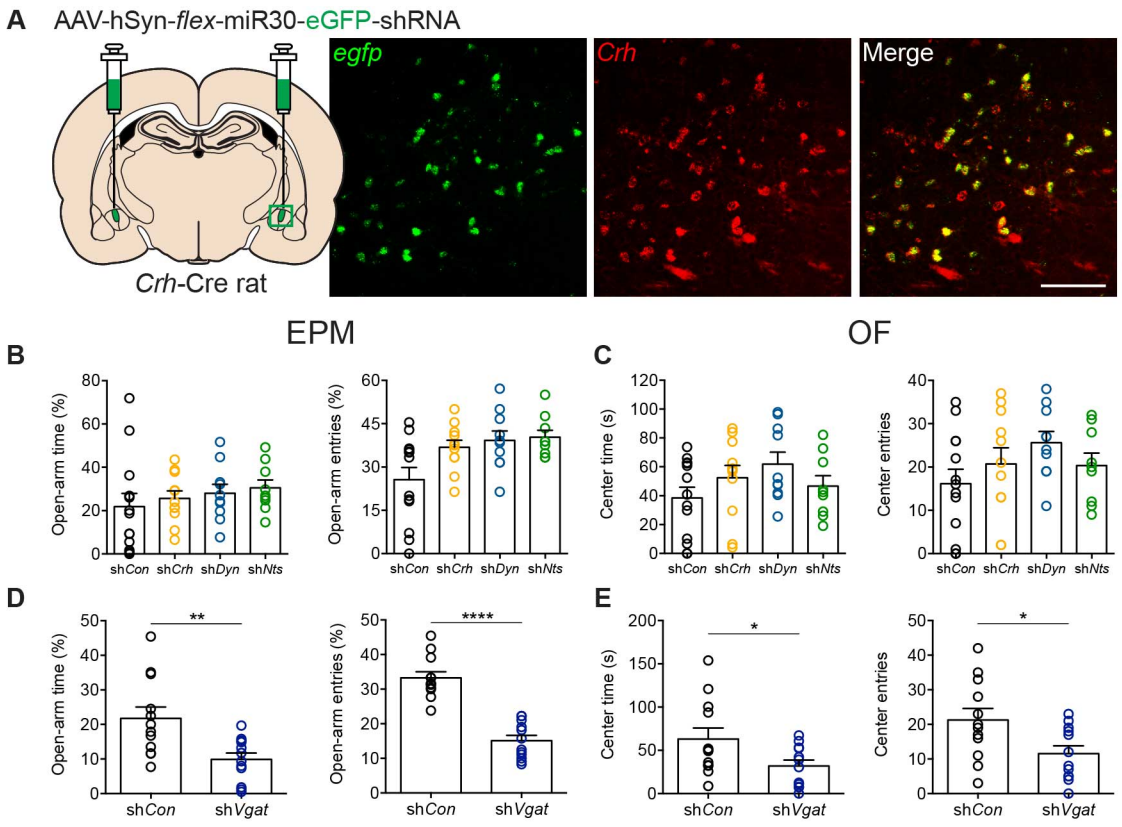

Figure 3.2. Knockdown of *Vgat*, but not *Crh*, *Dyn*, or *Nts* in CeA^{CRF} neurons produces an anxiogenic state

(A) Injection schematic and representative image of *egfp* mRNA from AAV containing shRNA co-localizing with *Crh* mRNA. Scale bar, 200 μm. **(B)** Knockdown of *Crh*, *Dyn*, or *Nts* leads to no changes in time spent in the open arms of the elevated plus maze [F(3,39) = 0.5965, P = 0.6211, one-way ANOVA, n = 13 sh*Con*, 11 sh*Crh*, 10, sh*Dyn*, 9 sh*Nts*] but does increase the number of entries into the open arms [F(3,39) = 2.139, P = 0.0092, one way ANOVA, n = 13 sh*Con*, 11 sh*Crh*, 10, sh*Dyn*, 9 sh*Nts*; *P < 0.05 compared with sh*Con* by Dunnett's test]. **(C)** Knockdown of *Crh*, *Dyn*, or *Nts* led to no changes in baseline anxiety-like behavior in the open field [time in the center: F(3,39) = 1.610, P = 0.2026,

one-way ANOVA; entries into the center: $F(3,39) = 1.477$, $P = 0.2356$, one-way ANOVA, $n = 13$ sh*Con*, 11 sh*Crh*, 10, sh*Dyn*, 9 sh*Nts*]. **(D)** Knockdown of *Vgat* in CeA^{CRF} neurons reduces time spent in the open arms [$t(22) = 3.158$, $^{**}P = 0.0046$; $n = 12$ both groups, unpaired t-test] and entries into the open arms [$t(22) = 7.858$, $^{****}P < 0.0001$, $n = 12$ both groups, unpaired t-test] on the elevated plus maze. **(E)** Knockdown of *Vgat* also reduces time spent in the center [$t(22) = 2.156$, $^{*}P = 0.0423$, $n = 12$ both groups, unpaired t-test] and entries into the center [$t(22) = 2.407$, $^{*}P = 0.0249$, $n = 12$ both groups, unpaired t-test] of the open field. Data are presented as mean ± SEM.

GABA release from CeA^{CRF} neurons regulates baseline anxiety

CeA^{CRF} neurons, like other neurons of the CeA, release GABA (Dabrowska et al., 2013a; Pomrenze et al., 2015; Veinante et al., 1997). An important question is whether GABA and neuropeptide release from these neurons cooperate to regulate behavior or play different roles. Since CRF is anxiogenic, we hypothesized that GABA relase from CeA^{CRF} neurons would synergize with CRF to generate anxiety-like behavior. To test this hypothesis, we reduced GABA release potential in these neurons by viral delivery of a Cre-dependent shRNA that targets the 3'-UTR of the transcript encoding the vesicular GABA transporter (*Vgat*). This shRNA has previously been extensively validated using single-cell qPCR and behavioral analysis (Yu et al., 2015). This construct was injected into the CeA of *Crh*-Cre rats and after 4-6 weeks to allow for expression and knockdown, rats were tested for baseline anxiety-like behavior. Surprisingly, we observed increased anxiety-like behavior in both the EPM and OF tests in animals with *Vgat* knockdown compared with animals expressing the control construct (Figures 3.12D and 3.2E). No effects on locomotion in either test were found (Figures 3.6C and 3.6D). This finding suggests that GABA release from CeA^{CRF} neurons is anxiolytic under baseline conditions, a role distinct from CRF, dynorphin, and neurotensin.

Knockdown of *Vgat* in CeA^{CRF} neurons could promote anxiety through disinhibition of downstream circuits. To investigate this possibility, we challenged a separate group of rats with *Vgat* knockdown by placing them in the OF for 10 min and used Fos as a readout for neural activity engaged by OF exposure (Figure 3.3A;(Heisler et al., 2007). Control rats exposed to the OF showed low levels of Fos in the CeA and in the oval BNST, a structure that is known to modulate anxiety and is strongly connected with the CeA as part of the "extended amygdala". In contrast to controls, rats with *Vgat* knockdown

displayed a large induction of Fos in both structures (Figures 3.3B-3.3E). Several Fos$^+$ neurons in the CeA and oval BNST expressed PKCδ, a marker for a subpopulation of non-CRF neurons that when activated can drive anxiety-like behaviors in mice (Botta et al., 2015). Together, these data suggest that CeA^{CRF} neurons release GABA to dampen baseline anxiety-like behavior through inhibition of other subpopulations of neurons in the extended amygdala.

Since CeA^{CRF} neurons appeared to disinhibit neurons of the dlBNST, we wondered whether the specific neurons that project to this region express dynorphin or neurotensin. Injection of the retrograde virus CAV2 carrying a Cre-dependent ZsGreen reporter construct resulted in substantial labeling of CRF neurons in the CeA. Using ZsGreen expression as a proxy for CRF, we next performed immunohistochemistry against dynorphin or neurotensin in ZsGreen infected CeA sections. We observed considerable co-staining of ZsGreen$^+$ neurons with dynorphin (Figure 3.4B) and neurotensin (Figure 3.4C). These results demonstrate that several CeA^{CRF} neurons targeting the dlBNST express dynorphin or neurotensin, and suggest that these neurons 1) may regulate anxiety through the dlBNST and 2) might release these neuropeptides in the dlBNST.

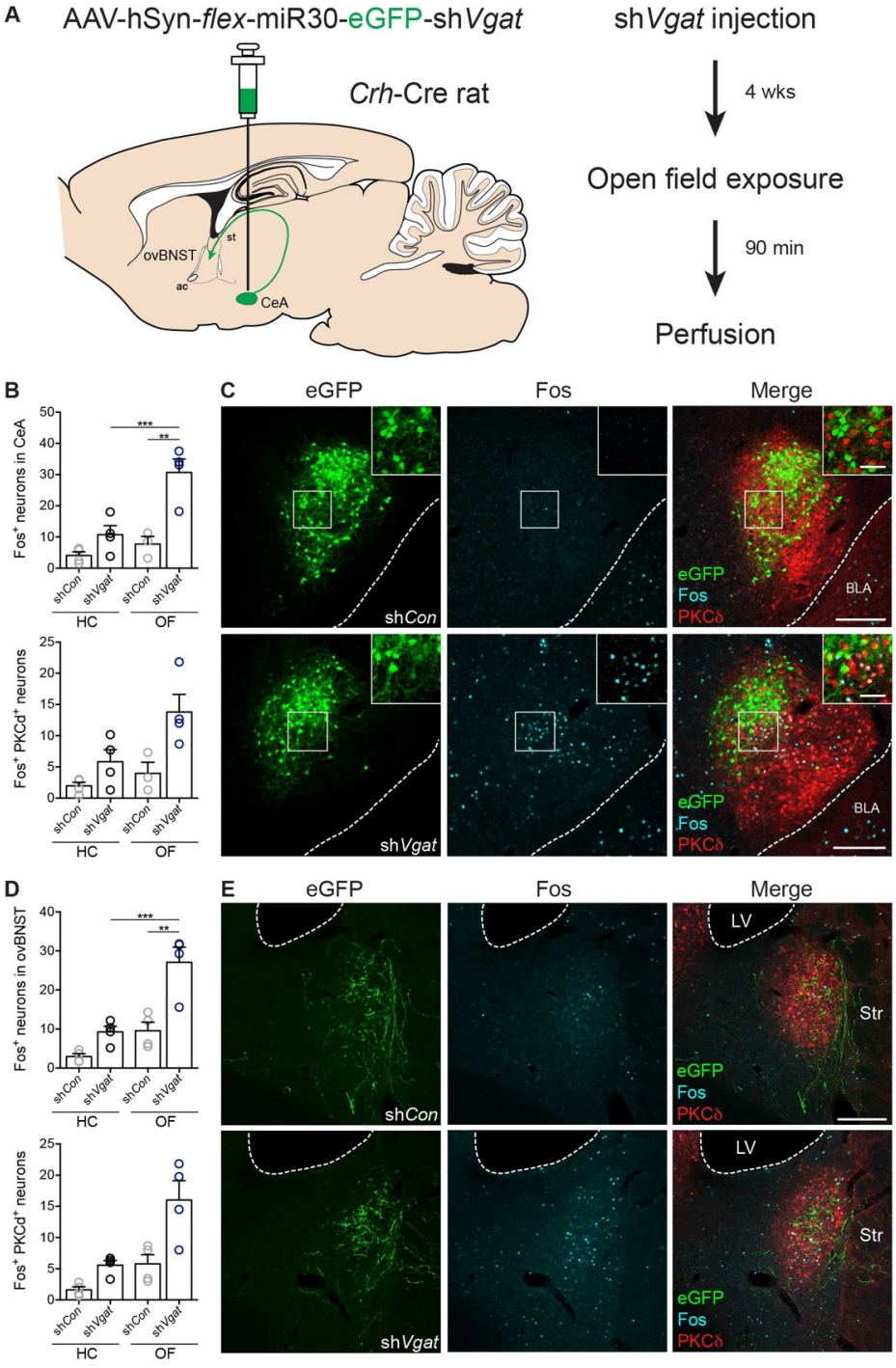

Figure 3.3. Suppression of GABA release from CeA^{CRF} neurons disinhibits the extended amygdala after open field exposure

(A) Right, viral injection schematic. Left, experimental protocol. **(B)** Top, knockdown of *Vgat* in CeA^{CRF} neurons promotes Fos expression in the CeA after open field exposure [$F_{sh\textit{Vgat} \times OF}(1,11) = 5.604$, $P = 0.0212$, two-way ANOVA, n = 3-4; $^{**}P = 0.0025$ for sh*Vgat*:HC compared with sh*Vgat*:OF and $^{**}P = 0.0015$ for sh*Con*:OF compared with sh*Vgat*:OF by Tukey's tests]. Bottom, several Fos^{+} neurons also expressed PKCδ. **(C)** Representative images demonstrating increased Fos induction in the CeA of rats expressing sh*Vgat* in CeA^{CRF} neurons. Scale bars, 200 μm. Boxed region is enlarged in inset (scale bar, 50 μm). **(D)** Top, knockdown of *Vgat* in CeA^{CRF} neurons promotes Fos expression in the oval BNST after open field exposure [$F_{sh\textit{Vgat} \times OF}(1,12) = 5.604$, $P = 0.0356$, two-way ANOVA, $n = 4$ for all groups; $^{***}P = 0.0009$ for sh*Vgat*:HC compared with sh*Vgat*:OF and $^{**}P = 0.0011$ for sh*Con*:OF compared with sh*Vgat*:OF by Tukey's tests]. Bottom, several Fos^{+} neurons also expressed PKCδ. **(E)** Representative images demonstrating increased Fos induction in the oval BNST of rats expressing sh*Vgat* in CeA^{CRF} neurons. eGFP^{+} axons emerging from CeA^{CRF} neurons are clearly visible in the oval nucleus. Scale bars, 200 μm. Data are presented as mean ± SEM.

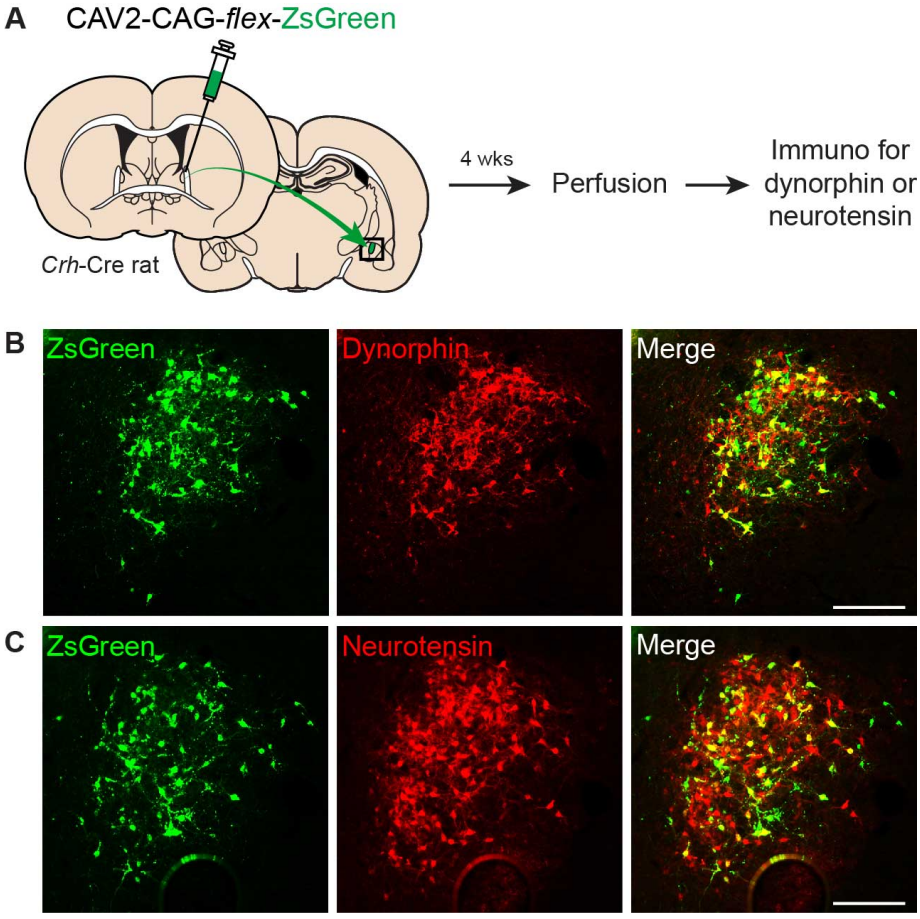

Figure 3.4. CeA^{CRF} neurons that project to the dorsolateral BNST express dynorphin and neurotensin

(A) Experimental design and injection schematic of CAV2 carrying Cre-dependent ZsGreen construct for retrograde labeling of CeA^{CRF} neurons. **(B)** Example of dynorphin expression in dlBNST-projecting CeA^{CRF} neurons. Scale bar, 200 μm. **(C)** Example of neurotensin expression in dlBNST-projecting CeA^{CRF} neurons. Scale bar, 200 μm.

Activation of CeA^{CRF} neurons promotes anxiety through CRF and dynorphin

CeA^{CRF} neurons can promote anxiety-like behavior when stimulated (McCall et al., 2015; Pliota et al., 2018) Chapter 2) and overexpression of CRF in the CeA of rats and primates is anxiogenic (Flandreau et al., 2012; Kalin et al., 2016; Keen-Rhinehart et al., 2009). Therefore, we investigated whether CRF is necessary for the increased anxiety-like behavior observed when CeA^{CRF} neurons are activated. To stimulate CeA^{CRF} neurons, we transduced them with a cocktail of the Cre-dependent excitatory designer receptor hM3Dq and the shRNA against *Crh*. Our previous work showed that hM3Dq stimulation of CeA^{CRF} neurons can increase anxiety-like behavior in EPM and OF assays (Chapter 2), consistent with a recent report in mice (Pliota et al., 2018). All animals received an injection of CNO (2 mg/kg, *i.p.*) and shortly after were placed on the EPM or in the OF. Rats with *Crh* knockdown showed less anxiety-like behavior in the EPM test compared with controls, but no differences in the OF test (Figures 3.5B and 3.5C). These data suggest that CRF release promotes anxiety on the EPM but not in the OF, similar to the results obtained using hM3Dq and the CRF1 receptor antagonist R121919 (Figure 2.4, Chapter 2).

Many CeA^{CRF} neurons express dynorphin, and it has been reported that the anxiogenic effects of central CRF administration are dependent on dynorphin/kappa opioid receptor signaling (Bruchas et al., 2009). To investigate whether stimulation of CeA^{CRF} neurons and the resulting anxiety-like behavior depends on release of dynorphin, we repeated the hM3Dq experiment above but injected rats with an shRNA targeting *Dyn* instead of *Crh*. Compared with control animals, rats with *Dyn* knockdown showed reduced anxiety-like behavior in both the EPM and OF tests (Figures 3.5D and 3.5E). Injections of neurotensin into the CeA do not modulate anxiety-like behavior (Laszlo et al., 2010). To determine whether neurotensin release from CeA^{CRF} neurons contributes to evoked anxiety,

we repeated this same experiment once again but with knockdown of *Nts*. Disrupting *Nts* expression in CeA^{CRF} neurons lead to no detectable differences in either the EPM or OF tests after stimulation with hM3Dq (Figures 3.5F and 3.5G). Altogether, these results indicate that CRF and dynorphin, but not neurotensin expression in CeA^{CRF} neurons regulate anxiety-like behavior.

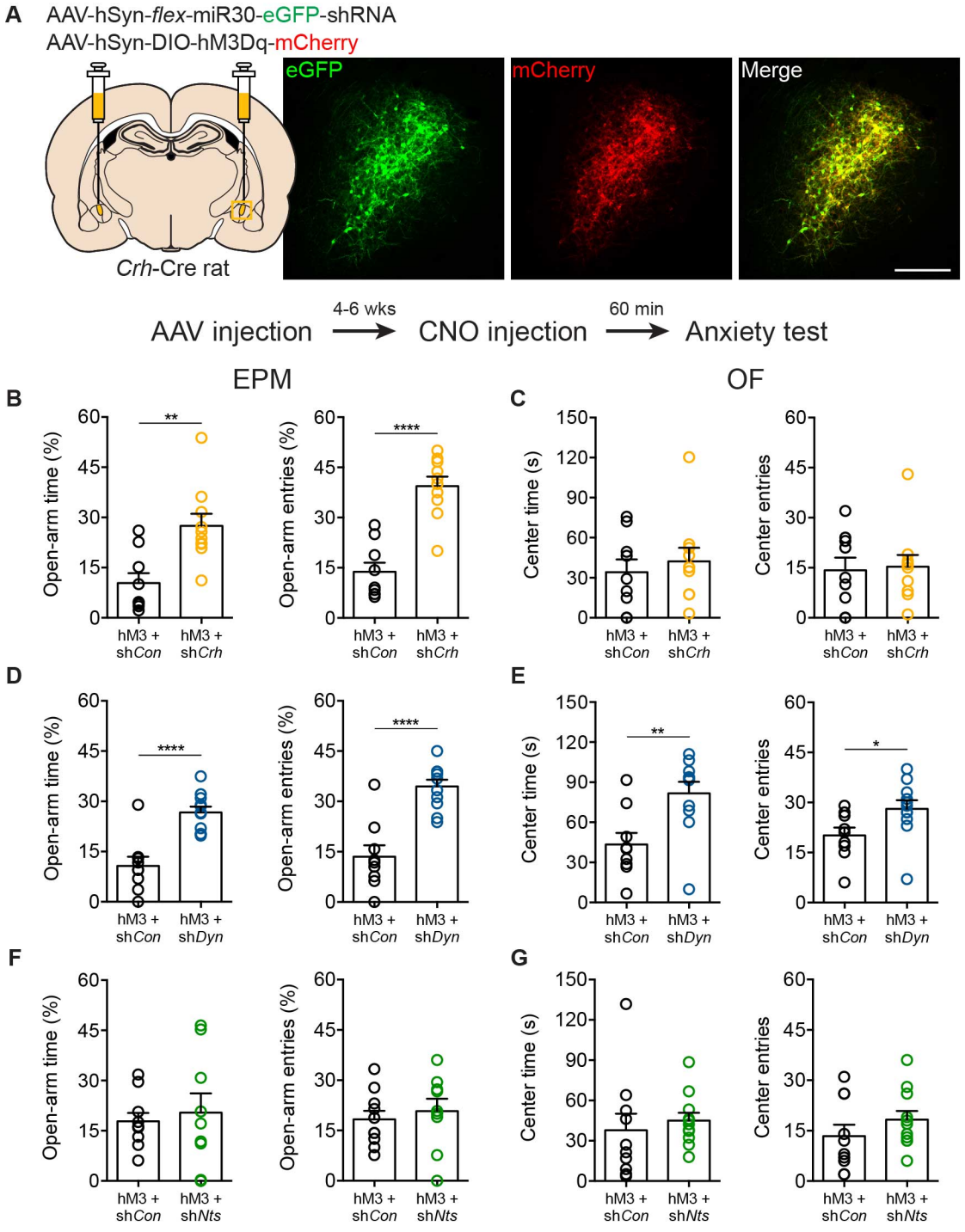

Figure 3.5. CeA^{CRF} neurons promote anxiety with CRF and dynorphin, but not neurotensin

(A) Top, example image of dual infection of CeA^{CRF} neurons with cocktail of AAVs carrying shRNAs and hM3Dq. Scale bar, 200 μm. Bottom, experimental protocol. **(B)** Knockdown of *Crh* lead to more time spent on the open arms [$t(17) = 3.613$, $^{**}P = 0.0021$, $n = 9$ sh*Con*, 10 sh*Crh*, unpaired t-test] and more entries into the open arms [$t(17) = 6.468$, $^{****}P < 0.0001$, $n = 9$ sh*Con*, 1 sh*Crh*, unpaired t-test] of the elevated plus maze after activation of CeA^{CRF} neurons with hM3Dq and CNO (2 mg/kg, *i.p.*). **(C)** Knockdown of *Crh* did alter anxiety-like behavior in the open field [center time: $t(17) = 0.854$, $P = 0.5669$, unpaired t-test; center entries: $t(17) = 0.208$, $P = 0.8376$, $n = 9$ sh*Con*, 10 sh*Crh*, unpaired t-test] after activation of CeA^{CRF} neurons with hM3Dq and CNO (2 mg/kg, *i.p.*). **(D)** Knockdown of *Dyn* also lead to more time spent on the open arms [$t(18) = 5.151$, $^{****}P < 0.0001$, $n = 9$ sh*Con*, 11 sh*Dyn*, unpaired t-test] and more entries into the open arms [$t(18) = 5.589$, $^{****}P < 0.0001$, $n = 9$ sh*Con*, 11 sh*Dyn*, unpaired t-test] of the elevated plus maze after activation of CeA^{CRF} neurons. **(E)** Knockdown of *Dyn* lead to more time spent in the center [$U = 15$, $^{**}P = 0.0074$, $n = 9$ sh*Con*, 11 sh*Dyn*, Mann-Whitney test] and more entries into the center [$U = 17.5$, $^{*}P = 0.013$, $n = 9$ sh*Con*, 11 sh*Dyn*, unpaired t-test] of the open field after activation of CeA^{CRF} neurons. **(F)** Knockdown of *Nts* did not change the time spent on the open arms [$t(17) = 0.4315$, $P = 0.6716$, $n = 10$ sh*Con*, 9 sh*Nts*, unpaired t-test] or entries into the open arms [$t(17) = 0.5536$, $P = 0.5871$, $n = 10$ sh*Con*, 9 sh*Nts*, unpaired t-test] of the elevated plus maze after activation of CeA^{CRF} neurons. **(G)** Knockdown of *Nts* did not change the time spent in the center [$U = 30$, $P = 0.2428$, $n = 10$ sh*Con*, 9 sh*Nts*, Mann-Whitney test] and more entries into the center [$t(17) = 1.319$, $P = 0.2046$, $n = 10$ sh*Con*, 9 sh*Nts*, unpaired t-test] of the open field after activation of CeA^{CRF} neurons. Data are presented as mean ± SEM.

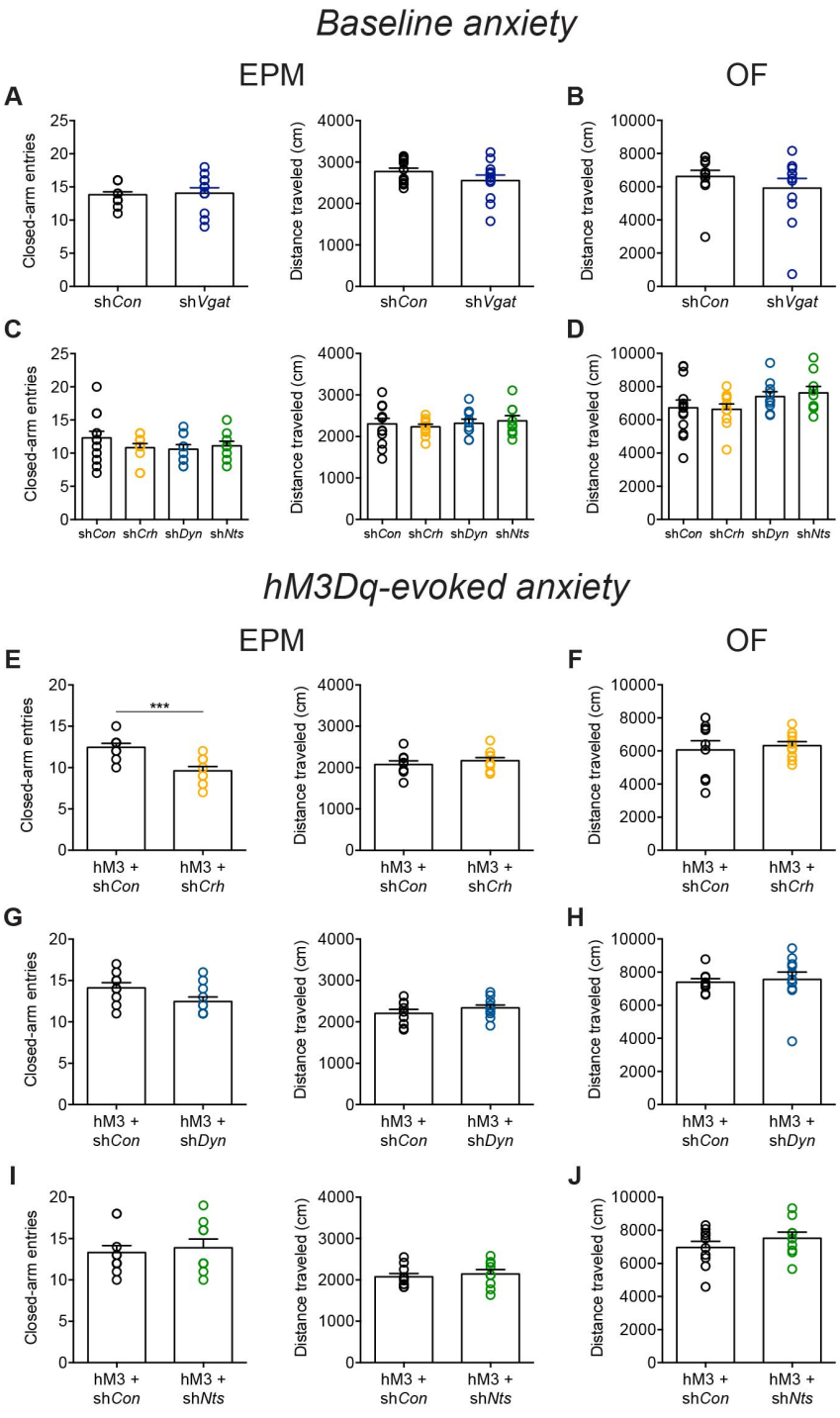

Figure 3.6. Locomotor data for anxiety testing after gene knockdown in CeA^{CRF} neurons

(A) Neuropeptide knockdown had no effects on baseline closed-arm entries [F(3,39) = 0.9954, $P = 0.64051$, one-way ANOVA, $n = 13$ sh*Con*, 11 sh*Crh*, 10, sh*Dyn*, 9 sh*Nts*] or distance traveled [F(3,39) = 0.2879, $P = 0.8338$, one-way ANOVA, $n = 13$ sh*Con*, 11 sh*Crh*, 10, sh*Dyn*, 9 sh*Nts*] on the EPM. **(B)** Neuropeptide knockdown had no effect on baseline locomotion in the OF [F(3,39) = 1.516, $P = 0.2255$, one-way ANOVA, $n = 13$ sh*Con*, 11 sh*Crh*, 10, sh*Dyn*, 9 sh*Nts*]. **(C)** *Vgat* knockdown had no effects on baseline closed-arm entries [t(22) = 0.271, $P = 0.789$, $n = 12$ both groups, unpaired t-test] or distance traveled [t(22) = 1.382, $P = 0.181$, $n = 12$ both groups, unpaired t-test] on the EPM. **(D)** *Vgat* knockdown had no effect on baseline locomotion in the OF [t(22) = 1.01, $P = 0.323$, $n = 12$ both groups, unpaired t-test]. **(E)** Knockdown of *Crh* in hM3Dq-stimulated CeA^{CRF} neurons reduced closed-arm entries [t(17) = 4.005, ***$P = 0.0009$; $n = 9$ sh*Con*, 10 sh*Crh*, unpaired t-test] but did not affect locomotion [t(17) = 0.7922, $P = 0.391$; $n = 9$ sh*Con*, 10 sh*Crh*, unpaired t-test] on the EPM. **(F)** Knockdown of *Crh* in hM3Dq-stimulated CeA^{CRF} neurons had no effect on locomotor activity [t(17) = 0.4322, $P = 0.06711$; $n = 9$ sh*Con*, 10 sh*Crh*, unpaired t-test] in the OF. **(G)** Knockdown of *Dyn* in hM3Dq-stimulated CeA^{CRF} neurons had no effect on closed-arm entries [t(18) = 1.992, $P = 0.0618$; $n = 9$ sh*Con*, 11 sh*Dyn*, unpaired t-test] or locomotion t(18) = 1.142, $P = 0.2685$; $n = 9$ sh*Con*, 11 sh*Dyn*, unpaired t-test] on the EPM. **(H)** Knockdown of *Dyn* in hM3Dq-stimulated CeA^{CRF} neurons had no effect on locomotor activity [t(18) = 0.3223, $P = 0.7509$; $n = 9$ sh*Con*, 11 sh*Dyn*, unpaired t-test] in the OF. **(I)** Knockdown of *Nts* in hM3Dq-stimulated CeA^{CRF} neurons had no effect on closed-arm entries [t(17) = 0.4389, $P = 0.6663$; $n = 10$ sh*Con*, 9 sh*Nts*, unpaired t-test] or locomotion [t(17) = 0.5074, $P = 0.6184$; $n = 10$ sh*Con*, 9 sh*Nts*, unpaired t-test] on the EPM. **(J)** Knockdown of *Nts* in hM3Dq-stimulated CeA^{CRF} neurons had no effect on [t(17) = 1.043, $P = 0.3118$; $n = 10$ sh*Con*, 9 sh*Nts*, unpaired t-test] in the OF.

CRF, dynorphin, and neurotensin, but not GABA release from CeA^{CRF} neurons modulates fear learning

The contribution of CRF in the CeA to fear learning appears somewhat inconsistent. In mice, knockdown of *Crh* in the CeA had little effect on fear behavior (Regev et al., 2012), yet *Crh* knockout *via* Cre-mediated gene deletion disrupted fear acquisition (Sanford et al., 2017). Knockdown of *Crh* in rat CeA lead to deficits in contextual fear memory consolidation (Pitts et al., 2009). Using our Cre-dependent shRNA targeting *Crh*, we observed no effects on shock-induced freezing during the conditioning session of a standard fear learning procedure (Figure 3.7B). However, freezing to the fear context and tone cues was significantly reduced in rats with *Crh* knockdown (Figure 3.7C). These data are consistent with previous studies done in rats. Similar to CRF, blockade of kappa opioid receptors in the amygdala decreased conditioned fear in rats (Knoll et al., 2011). *Crh*-Cre rats with *Dyn* knockdown in CeA^{CRF} neurons exhibited similar disruptions in contextual and cued fear retrieval (Figure 3.7C).

Neurotensin signaling has also been reported to regulate fear behaviors. Neurotensin 1 receptor knockout mice displayed enhanced fear expression and neurotensin receptor agonists reduced conditioned footshock-induced ultrasonic vocalizations in rats (Prus et al., 2014; Steele et al., 2017; Yamada et al., 2010). Additionally, neurotensin receptor antagonists enhance whereas agonists dampen conditioned fear when injected into the CeA (Toda et al., 2014). *Crh*-Cre rats with *Nts* knockdown in CeA^{CRF} neurons showed no differences in shock-induced freezing or contextual fear expression. However, cued freezing was significantly enhanced by lack of neurotensin in these neurons. These data suggest that different neuropeptides secreted by CeA^{CRF} neurons play distinct roles in regulating fear behaviors.

The data presented above demonstrate the necessity of CeA^{CRF} neuron secretion of CRF, dynorphin, and neurotensin in the modulation of fear learning. We next asked whether GABA transmission from these neurons plays a similar role. *Crh*-Cre rats were injected with AAV carrying the sh*Vgat* construct and subjected to fear conditioning. Surprisingly, knockdown of *Vgat* in CeA^{CRF} neurons had little effect on fear learning or expression (Figure 3.7C). Together, these data demonstrate the differential roles of neuropeptides and GABA from CeA^{CRF} neurons in fear learning.

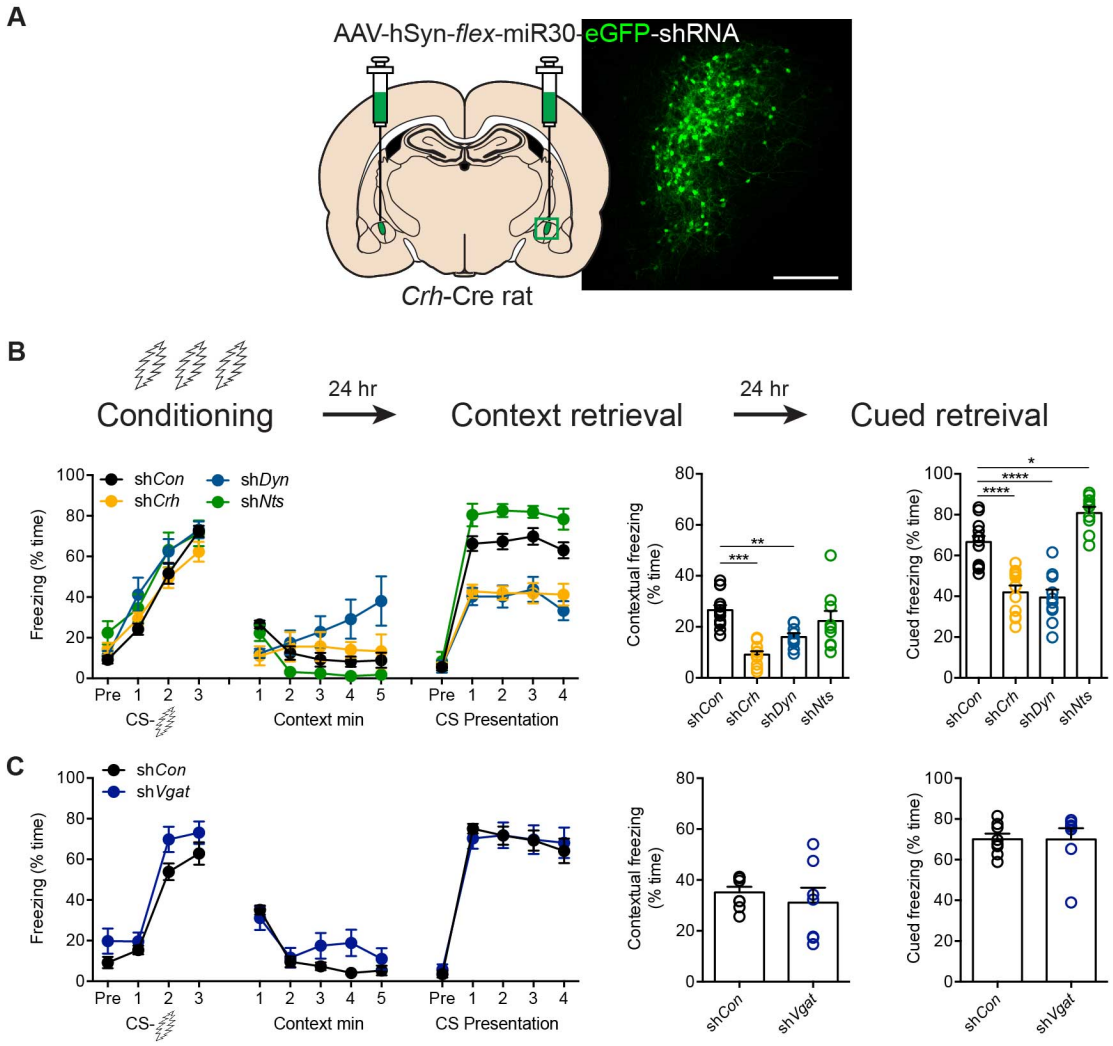

Figure 3.7. CeA^{CRF} neurons differentially modulate fear learning with CRF, dynorphin, and neurotensin

(A) Injection schematics and example of viral expression in CeA^{CRF} neurons for shRNA knockdown. Scale bar, 200 μm. **(B)** Top, experimental protocol. Bottom, shRNA-mediated knockdown of *Crh* and *Dyn*, but not *Nts* in CeACRF neurons blunted contextual fear retrieval during the first minute [F(3,38) = 12.53, $P < 0.0001$, one-way ANOA, $n = 13$ sh*Con*, 11 sh*Crh*, 9 sh*Dyn*, 9 sh*Nts*; ***$P < 0.0001$ sh*Crh* compared with sh*Con*; **$P =$

0.0054 sh*Dyn* compared with sh*Con* by Dunnett's test]. Knockdown of *Crh* and *Dyn* also reduced cued freezing, yet knockdown of *Nts* enhanced cued freezing [$F(3,39) = 34.13$, $P < 0.0001$, one-way ANOVA, $n = 13$ sh*Con*, 11 sh*Crh*, 10 sh*Dyn*, 9 sh*Nts*; ****$P < 0.0001$ sh*Crh* compared with sh*Con*; ****$P < 0.0001$ sh*Dyn* compared with sh*Con*; *$P = 0.0115$ sh*Nts* compared with sh*Con* by Dunnett's test]. **(C)** Knockdown of *Vgat* in CeA^{CRF} neurons did not affect contextual [$t(13) = 0.6684$, $P = 0.5156$, $n = 8$ sh*Con*, 7 sh*Vgat*, unpaired t-test] or cued fear learning [$t(13) = 0.0125$, $P = 0.9902$, $n = 8$ sh*Con*, 7 sh*Vgat*, unpaired t-test]. Data are presented as mean ± SEM.

DISCUSSION

We have demonstrated that CRF neurons of the central amygdala release different neurotransmitters to differentially regulate fear and anxiety-like behaviors. We show that at baseline under non-stressful conditions, the expression of CRF, dynorphin, and neurotensin and presumably their release contributes minimally to anxiety-like behavior, implying minimal neuropeptide tone in the non-stressed state. However, the release of GABA, as determined by knockdown of *Vgat* in these neurons, is critically important in maintaining a low baseline level of anxiety as measured by the EPM and OF tests. We further find that in rats with chemogenetic stimulation of CeA^{CRF} neurons, the evoked anxiety-like behavior is prevented by knockdown of *Crh* and *Dyn*, but not *Nts*. Together these results suggest that different neurotransmitters released from CeA^{CRF} neurons regulate anxiety behavior through divergent signaling mechanisms.

At baseline, a tonic and anxiolytic GABA tone from CeA^{CRF} neurons may help balance microcircuits local to the CeA and remotely in the oval BNST. In this manner GABA released from CeA^{CRF} neurons could act as a gate of neuronal output that promotes anxiety. The absence of neuropeptide release under non-stressful conditions is consistent with previous studies showing that neuropeptide receptor antagonists block stress-induced behaviors but not those at baseline (Berridge and Dunn, 1987; Bruchas et al., 2009; Normandeau et al., 2018b). This is also consistent with the idea that high frequency neuronal stimulation is required for neuropeptide release (van den Pol, 2012). We used the stimulatory designer receptor hM3Dq to drive the activity of CeA^{CRF} neurons, a procedure that has been demonstrated as being anxiogenic (Pliota et al., 2018)Chapter 2). Under this condition, we were able to prevent anxiety-like behavior with knockdown of *Crh* or *Dyn*. These data are supported by previous studies evaluating the role of these peptides in anxiety

(Crowley et al., 2016; Knoll et al., 2007; Knoll et al., 2011; McCall et al., 2015; Regev et al., 2012) and help confirm the hypothesis that CRF and dynorphin synergize to modulate anxiety (Bruchas et al., 2009). Interestingly, knockdown of *Nts* had no detectable effects on hM3Dq-evoked anxiety. Consistent with this result, neurotensin signaling in the CeA has been reported to play minimal roles in baseline anxiety-like behavior (Laszlo et al., 2010), but does mediate chronic stress-induced anxiety in the oval BNST (Normandeau et al., 2018b). This suggests that neurons might release different neurotransmitters to achieve a 'balanced' effect on behavioral output. How a neuron coordinates the release of different peptides for different purposes, and how the co-release of multiple peptides coordinates downstream signaling to achieve a common goal is most likely complex and should be the focus of future studies.

One interesting observation was the effect of disrupting CeA^{CRF} release on evoked anxiety behavior. Both *Crh* knockdown and blockade of CRF1 receptors with R121919 (Figure 2.4) prevented induced anxiety on the EPM, but not in the OF test. However knockdown of *Dyn* prevented anxiety in both assays. It is possible that differences in the two tests could explain this divergent result. The plus maze could be considered a less stressful and anxiogenic apparatus since the closed arms represent 'safety' areas, whereas the open field offers less protection and could lead to behaviors more characteristic of despair, aversion, and helplessness. In the open field, other peptides, such as dynorphin, could wash out the effects of CRF due to its relative inescapable properties. As such, there have been reports of brain manipulations having effects in certain anxiety tests and not others (Schmidt and Duman, 2010). Future studies should dissect the role of different peptides in different anxiety tests and determine where in the brain these might be mediated.

We used the inhibitory designer receptor hM4Di to inhibit all CeA^{CRF} neurons during a standard fear conditioning procedure. These neurons mediated fear learning during the conditioning session when shocks were delivered since inhibition at other time points (immediately after conditioning or before retrieval trials) had no effects. This is consistent with previous studies done in mice (Sanford et al., 2017) and rats (Asok et al., 2018). We next asked which neurotransmitters were responsible for CeA^{CRF} neuron contributions to fear learning. Knockdown of *Crh* or *Dyn* in these neurons disrupted contextual and cued fear responses during retrieval trials, whereas knockdown of *Nts* enhanced cued fear responding. Since gene knockdown is a chronic manipulation, it is typically unclear how the genes of interest contribute to learned behaviors since there could be effects on learning and/or expression. Our experiment with hM4Di demonstrates CeA^{CRF} neurons as critical to conditioning, but not expression. Thus, it is likely that the CeA-derived peptides we assessed are contributing to fear learning and not fear expression.

Our data are supported by previous reports showing that in the CeA, CRF and dynorphin promote fear behaviors (Fanselow et al., 1991; Knoll et al., 2007; Knoll et al., 2011; Pitts et al., 2009; Sanford et al., 2017), whereas neurotensin signaling dampens fear (Prus et al., 2014; Steele et al., 2017; Yamada et al., 2010). Therefore, using the CRF gene as a cellular entry point, we have demonstrated that the same population of central amygdala neurons can play multimodal roles fear and anxiety behaviors. Future efforts should determine which signaling molecules released from CeA^{CRF} neurons play critical roles in other emotional behaviors, such as those associated with reward, pain, and feeding.

Our results suggest opposing roles of different peptides in aversive learning. This could explain why stimulation of CRF neurons can lead to both appetitive (Dedic et al., 2018; Kim et al., 2017) and aversive behavioral outputs. Thus, when CeA^{CRF} neurons are

stimulated, the release of multiple neuropeptides could lead to complex behavioral results depending on the testing environment. It is paradoxical that animals will self-stimulate neurons that also mediate negative emotions and learning (Asok et al., 2018; Kim et al., 2017; Sanford et al., 2017). However, this is relatively unsurprising given that key components of these behaviors involve arousal and attention, which may drive self-stimulation independent of its rewarding components. In addition, parallel antagonistic circuits nested within the CRF system may control behaviors with different emotional valence (Dedic et al., 2018). In any case, all of the studies discussed so far have led us to the conclusion that CeA^{CRF} neurons contribute globally to behavioral responses associated with extreme valence (whether positive or negative).

Our study has demonstrated the versatility of CeA^{CRF} neurons in regulating fear and anxiety at the level of their released neurotransmitters. CRF and dynorphin promote fear and anxiety, whereas neurotensin and GABA play more complex roles in these behaviors. Our data show that amygdala neurons are not dedicated to subserving just one type of process. Furthermore, our findings suggest that CRF neurons, and perhaps the CRF system as whole, interacts strongly with other neuropeptide systems. This property could account for the negative results obtained in clinical trials evaluating CRF receptor antagonists in the treatment of stress-induced alcohol craving and negative emotions associated with PTSD. Our results should contribute to a more fundamental understanding of how brain systems interact to regulate behavior and to developing more effective therapeutic strategies for neuropsychiatric disorders associated with both positive and negative emotional states.

ACKNOWLEDGMENTS

For assistance with these studies, I am indebted to Simone Giovanetti for generating final shRNA constructs, testing their efficacies both *in vitro* and *in vivo*, and her intellectual contributions. I am also indebted to Dr. Rajani Maiya for her assistance gathering data and her intellectual contributions. I also thank Dr. Larry Zweifel from the University of Washington in Seattle for his generous contribution of the CAV2-*flex*-ZsGreen virus. Finally, I am grateful to Dr. Robert Messing for providing space and funding for the project, and his intellectual contributions. And of course, the National Science Foundation for my funding (NSF fellowship DGE-1110007).

CHAPTER 4: CENTRAL AMYGDALA CRF NEURONS INTERACT WITH BNST CRF NEURONS TO REGULATE ANXIETY

ABSTRACT

The central amygdala (CeA) is important for fear responses to discrete cues. Recent findings indicate that the CeA also contributes to states of sustained apprehension that characterize anxiety, although little is known about the neural circuitry involved. The stress neuropeptide corticotropin releasing factor (CRF) is anxiogenic and is produced by subpopulations of neurons in the lateral CeA and the dorsolateral BNST (dlBNST). Here we investigated the function of these CRF neurons in stress-induced anxiety using chemogenetics in rats that express Cre recombinase from a *Crh* promoter. Anxiety-like behavior was mediated by CRF projections from the CeA to the dlBNST and depended on activation of CRF1 receptors and CRF neurons within the dlBNST. These findings identify a $CeA^{CRF} \rightarrow dlBNST^{CRF}$ circuit for generating anxiety-like behavior and provide mechanistic support for recent human and primate data suggesting that the CeA and BNST act together to generate states of anxiety.

INTRODUCTION

Threatening environments evoke fear and anxiety, which are two ethologically different defensive behavioral responses that are driven by conserved brain circuits and promote survival (LeDoux and Brown, 2017; Panksepp, 2011). Fear responses are acute and generated when animals are presented with an imminent threat or a cue that predicts the threat. In contrast, environments providing ambiguous or diffuse cues for threat prediction promote a sustained state of avoidance, apprehension, and risk-assessment, i.e. anxiety. Both of these behavioral profiles are adaptive and essential to survival, yet exaggerated and persistent fear and anxiety reactions can be maladaptive and hinder survival. Unfortunately, anxiety disorders are prevalent psychiatric conditions that cause substantial morbidity worldwide (Baxter et al., 2013).

The neuronal circuitry underlying fear has been extensively studied and the amygdala has emerged as a critical component. The circuits governing anxiety are less understood but were originally considered to be independent of the amygdala. An influential conceptual framework that emerged from early lesion and inactivation studies proposed that the central nucleus of the amygdala (CeA) mediates fear responses to discrete threats, while the bed nucleus of the stria terminalis (BNST), a forebrain structure with strong connections to the amygdala (together referred to as the extended amygdala), mediates states of anxiety (Walker et al., 2003). However, with the advent of new tools allowing access to genetically-defined neuronal populations, recent work has demonstrated the CeA as a potent driver of anxiety-like behavior in mice (Ahrens et al., 2018; Botta et al., 2015; McCall et al., 2015; Pliota et al., 2018) and rats (Chapters 2 and 3).

A role for the neuropeptide corticotropin releasing factor (CRF) in anxiety has been suspected because of its control over neuroendocrine responses to stress (Bale and Vale,

2004; Binder and Nemeroff, 2010; Koob, 2009) and its high expression in the extended amygdala (Asan et al., 2005; Nguyen et al., 2016; Pomrenze et al., 2015; Sanford et al., 2017). In agreement with this hypothesis, CRF administration into the ventricles or the dorsolateral BNST (dlBNST) in rats generates anxiety-like behaviors (Lee and Davis, 1997; Liang et al., 1992b; Sahuque et al., 2006; Swerdlow et al., 1986) that are reduced by CRF1 receptor antagonists injected into the BNST, but not into the CeA (Lee and Davis, 1997; Sahuque et al., 2006). Thus, the BNST appears to orchestrate anxiety-like responses that are dependent on CRF.

The source of CRF that acts in the BNST to generate anxiety is not certain. One possibility is the population of CRF neurons that reside within the BNST. Another source could be CeA^{CRF} neurons since activation of those neurons can produce anxiety-like behavior in mice (McCall et al., 2015; Pliota et al., 2018; Regev et al., 2012) and rats (Chapters 2 and 3), and in rats a considerable portion of CRF in the dorsolateral BNST (dlBNST) originates from CeA^{CRF} neurons (Sakanaka et al., 1986). In addition, neuropeptides that have been reported to be anxiogenic in the BNST, such as dynorphin and neurotensin (Crowley et al., 2016; Normandeau et al., 2018b) are co-expressed in CeA^{CRF} neurons (Figure 3.4, Chapter 3). However, a role for CeA^{CRF} projections to the BNST in anxiety has not yet been demonstrated.

Here, we provide evidence in rats that stress-induced anxiety is critically dependent on CeA^{CRF} projections to the dlBNST and on activation of CRF1 receptors and CRF neurons in the dlBNST. Our findings identify a circuit by which CRF neurons in the CeA and BNST cooperate in series to generate anxiety. These results support recent human and primate data suggesting that the CeA and BNST work together as a functional unit to generate anxiety (Gungor and Paré, 2016; Shackman and Fox, 2016).

MATERIALS AND METHODS

Subjects

All experiments and procedures were approved by the University of Texas at Austin Institutional Animal Care and Use Committee. We used male heterozygous *Crh*-Cre rats (Pomrenze et al., 2015) outcrossed to wild-type Wistar rats (Envigo, Houston, TX), aged 5-6 weeks at the start of the surgical procedures and 10-14 weeks at the start of experimental procedures. Rats were group housed and maintained on a 12 hr light:dark cycle (lights on 4AM to 4PM) with food and water available *ad libitum*. Rats prepared with guide cannulas were singly housed. All experiments were done between 9AM and 3PM. Rats were randomly assigned to either experimental or control groups within each litter.

Drugs and viral vectors

Clozapine-N-oxide (CNO) was supplied through the NIMH Chemical Synthesis and Drug Supply Program. CNO (2 mg/kg body weight) was dissolved in 5% dimethyl sulfoxide (DMSO) and then diluted to 2 mg/mL with 0.9% saline. For intracerebral administration, CNO was dissolved in 0.5% DMSO and then diluted to 1mM in aCSF (Harvard Apparatus, Holliston, MA) (Mahler et al., 2014). The selective CRF1 receptor antagonist R121919 (3-[6-(dimethylamino)-4-methyl-pyrid-3-yl]-2,5-dimethyl-N,N-dipropyl-pyrazolo[2,3-a]pyrimidin-7-amine, NBI 30775, was a gift from Dr. Kenner Rice (Chemical Biology Research Branch, Drug Design and Synthesis Section, National Institute on Drug Abuse and National Institute on Alcohol Abuse and Alcoholism, Rockville, MD) and dissolved in a 1:1 solution of 0.9% saline and 1N HCl before adding 25% hydroxypropyl-β-cyclodextrin (HBC) to yield a final concentration of 10mg/mL R121919 in 20% HBC, pH 4.5. For intracerebral infusion, R121919 was prepared in 4% kolliphor RH 40 in aCSF, pH

5. Salvinorin B (SalB; Apple Pharms, Asheville, NC) was dissolved in 100% DMSO at 15 mg/mL, followed by 5 min of sonication. SalB was administered at 15 mg/kg body weight. All systemic injections were administered at 1mL/kg, except for R121919 which was administered at 2 mL/kg.

Cre-dependent adeno-associated viral vectors AAV8-hSyn-DIO-hM3Dq-mCherry, AAV8-hSyn-DIO-hM4Di-mCherry, AAV8-hSyn-DIO-mCherry, AAV5-EF1α-DIO-eYFP, AAV2-Ef1α-flex-taCaspase3-TEVp, and AAV9-hSyn-DIO-KORD-IRES-mCitrine were obtained from the University of North Carolina Viral Vector Core and were injected at 4-6 × 10^{12} infectious units per mL. Canine adeno virus 2 (CAV2) carrying a *flex*-ZsGreen reporter expressed from the CAG promoter (CAV2-CAG-flex-ZsGreen) was a gift from Dr. Larry Zweifel (University of Washington, Seattle, WA) and was injected at 2 × 10^{12} infectious units per mL.

Stereotaxic surgery

At the start of surgical procedures, rats were anesthetized with isoflurane (5% v/v) and placed in a stereotaxic frame (David Kopf Instruments, Tujunga, CA, USA). Viruses were injected into the CeA (AP: -2.1; ML: ± 4.5; DV: -8.0 from skull) or dlBNST (AP: -0.0; ML: ± 3.5; DV: -6.8 from skull, 16° angle) at a rate of 150nL min-1 over 5 min (750-800nL total volume per hemisphere) with a custom 32-gauge injector cannula coupled to a pump-mounted 2μL Hamilton syringe. Injectors were slowly retracted after a 5-min diffusion period. Rats were 190-220 g at the time of viral injection. Virus-injected rats were group housed to recovery for 1-2 months before behavioral or histological examination.

Two to three months after viral injection, rats used for intracerebral targeting were bilaterally implanted with stainless steel guide cannulas (Plastics One) directed to the

dlBNST (AP: -0.2; ML: ± 3.55; DV: -5.1 from skull, 18° angle; injector tips emerged 2 mm from the cannula tips). Cannulas were affixed to the skull with stainless steel screws and dental acrylic (H00325, Coltene, Altstätten, Switzerland). Cannula-implanted rats were administered the antibiotic cefazolin (100 mg/kg, *s.c.*) and singly housed during a 1-2 week recovery period before experiments.

Immobilization stress (IMS)

Rats were transferred to an experimental room distinct from the behavioral testing room and placed in ventilated plastic Decapicone bags (Braintree Scientific, Braintree, MA, USA) for 30 min. Each rat was monitored every 5 min to ensure sufficient immobilization and respiration rate. Rats were tested for anxiety-like behavior 10 min later. Some rats received injections of the CRF1 receptor antagonist R121919 (20 mg/kg, *s.c.*) 60 min prior to stress. Separate groups of rats received CNO 1mM in 0.3μL (300 pmol) via cannula 5 min prior to stress.

Behavior

We used three assays to evaluate anxiety-like behavior: the elevated plus maze (EPM), the open field test (OF) and the social interaction test. Anxiety testing occurred in a room that was different than the one used to immobilize and administer drugs. The elevated plus maze consisted of two open arms (50 x 10 cm) and two enclosed arms (50 x 10 x 40 cm) connected by a central area measuring 10 x 10 cm, 50 cm above the floor. At the beginning of each trial, rats were placed in the center facing one open arm. Trials lasted for 6 min and were performed under red lighting to promote exploration. The open field consisted of an open topped arena (100 x 100 x 50 cm) situated on the floor. The center area was designated

as a central zone measuring 55 x 55 cm. Rats were placed into a corner of the arena at the beginning of each trial. Each test lasted for 10 min and was performed under red lighting to promote exploration of the center. Social interaction was measured by placing a novel juvenile rat (4-5 weeks) into a 70 x 70 cm arena and then placing an experimental adult rat into the arena. The adult rat was allowed to interact with the juvenile rat for 5 min under red lighting. Exploratory behaviors such as allogrooming, sniffing, and pinning initiated by the adult rat were considered interactions (Christianson et al., 2010). All testing equipment was cleaned with 70% ethanol between trials. Behaviors were tracked with EthoVision (Noldus Information Technology, Leesburg, VA, USA).

Chemogenetic manipulations

Crh-Cre rats were microinjected bilaterally in the CeA with AAV8-hSyn-DIO-hM3Dq-mCherry, AAV8-hSyn-DIO-hM4Di-mCherry, or AAV8-hSyn-DIO-mCherry. To manipulate CeA^{CRF} projections to dlBNST, we bilaterally injected AAV8-hSyn-DIO-hM4Di-mCherry, AAV8-hSyn-DIO-hM3Dq-mCherry, or AAV8-hSyn-DIO-mCherry into the CeA and after 8-10 weeks implanted bilateral guide cannulas directed at the dlBNST. After 1-2 weeks of recovery, we administered CNO (1mM in 0.3µL) through the BNST cannulas prior to immobilization stress and behavioral testing. To inhibit CRF1 receptors, we administered R121919 systemically at 20 mg/kg *s.c.*, 30 min prior to administering CNO, or into the dlBNST at 1µg in 0.3µL, 5 min prior to injecting CNO.

To investigate the interdependence of CeA^{CRF} and $dlBNST^{CRF}$ neurons, we unilaterally injected AAV8-hSyn-DIO-hM3Dq-mCherry into the CeA and AAV9-hSyn-DIO-KORD-IRES-mCitrine that expresses the inhibitory kappa opioid receptor DREADD (KORD) into the ipsilateral dlBNST, counterbalanced with respect to the injected

hemisphere. After a 4-6-week recovery rats were administered CNO (2 mg/kg, *i.p.*), SalB (15 mg/kg, *s.c.*) or CNO plus SalB (separate injections), and tested for anxiety-like behavior 15 min later.

CRF circuit disconnection

Rats were unilaterally injected with a 1:2 ratio of AAV5-EF1α-DIO-eYFP and AAV2-Ef1α-flex-taCaspase3-TEVp into the CeA and the contralateral dlBNST. Control rats were injected with eYFP+Caspase3 into the CeA of one side and eYFP+PBS into the contralateral dlBNST. Additional controls received eYFP+Caspase3 in the dlBNST of one side and eYFP+PBS into the contralateral CeA. A final group was injected with eYFP+Caspase3 into the CeA and the ipsilateral dlBNST. eYFP was diluted (1:2) in sterile PBS for controls so an equivalent volume of eYFP was injected into the CeA and dlBNST in all animals. All injections were counterbalanced with respect to injected hemispheres. The experiment in Figure 4.6E had similar viral injection parameters for bilateral CeA injection (controls received eYFP+PBS). After 4-6 weeks recovery rats were subjected to IMS and tested for anxiety-like behavior.

Histology

All rats were checked for virus expression and implanted cannula locations after behavioral studies were completed. For immunofluorescence, rats were anesthetized with isoflurane and perfused transcardially with 1X PBS followed by 4% paraformaldehyde in PBS, pH 7.4. Brains were extracted, allowed to postfix overnight in the same fixative and cryoprotected in 30% sucrose in PBS at 4º C. Each brain was sectioned at 40 µm on a

cryostat (Thermo Scientific) and collected in PBS. Staining for injected viruses (except KORD-IRES-mCitrine) was omitted due to strong native fluorescence.

For immunohistochemistry, free-floating sections were washed three times in PBS with 0.2% Triton X-100 (PBST) for 10 min at room temperature. Sections were then incubated in blocking solution made of PBST with 3% normal donkey serum (Jackson ImmunoResearch, number 017-000-121) for 1 hr. Sections were next incubated in primary antibodies rabbit anti-GFP (1:1000, Abcam, ab290, Lot #GR135929-1) or rabbit anti-PKCδ (1:2000, Santa Cruz Biotechnology, sc-213, Lot #D2210) in blocking solution rotating at 4° C for 18-20 hr. After three 10 min washes in PBST, sections were incubated in species-specific secondary antibodies Alexa Fluor 488, 594, or 647 (1:700, Life Technologies, A-21206, A-11055, A-21208, A11073, A-21447, A-31573) in blocking solution for 1 hr at room temperature. Finally, sections were washed three times for 10 min in 1X PBS. Sections were then mounted in 0.2% gelatin water onto SuperFrost Plus glass slides (Fisherbrand, 12-550-15), coverslipped with Fluoromount-G with DAPI (Southern Biotech, 0100-20), and stored in the dark. Fluorescent images were collected on a Zeiss 710 LSM confocal microscope or a Zeiss Axio Zoom stereo microscope. Quantification of fluorescence was performed on 3-6 sections per rat from 5 rats spanning the rostral-caudal axis of the CeA (from approximately Bregma -1.90 to -3.00) using the cell-counter plugin in Fiji (Schindelin et al., 2012).

Fluorescence *in situ* hybridization

For examination of gene expression in the dlBNST, coronal sections were processed for fluorescent in situ hybridization by RNAscope according to manufacturer's guidelines. Genes examined in the dlBNST were *Crh* (ACDBio cat# 318931) and *proEnkephalin*

(ACDBio cat# 417431) and hybridization was performed using RNAscope Fluorescent Multiplex Kit (Advanced Cell Diagnostics). Slides were coverslipped with Fluoromount-G with DAPI (Southern Biotech, 0100-20) and stored at 4°C in the dark before imaging.

Statistical analyses

We calculated sample sizes of n = 8-12 animals per condition using SD values measured in pilot studies of IMS-induced anxiety-like behavior, $\alpha = 0.05$, and power = 0.80, with the goal of detecting a 25-35% difference in mean values for treated and control samples, using the program G*Power (Faul et al., 2007). Studies were performed with the experimenter blind to the identity of the drugs that were administered. All results were expressed as mean ± S.E.M. values and analyzed using Prism (GraphPad Software, San Diego, CA). Data distribution and variance were tested using Shapiro-Wilk normality tests. Normally distributed data were analyzed by unpaired, two-tailed t-tests, or one or two factor ANOVA with post-hoc Tukey's or Bonferroni's multiple comparisons tests. Data that were not normally distributed were analyzed by Mann-Whitney U tests when comparing two conditions, or were transformed to square root values, as noted, before performing a two-factor ANOVA. Differences were considered significant when $P < 0.05$.

RESULTS

CeA^{CRF} neurons project their axons to the BNST

If the CRF that mediates stress-induced anxiety originates in the CeA (Chapters 2 and 3) and signals in the BNST, then CeA^{CRF} projections should be present in the BNST. Using an AAV to express Cre-dependent mCherry (Figure 4.1A), we identified CeA^{CRF} fibers in the dorsolateral oval and ventral fusiform nuclei of the BNST on the same side (Figures 4.1B and 4.2E). Importantly, CeA^{CRF} axons were clustered in a region of the dlBNST in which local $dlBNST^{CRF}$ neurons were concentrated (Figure 4.1B), along with PKCδ- or enkephalin-expressing cells, which are distinct from CRF neurons (Figures 4.2B-D). In addition, injection of the retrograde tracer canine adenovirus 2 (CAV2) encoding flex-ZsGreen into the dlBNST (Figure 4.1C) labeled 46.1% of 1465 CeA^{CRF} neurons spanning the entire rostral-caudal axis of the CeA (Figures 4.1D and 4.1E), indicating that roughly half of CeA^{CRF} neurons project to and have terminals within the dlBNST. There was no labeling of contralateral CeA neurons.

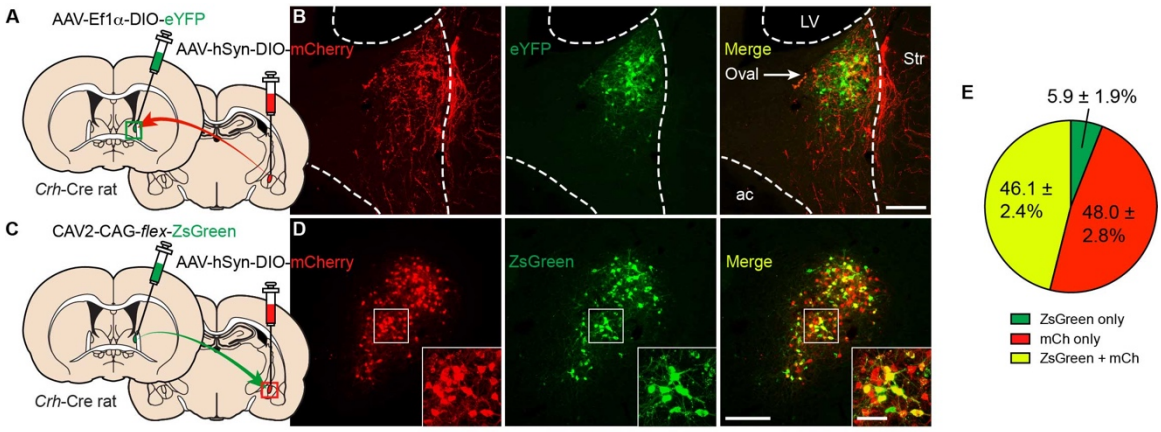

Figure 4.1. CeA^{CRF} neurons target the dlBNST

(A) Configuration of dual viral injections into the dlBNST and CeA of *Crh*-Cre rats for anterograde tracing. **(B)** A dense plexus of mCherry^{+} CeA^{CRF} fibers was detected in the dlBNST in the vicinity of eYFP^{+} dlBST^{CRF} neurons. Scale bar, 200 μm. LV, lateral ventricle. Str, striatum. ac, anterior commissure. **(C)** Configuration of dual viral injections into the dlBNST and CeA of *Crh*-Cre rats for retrograde tracing. **(D)** Many mCherry^{+} CRF neurons in the CeA were retrogradedly labeled with CAV2-packaged ZsGreen. Scale bar, 200 μm. Boxed region is enlarged in inset (scale bar, 50 μm). **(E)** Quantification of ZsGreen expressed in CeA cell bodies revealed that approximately 46.1% (total of 1465 neurons counted from 3-6 BNST sections from 5 rats) of CeA^{CRF} (mCh^{+}) neurons project to the dlBNST.

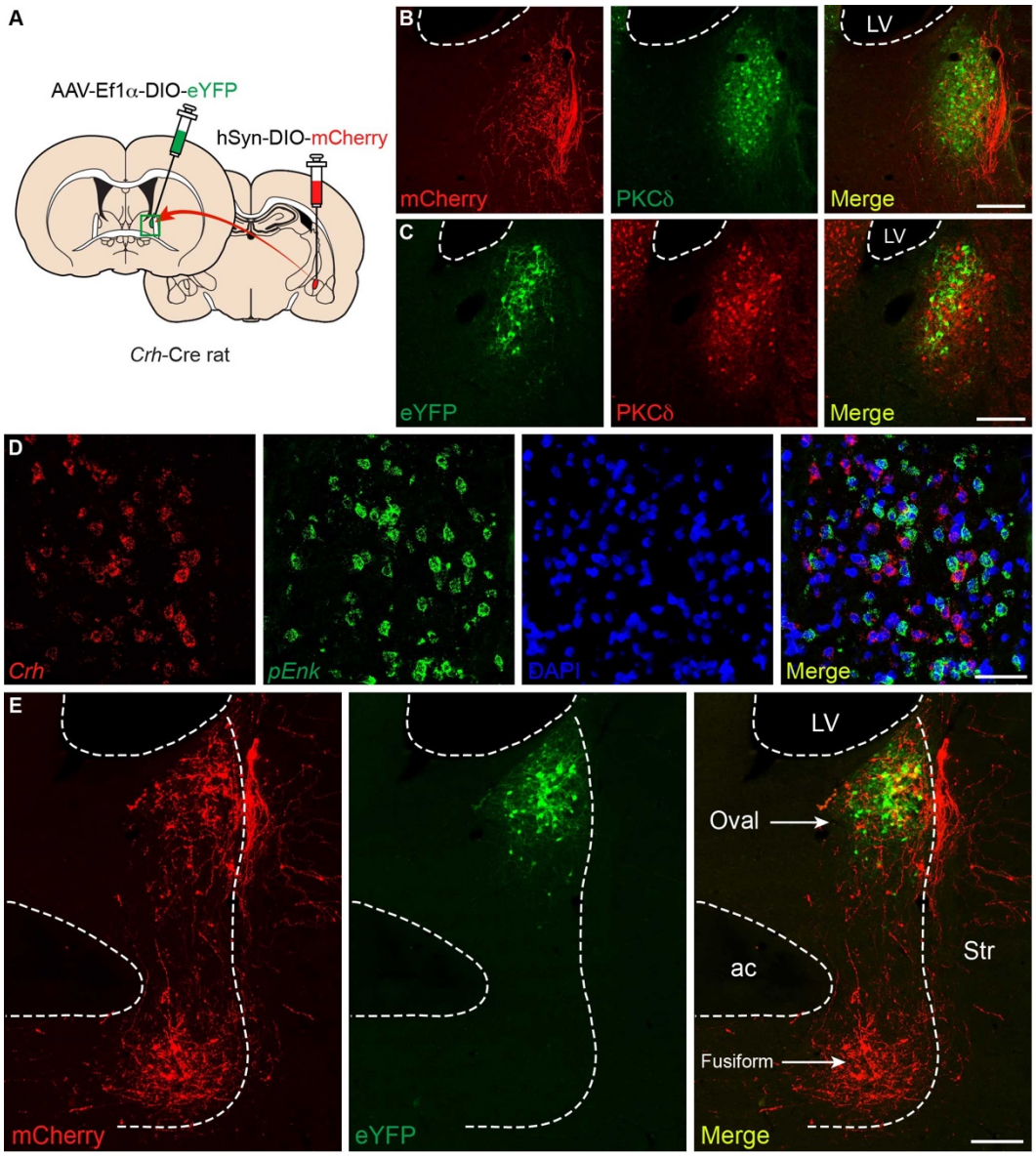

Figure 4.2. Anatomy of CeA^{CRF} inputs to neurons of the dlBNST

(A) Dual AAV injection into the extended amygdala. **(B)** CeA^{CRF} inputs cluster around PKCδ neurons in the oval nucleus. Scale bar, 200 μm. dlBNST^{CRF} neurons are distinct from PKCδ neurons (Scale bar, 200 μm) **(C)** and from cells expressing *proenkephalin* (Scale bar, 50 μm) **(D)**. **(E)** CeA^{CRF} projections are mainly found in the oval and fusiform nuclei

of the BNST. Scale bar, 200 μm. LV, lateral ventricle. Str, striatum. ac, anterior commissure.

CeA^{CRF} projections to the dlBNST promote anxiety

Since CeA^{CRF} neurons projected to a region of the dlBNST containing CRF neurons, we next investigated whether CeA^{CRF} projections within the dlBNST are important for stress-induced anxiety. We expressed hM4Di in CeA^{CRF} neurons and targeted guide cannulas to the dlBNST for delivery of CNO (Figure 4.3A). We used a dose of CNO (1mM in 0.3μL; 300 pmol) previously reported to be effective in activating DREADDs in nerve terminals (Mahler et al., 2014). In *Crh*-Cre rats that expressed hM4Di in CeA^{CRF} neurons, silencing CeA^{CRF} terminals in the dlBNST with CNO at this dose suppressed IMS-induced anxiety-like behavior (Figures 4.3B and 4.4A). CNO increased the percentage of time spent on the open arms of the EPM and the percentage of open arm entries on the EPM without affecting the number of closed arm entries (Figures 4.3B and 4.4A). CNO also increased time spent and distance traveled in the center of the OF after IMS without altering the total distance traveled (Figures 4.3B and 4.4A).

Next, to investigate whether CeA^{CRF} inputs to the dlBNST were sufficient to enhance anxiety, we expressed hM3Dq in CeA^{CRF} neurons and directed guide cannulas to the dlBNST to activate CeA^{CRF} terminals (Wang et al., 2015) (Figure 4.3A). Microinfusion of CNO (1mM in 0.3μL; 300 pmol) into the dlBNST (Figures 4.3D and 4.4B) reduced the percentage of time spent on the open arms of the EPM, which was prevented with local injection of R121919 (1μg in 0.3μL). Likewise, microinfused CNO reduced the percentage of open arm entries on the EPM, which was also prevented by administration of R121919 in the dlBNST (Figure 4.4B). Similar results were observed in the OF test. CNO reduced time spent in the center of the OF, which was prevented by local blockade of CRF1 receptor (Figure 4D). CNO also reduced the percentage of total distance traveled that was in the center of the OF, and this was also prevented by R121919 (Figure 4.4B). CNO modestly

reduced the total distance traveled in the OF in animals that expressed hM3Dq in CeA^{CRF} neurons, but R121919 in the dlBNST had no effect on this measure (Figure 4.4B). Finally, CNO infusion into the dlBNST reduced social interaction time, which was also reversed by R121919 infusion (Figure 4.3D). To ensure that the dose of CNO we used did not produce off-target effects, we implanted guide cannulas over the dlBNST of non-transgenic Wistar rats and found no effect of 300 pmol CNO on IMS-induced anxiety (Figure 4.4C). Importantly, these findings indicate that CeA^{CRF} inputs to the dlBNST are necessary and sufficient for increasing anxiety-like behavior, likely through release of CRF and activation of CRF1 receptors in the dlBNST.

Since systemic administration of R121919 inhibited IMS-induced anxiety-like behavior (Figure 2.2, Chapter 2), we investigated whether R121919 could also block anxiety-like behavior induced by activation of CeA^{CRF} inputs to the dlBNST. Systemic administration of R121919 (20 mg/kg, *s.c.*) prevented anxiety like behavior induced by microinfusion of CNO into the dlBNST in rats that expressed hM3Dq in CeA^{CRF} neurons. CNO decreased the percentage of time in the open arms and the percentage of open arm entries on the EPM, without altering the number of closed arm entries (Figure 4.5A). Likewise, CNO microinfusion decreased the percentage of time spent in the OF and this effect was prevented by systemic R121919 (Figure 4.5B). CNO also reduced the distance traveled in the center of the OF and this effect was prevented by systemic R121919 (Figure 4.5B). Since both systemic and local administration of R121919 into the dlBNST reversed anxiety-likely behavior induced by activation of CeA^{CRF} inputs to the dlBNST, it is likely that that systemic R121919 inhibits anxiety-like behavior through actions at CRF1 receptors in the dlBNST.

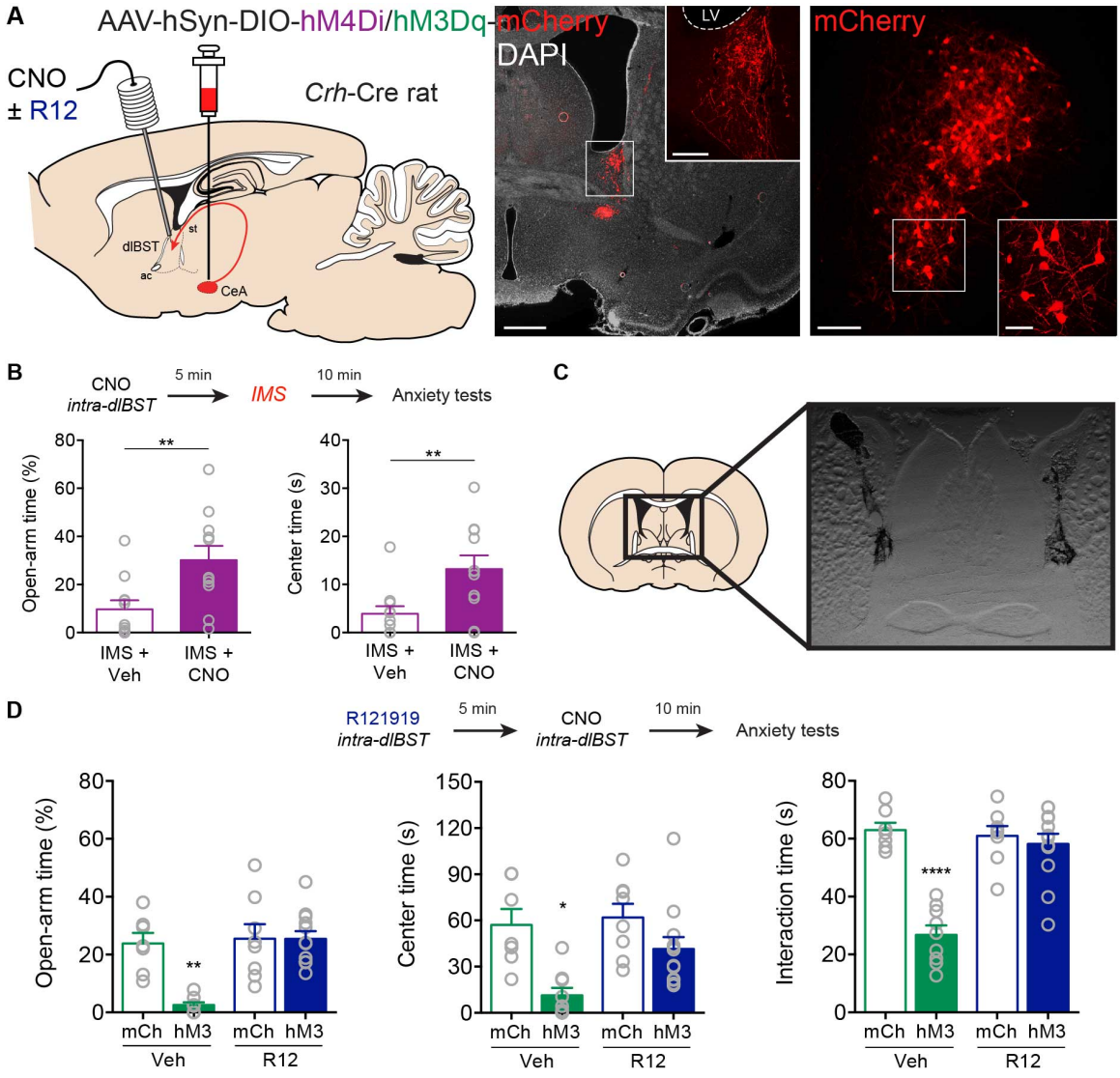

Figure 4.3. CeA^{CRF} projections to dlBNST mediate anxiety

(A) AAV encoding Cre-dependent inhibitory hM4Di or excitatory hM3Dq was injected into the CeA with guide cannulas directed to the dlBNST for targeted CNO microinjection. Left image, CeA^{CRF} fibers targeting the dlBNST. Scale bar, 200 µm. Boxed region is enlarged in inset (scale bar, 20 µm). Right image, dlBNST-projecting CeA^{CRF} neurons. Scale bar, 500 µm. Boxed region is enlarged in inset (scale bar, 20 µm). **(B)** Top,

experimental protocol. Bottom, inhibition of CeA^{CRF} terminals in the dlBNST with CNO (1mM in 0.3μL) increased the percentage of time spent on the open arms of the EPM [U = 20, $^{**}P = 0.0065$, $n = 11$ both groups, Mann-Whitney test] and time spent in the center of the OF after IMS [U = 21, $^{**}P = 0.0081$, $n = 11$ both groups, Mann-Whitney test]. **(C)** Representative ink injection demonstrating targeted microinjection into the dlBNST. **(D)** Top, experimental protocol. Bottom, activation of CeA^{CRF} terminals in the dlBNST with CNO (1mM in 0.3μL) reduced the percentage of time spent on the open arms of the EPM, which was prevented with local injection of R121919 (1μg in 0.3μL) [$F_{hM3Dq \times R12}(1,31) = 9.83$, $^{**}P = 0.0037$, two-way ANOVA, $n = 8$-12; $^{***}P = 0.0012$ mCh:Veh compared with hM3:Veh; $^{****}P < 0.0001$ hM3:Veh compared with hM3:R12 by Tukey's test]. Activation of terminals also reduced time spent in the center of the OF, which was prevented by local blockade of CRF1 receptors [$F_{hM3Dq \times R12}(1,32) = 6.224$, $^{*}P = 0.0180$, two-way ANOVA, $n = 8$-12; $^{****}P = 0.0001$ for mCh:Veh compared with hM3:Veh and $^{***}P = 0.0009$ for hM3:Veh compared with hM3:R12 by Tukey's tests]. Terminal activation reduced social interaction time, which was CRF1 receptor-dependent [$F_{hM3Dq \times R12}(1,33) = 24.22$, $^{****}P < 0.0001$, two-way ANOVA, $n = 8$-12; $^{****}P < 0.0001$ for mCh:Veh compared with hM3:Veh and for hM3:Veh compared with hM3:R12 by Tukey's tests]. Data are represented as mean ± SEM.

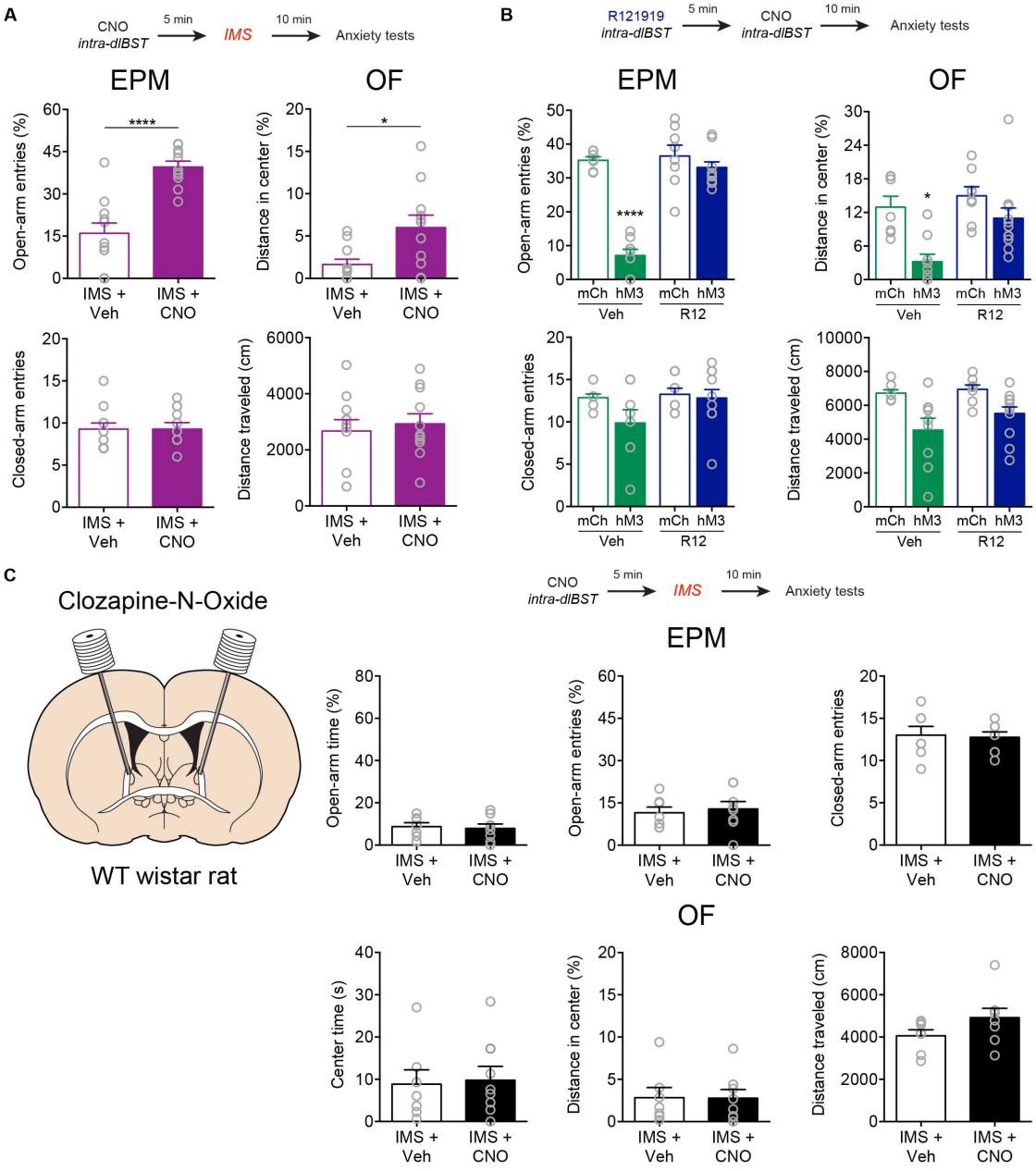

Figure 4.4. Effects of DREADD manipulation of CeA^{CRF} fibers in dlBNST on other measures of anxiety-like behavior

(A) hM4Di was expressed in CeA^{CRF} fibers projecting to the dlBNST. CNO (1mM in 0.3µL) administration in the dlBNST during IMS increased the percentage of open arm

entries on the EPM [t(20) = 5.647, ****$P < 0.0001$, $n = 11$ both groups, unpaired t-test] without affecting the number of closed arm entries [U = 57, $P = 0.8451$, $n = 11$ both groups, Mann-Whitney test]. CNO also increased distance traveled in the center of the OF [U = 24, *$P = 0.0153$, $n = 11$ both groups, Mann-Whitney test] without altering the total distance traveled in the OF [t(20) = 0.4655, $P = 0.6466$, $n = 11$ both groups, unpaired t-test]. **(B)** hM3Dq was expressed in CeA^{CRF} fibers projecting to the dlBNST. CNO administration in the dlBNST CNO also reduced the percentage of total distance traveled that was in the center of the OF, which was prevented by R121919 [$F_{hM3Dq \times R12}(1,32) = 6.56$, $P = 0.0153$, n = 8-12, two-way ANOVA; ***$P = 0.002$ for mCh:Veh compared with hM3:Veh, and ***$P = 0.003$ for hM3:Veh compared with hM3:R12 by Tukey's test]. CNO modestly reduced the total distance traveled in the OF in animals that expressed hM3Dq in CeA^{CRF} neurons, while R121919 in the dlBNST had no effect [$F_{hM3Dq \times R12}(1,33) = 0.65$, $P = 0.426$, n = 8-12, two-way ANOVA; $F_{hM3Dq}(1,32) = 14.77$, $P = 0.0005$; $F_{R12}(1,32) = 1.645$, $P = 0.209$]. **(C)** Left, experimental configuration. Right, WT wistar rats were cannulated in the dlBNST and microinjected with CNO (1mM in 0.3µL) prior to stress. CNO administration in the dlBNST in the absence of DREADD expression in CeA^{CRF} terminals had no effects time spent in the open arms [t(13) = 0.2981, $P = 0.7703$, n = 7 Veh, 8 CNO, unpaired t-test], entries into the open arms [t(13) = 0.4071, $P = 0.6906$, n = 7 Veh, 8 CNO, unpaired t-test], or entries into the closed arms of the EPM [t(13) = 0.2089, $P = 0.8378$, n = 7 Veh, 8 CNO, unpaired t-test]. CNO also lead to no changes in time spent in the center [t(13) = 0.2022, $P = 0.8429$, n = 7 Veh, 8 CNO, unpaired t-test], distance traveled in the center [U = 26, $P = 0.8665$, n = 7 Veh, 8 CNO, Mann-Whitney test], or total distance traveled in the OF [t(13) = 1.573, $P = 0.1397$, n = 7 Veh, 8 CNO, unpaired t-test]. Data are represented as mean ± SEM.

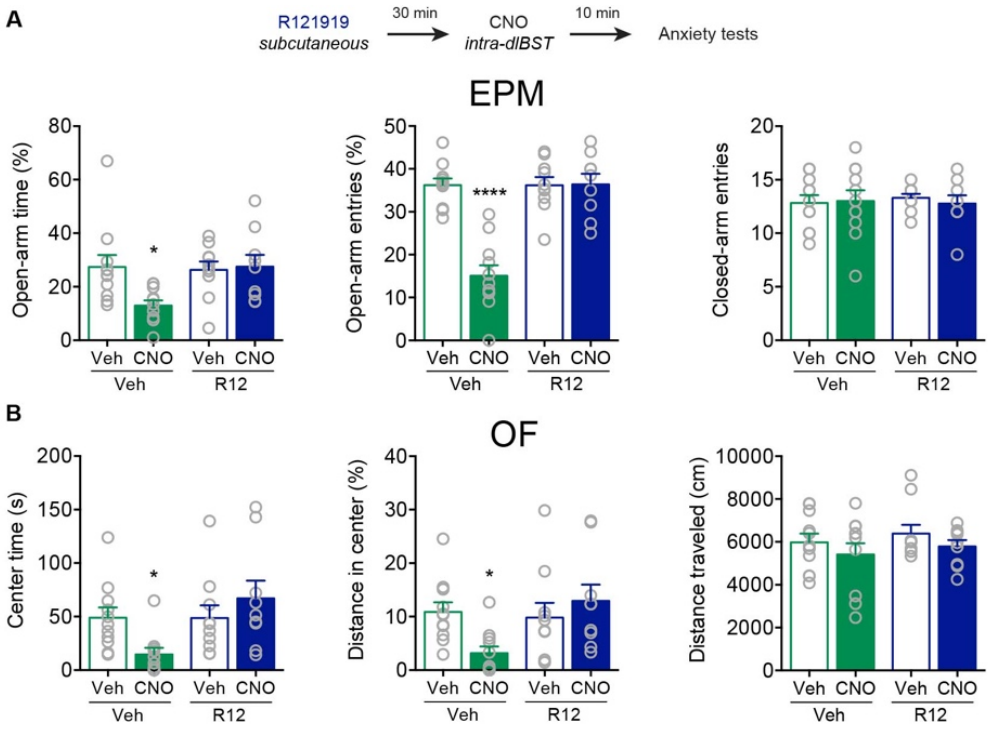

Figure 4.5. Systemic CRF1 receptor blockade prevents anxiety produced by CeA^{CRF} terminal stimulation in the dlBNST

(A) Top, experimental protocol. Bottom, systemic administration of R121919 prevented hM3Dq-induced decreases in the percentage of time in the open arms [$F_{CNO \times R12}(1,37) = 4.678$, $^{*}P = 0.0371$, two-way ANOVA, $n = 9$-11; $^{*}P = 0.0282$ for Veh:Veh compared with Veh:CNO, and $^{*}P = 0.0378$ for Veh:CNO compared with R12:CNO by Tukey's test] and the percentage of open arm entries [$F_{CNO \times R12}(1,37) = 25.69$, $^{****}P < 0.0001$, two-way ANOVA, $n = 9$-11; $^{****}P < 0.0001$ compared with other conditions by Tukey's test], without altering the number of closed arm entries [$F_{CNO \times R12}(1,37) = 0.2072$, $P = 0.6517$, two-way ANOVA, $n = 9$-11]. **(B)** Systemic administration of R121919 also prevented hM3Dq-induced decreases in the percentage of time spent in the OF [$F_{CNO \times R12}(1,37) = 5.999$, $^{*}P = 0.0192$, two-way ANOVA, $n = 9$-11; $^{**}P = .0086$ for Veh:CNO compared

with R12:CNO by Tukey's test] and the distance traveled in the center [$F_{CNO \times R12}(1,37) = 5.886$, $^{*}P = 0.0203$, two-way ANOVA, $n = 9$-11; $^{*}P = .0212$ for Veh:CNO compared with R12:CNO by Tukey's test] without affecting total distance traveled in the OF. Data are represented as mean ± SEM.

CeA^{CRF} neurons and dlBNST^{CRF} neurons act within a common network to regulate anxiety

Since activation of CeA^{CRF} inputs to the dlBNST can drive anxiety-like behavior and the dlBNST also contains neurons that produce CRF, we investigated whether CeA^{CRF} and dlBNST^{CRF} neurons act within a common network to drive anxiety. We infected the CeA of *Crh*-Cre rats with the excitatory designer receptor hM3Dq on one side of the brain and infected the ipsilateral dlBNST with a Cre-dependent KORD-IRES-mCitrine (kappa opioid receptor DREADD), a complementary inhibitory designer receptor (Figures 4.6A and 4.6B). Unstressed rats were administered CNO followed by the KORD-specific ligand salvinorin B (SalB - 15 mg/kg, *s.c.*), and then were tested for anxiety-like behavior. Rats given CNO to excite CeA^{CRF} neurons displayed significant anxiety-like behavior on the EPM and in the OF. Importantly, co-administration of SalB to inhibit dlBNST^{CRF} neurons blocked the anxiety-like behaviors evoked by activating CeA^{CRF} neurons (Figures 4.6C). As expected, systemic administration of CNO (2 mg/kg, *i.p.*) decreased in the percentage of open arm time in the EPM and this effect was prevented by inhibiting dlBNST^{CRF} neurons with SalB (Figure 4.6C). CNO also reduced the percentage of open arm entries on the EPM and co-administration of SalB also prevented this effect, while no effect on the number of closed arm entries was detected (Figure 4.6C). SalB also prevented CNO-induced decreases in time spent in the center of the OF, and in the distance traveled in the center, without affecting the total distance traveled in the OF (Figure 4.6D). These results are consistent with the hypothesis that CeA^{CRF} neurons engage dlBNST^{CRF} neurons to drive anxiety-like behavior. They also demonstrate that unilateral activation of CeA^{CRF} neurons is sufficient to increase anxiety-like behavior.

Since dlBNST^{CRF} neurons were necessary for the anxiety-like behaviors produced by activating CeA^{CRF} neurons, we next examined whether this CRF-to-CRF cell network

interaction was important for anxiety induced by stress. We disconnected this postulated CRF network by injecting Cre-dependent Caspase3, which lesions neurons, into the CeA of one side of the brain and into the contralateral dlBNST (Figure 4.7A). This disconnection procedure prevented IMS-induced anxiety in the EPM and social interaction tests, while unilateral ablation in either the CeA or dlBNST alone, or ablation of CRF neurons in the CeA and dlBNST of the same side, had no effect on stress-induced anxiety (Figure 4.7C). Expression of Caspase3 in contralateral CeA^{CRF} and $dlBNST^{CRF}$ neurons increased the percentage of time spent on the open arms of the EPM (Figure 4.7C). Expression of Caspase3 in contralateral CeA^{CRF} and $dlBNST^{CRF}$ neurons also increased the percentage of open arm entries on the EPM without significantly affecting the number of closed arm entries (Figure 4.7C). Finally, expression of Caspase3 in contralateral CeA^{CRF} and $dlBNST^{CRF}$ neurons reduced time spent in social interaction (Figure 4.7C). Together, these results indicate that CeA^{CRF} and $dlBNST^{CRF}$ neurons function within a common network to mediate stress-induced anxiety-like behavior in rats.

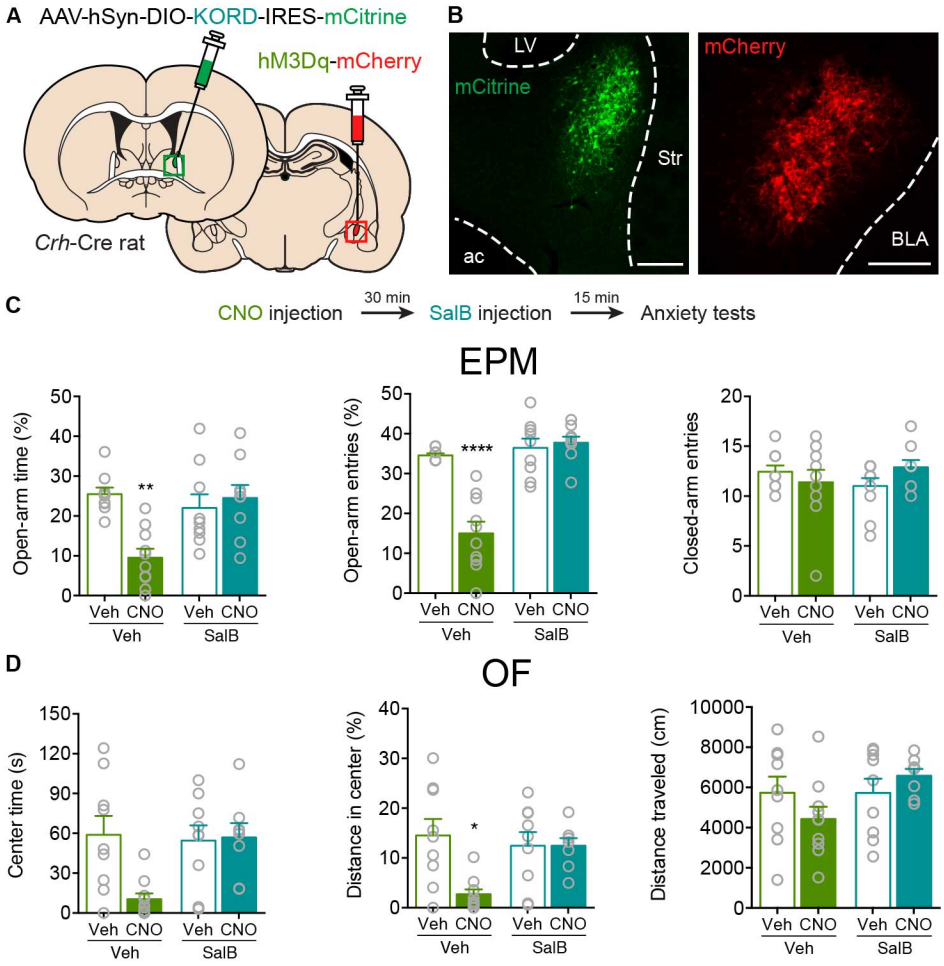

Figure 4.6. Extended amygdala CRF network for eliciting anxiety

(A) AAV encoding Cre-dependent KORD was injected into the dlBNST and AAV encoding Cre-dependent hM3Dq was injected into the ipsilateral CeA. **(B)** Example of antibody-amplified mCitrine fluorescence in dlBNST^{CRF} neurons and native mCherry in CeA^{CRF} neurons. Scale bars, 200 μm. **(C)** Top, experimental protocol. Bottom, inhibition of dlBNST^{CRF} neurons with SalB prevented CNO-induced decreases in the percentage of time in the open arms of the EPM [$F_{CNO \times SalB}(1,34) = 10.33$, $^{**}P = 0.0029$, two-way ANOVA, $n = 9$-10; $^{**}P = 0.0011$ for Veh:Veh compared with Veh:CNO and $^{**}P = 0.0023$

for Veh:CNO compared with SalB:CNO by Tukey's tests]. CNO also reduced the percentage of open arm entries on the EPM but co-administration of SalB prevented this effect [$F_{CNO \times SalB}$ (1,33) = 24.54, ****$P < 0.0001$, two-way ANOVA, n = 9-10; ****$P <$ 0.0001 compared with other conditions by Tukey's test]. No effect on the number of closed arm entries were detected [$F_{CNO \times SalB}$ (1,33) = 2.610, $P = 0.1155$, two-way ANOVA, n = 9-10]. **(D)** SalB prevented CNO-induced decreases in time spent in the center of the OF [$F_{CNO \times SalB}$ (1,32) = 5.751, *P = 0.0225, two-way ANOVA, n = 8-10; *P = 0.0113 for Veh:Veh compared with Veh:CNO and *P = 0.0203 for Veh:CNO compared with SalB:CNO by Tukey's tests]. CNO also reduced the distance traveled in the center but co-administration of SalB prevented this effect [$F_{CNO \times SalB}$ (1,32) = 6.475, *P = 0.0160, two-way ANOVA, n = 8-10; **P = 0.0042 for Veh:Veh compared with Veh:CNO, and *P = .0275 for Veh:CNO compared with SalB:CNO by Tukey's test] without affecting the total distance traveled in the OF [$F_{CNO \times SalB}$ (1,32) = 2.718, P = 0.1090, two-way ANOVA, n = 8-10]. Data are represented as mean ± SEM.

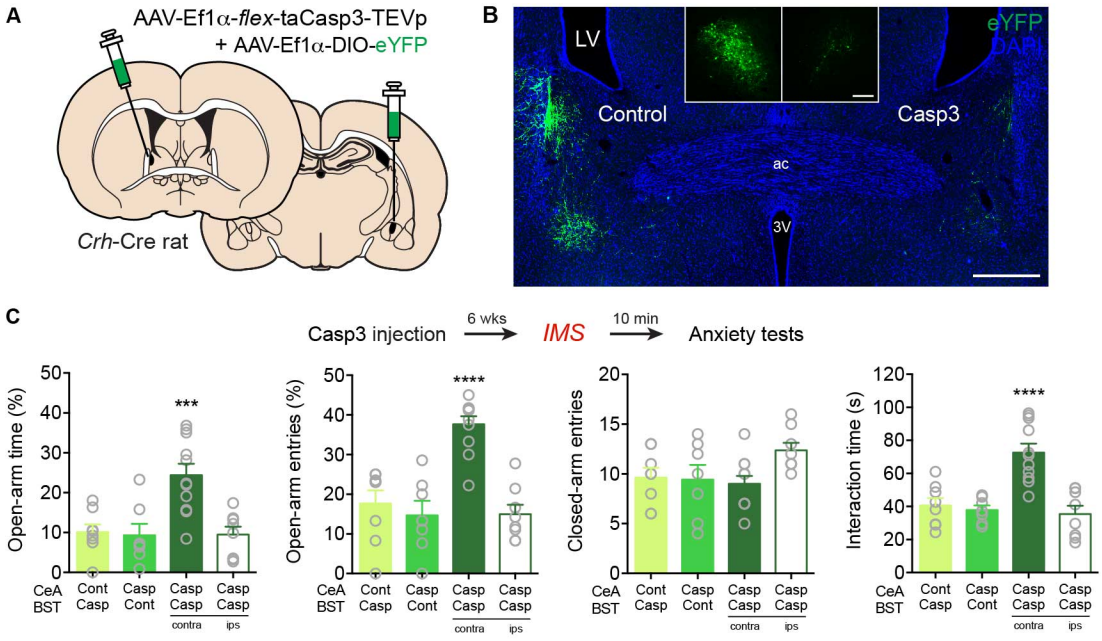

Figure 4.7. Caspase3-mediated CRF circuit disconnection disrupts stress-induced anxiety

(A) AAV carrying *flex*-Caspase3 was injected into the dlBNST and the contralateral CeA for disconnection of the extended amygdala CRF network. **(B)** Caspase3 ablates CeA^{CRF} neurons and their fibers in the BNST. Example image of CeA^{CRF} terminal eYFP expression in the dlBNST of animal injected with eYFP+PBS (Control) in the left CeA and eYFP+Caspase3 in the right CeA. Scale bar, 500 µm. Inset shows eYFP expression in the respective CeA for each side. Scale bar, 200 µm. **(C)** Top, experimental protocol. Bottom, expression of Caspase3 in contralateral CeA^{CRF} and $dlBNST^{CRF}$ neurons increased the percentage of time spent on the open arms of the EPM [$F(3,30) = 9.675$, $^{***}P = 0.0001$, one-way ANOVA, $n = 7$-11; $^{**}P = 0.0015$ for contralateral ablation compared with either eYFP group and $^{***}P = .0009$ for contralateral ablation compared with ipsilateral ablation, by Tukey's test] and increased the percentage of open arm entries on the EPM [$F(3,30) = 18.49$, $P < 0.0001$, one-way ANOVA, $n = 7$-11; $^{****}P < 0.0001$ compared with other

conditions by Tukey's test] without significantly affecting locomotion [$F(3,30) = 2.424$, $P = 0.0852$, one-way ANOVA, $n = 7\text{-}11$]. CRF circuit disconnection also increased social interaction in time [$F(3,30) = 15.07$, $^{****}P < 0.0001$, one-way ANOVA, $n = 7\text{-}11$ rats; $^{***}P = 0.0002$ for contralateral ablation compared with either eYFP group and $^{****}P < 0.0001$ for contralateral ablation compared with ipsilateral ablation by Tukey's test]. Data are represented as mean ± SEM.

DISCUSSION

Here we demonstrate the existence of a CeA^{CRF} to $dlBNST^{CRF}$ neuronal network that drives stress-induced anxiety-like behavior in rats. This network involves CeA^{CRF} inputs to the dlBNST and activation of CRF1 receptors and CRF neurons in the dlBNST. Importantly, our findings indicate that CRF neurons in the CeA and BNST cooperate to generate a state of anxiety following stress, which concurs with recent evidence of CeA and BNST coupling in humans and nonhuman primates exhibiting anxiety (Gungor and Paré, 2016; Shackman and Fox, 2016).

Two previous studies have suggested a role for CeA^{CRF} neurons in driving anxiety-like behaviors in mice. In one, CRF knockdown in the CeA reduced stress-induced anxiety (Regev et al., 2012), and in the other, optogenetic stimulation of CeA^{CRF} terminals in the brainstem evoked anxiety-like behavior (McCall et al., 2015). Our study adds important new findings to the evolving literature on anxiety circuitry by demonstrating in rats that CeA^{CRF} projections to the dlBNST and functional coupling of CeA^{CRF} and $dlBNST^{CRF}$ neurons are necessary and sufficient for expression of stress-induced anxiety. One caveat is that optogenetic or chemogenetic activation may provide stronger drive than occurs endogenously, and the sufficiency of activating a given cell type to cause anxiety does not imply that other circuit elements are not also important with respect to endogenous activity of the CRF system. In this regard, since stimulation of CeA^{CRF} projections to the locus coeruleus (LC) (McCall et al., 2015) or the dlBNST (the current study) can generate anxiety-like behavior, one interesting and important question is whether these two pathways originate from the same or different CeA^{CRF} neurons. Thus, future studies are needed to determine whether subpopulations of CRF neurons have different projection targets, and how different CeA^{CRF} outputs could interact to drive anxiety-like behaviors.

Another important question is how CRF released from CeA^{CRF} neurons affects dlBNST circuitry to increase anxiety. We detected CeA^{CRF} fibers throughout the dlBNST but most were clustered in the oval nucleus (Figures 4.1B and 4.2B), which contains GABA neurons that promote anxiety, possibly through negative regulation of an anxiolytic anterodorsal subregion identified in mice (Kim et al., 2013). In rats, $dlBNST^{CRF}$ neurons cluster in the oval nucleus (Pomrenze et al., 2015), and are therefore more likely to be components of this circuitry than in mice where CRF neurons are scattered in the dlBNST (Nguyen et al., 2016). It is also likely that CeA^{CRF} neurons engage $dlBNST^{CRF}$ neurons that project to remote regions, such as the hypothalamus or ventral tegmental area, to modulate anxiety (Dedic et al., 2018; Marcinkiewcz et al., 2016).

We found that anxiety-like behaviors driven by CeA^{CRF} neuron activation (*via* hM3Dq) were dependent on $dlBNST^{CRF}$ neurons being active in the same hemisphere, supporting a cooperative role of the CeA and the BNST in stress-induced anxiety. How CeA^{CRF} neurons engage $dlBNST^{CRF}$ neurons is not known. A simple explanation could be that $dlBNST^{CRF}$ neurons express CRF1 receptors and are excited directly by CRF. However, only presynaptic effects of CRF in the dlBNST have been reported. In mice, CRF acting at CRF1 receptors can enhance glutamatergic neurotransmission in the dlBNST (Kash et al., 2008; Nobis et al., 2011; Silberman et al., 2013). Thus, CRF release from CeA terminals in the dlBNST might stimulate $dlBNST^{CRF}$ neurons by enhancing excitatory inputs onto those neurons. In addition, CeA^{CRF} neurons project their axons to other structures that also project to the dlBNST, such as the parabrachial nucleus and LC (McCall et al., 2015; Pomrenze et al., 2015). Thus, since our CNO injections were systemic, it is possible that ipsilateral network effects indirectly recruited $dlBNST^{CRF}$ neurons. For example, recent findings (McCall et al., 2015; Nobis et al., 2011) support a positive

feedforward circuit model (Koob, 1999) involving noradrenergic and CRF interactions in the LC, CeA and BNST that drive stress-related anxiety. Thus, regardless of the mechanism, the serial interaction of CeA^{CRF} and $dlBNST^{CRF}$ neurons that we have identified likely promotes anxiety-like behavior through actions within a larger circuit.

Additional evidence indicates that local circuits within the lateral CeA can contribute to anxiety-like behavior. We previously found that rat CeA^{CRF} neurons form inhibitory synapses with nearly half of non-CRF neurons in the lateral CeA (Pomrenze et al., 2015). A major subpopulation of non-CRF neurons expresses PKCδ, and in mice, optogenetic stimulation of CeA PKCδ neurons promotes anxiety-like behavior (Botta et al., 2015). Because many mouse PKCδ neurons express CRF1 receptors (Sanford et al., 2017), local release of CRF might activate CRF1 receptors on rat PKCδ neurons to promote anxiety. Another subpopulation of non-CRF neurons in the lateral CeA expresses the neuropeptide somatostatin. Compared with PKCδ neurons, somatostatin neurons show greater connectivity with CeA^{CRF} neurons (Fadok et al., 2017) and a larger proportion express CRF1 receptors in mice (Sanford et al., 2017). These characteristics agree with recent findings that CeA somatostatin neurons promote anxiety-like behavior through a circuit mechanism that recruits dlBNST somatostatin neurons (Ahrens et al., 2018). Additionally, a recent study reported that chemogenetic activation of CeA^{CRF} neurons in mice decreased locomotor activity and increased freezing on the EPM, which are behaviors proposed to model passive coping to environmental threats (Pliota et al., 2018). In that report, bath application of CRF increased the frequency of spontaneous excitatory postsynaptic currents in CeA somatostatin neurons when tested in brain slices. These findings suggest that active CRF neurons can modulate local circuits in the CeA to orchestrate anxiety and other defensive behaviors in addition to the critical role that their

dlBNST projections play in stress-induced anxiety, as demonstrated here. It will be interesting in future studies to uncover how local and distant CeA^{CRF} projections interact to generate anxiety-like behaviors.

In addition to CRF and GABA, CeA^{CRF} neurons express other neuropeptides (Kim et al., 2017; Pomrenze et al., 2015). Neurotensin in the rat oval BNST can promote chronic stress-induced anxiety and cooperates with CRF to modulate synaptic transmission (Normandeau et al., 2018b). In mice, the anxiogenic actions of dynorphin involve activation of kappa opioid receptors and inhibition of glutamate release from basolateral amygdala terminals in the anterodorsal BNST (Crowley et al., 2016). Since several CeA^{CRF} neurons express dynorphin or neurotensin (Pomrenze et al., 2015), they could be the source of dynorphin involved in these effects. Indeed, a recent paper reports a population of dlBNST-projecting CeA neurons as integral to a genetic model of anxiety in mice *via* dynorphin release (Ahrens et al., 2018). In addition, since a considerable portion of dlBNST-projecting CeA^{CRF} neurons express dynorphin or neurotensin (Figure 3.4), the release of these peptides in the dlBNST after terminal stimulation with hM3Dq could contribute to the observed effects on anxiety. The contribution of other neuropeptides released from CeA^{CRF} neurons, and their coordinated effects on synaptic physiology both locally in the CeA and remotely in the BNST should be a major focus of future investigation.

The availability of modern imaging and genetic tools has allowed discoveries that challenge previous notions about the dissociable roles of CeA and BNST neurons in mediating fear and anxiety. Our results strongly support the hypothesis that both CeA^{CRF} and $dlBNST^{CRF}$ neurons are important for generating stress-induced anxiety-like behavior. In addition, our findings support the growing realization that the CeA and BNST can

interact as a tightly coupled functional unit (Shackman and Fox, 2016), and suggest that dysfunction of the CeA^{CRF}→BNST circuit could contribute to anxiety disorders in humans.

ACKNOWLEDGMENTS

The experiments in this chapter could not have been done without the help of others. I must thank Dr. Angelo Blasio for his massive contributions of viral injections, cannula surgery, drug microinjections, and behavior. I also thank Simone Giovanetti and Dr. Rajani Maiya for their assistance in data collection and their intellectual contributions to the project. Dr. Robert Messing was integral to this study because he provided space, funding, intellectual contribution, and oversaw the entire project. I also thank Dr. Larry Zweifel from the University of Washington in Seattle for his generous contribution of the CAV2-*flex*-ZsGreen virus. And finally, I acknowledge my own funding from NSF (Fellowship DGE-1110007).

GENERAL DISCUSSION

The objective of this dissertation was to determine whether CRF neurons of the rat central amygdala significantly contribute to fear and anxiety-like behaviors. Additionally, based on observations that CeA^{CRF} neurons co-express multiple other neuropeptides and release GABA, it was important and interesting to determine which of these neurotransmitters were involved in the impact that CeA^{CRF} neurons have on fear and anxiety. The final major focus was to establish whether the CRF projection from the CeA to the dorsolateral BNST was important for anxiety-like behaviors. These experiments were designed to challenge a long-standing neuroanatomical framework for fear and anxiety, and investigate an important hypothesis that remained unproven in the literature (Davis et al., 2010). The data collected and presented in this dissertation have demonstrated that the early anatomical model proposed by Davis and colleagues is not completely accurate, but the neurocircuit hypothesis is correct. Furthermore, these new data expand on the role of CeA^{CRF} neuron contributions to fear and anxiety by showing that different neurotransmitters released from these neurons play distinct roles in these phenotypes, and that these neurons recruit the population of CRF neurons in the dlBNST to orchestrate anxiety responses. Altogether, the data presented here determine novel roles for CeA^{CRF} neurons in anxiety, confirm a role for these neurons in fear learning, and confirm the previously untested hypothesis that the CeA^{CRF} projection to the dlBNST is critical for anxiety.

Amygdala and BNST dichotomy

Fear and anxiety behaviors are highly investigated topics in the field of neuroscience. This is because 1) they represent evolutionarily conserved processes essential to survival, 2) they are mediated by well conserved neurobiological systems, and 3) are central to some

of the most prevalent neuropsychiatric disorders in humans (Baxter et al., 2013). Neuroscientists and clinicians alike are interested in how these emotional states are generated and regulated by specific brain circuits. The earliest studies on the neurobiology of fear and anxiety used the best methods available (electrolytic or pharmacological lesions and pharmacological inactivation) to determine important brain regions. The massive body of work by Davis and colleagues laid the groundwork for understanding how the brain produces fear and anxiety-like emotional states. They determined that the canonical amygdala complex, including the CeA, was critical to the induction and expression of conditioned fear responses in rats, and that the BNST was critical to anxiety-like behaviors, but not vice versa (Davis, 1997; Davis et al., 1994b; Davis et al., 2010; Liang et al., 1992a; Walker and Davis, 1997b, 2008; Walker et al., 2009b; Walker et al., 2003). This allowed for the development of an anatomical framework that suggested that these two emotional states were mediated by two distinct brain regions, fear in the amygdala and anxiety in the BNST. Additionally, a role for the stress neuropeptide CRF was incorporated into the model since central CRF administration enhanced anxiety in a fear-potentiated startle procedure which was disrupted by CRF antagonists (Liang et al., 1992a; Liang et al., 1992b; Walker and Davis, 2008; Walker et al., 2009b).

Years of data supported this parsimonious framework. But shortly after, the advent of genetic tools that permitted cell-type and pathway specific interrogation of brain structures began to suggest this hypothesis was not entirely accurate. Studies manipulating discrete cell-types in the CeA revealed that some neuronal populations indeed were involved in anxiety-like behaviors in mice (Ahrens et al., 2018; Botta et al., 2015; McCall et al., 2015; Pliota et al., 2018; Regev et al., 2012). These findings countered the concept that Davis and colleagues proposed, implicating lesions as a less than ideal method to study

a given brain structure. These studies also highlight a mismatch in the literature. The anatomical segregation of fear and anxiety was assessed in rats, while essentially all studies evalutaing specific cell-types the CeA in fear and anxiety were performed in mice. Thus, the current set of experiments set out to determine whether a specific population of neurons in the CeA could modulate anxiety-behaviors in rats. Since CRF was known to contribute to anxiety, and the CeA harbors a large population of CRF neurons (Chapter 1), a simple hypothesis was that CeA^{CRF} neurons played a role in this anxiety. Indeed this was the case. Chemogenetic activation of CeA^{CRF} neurons generated an anxiogenic state and inhibiton prevented stress-induced anxiety (Chapter 2). These data demonstrate that the rat CeA can play a role in anxiety behavior (similar to recent studies in mice) and CeA^{CRF} neurons may be the source of CRF in the early Davis and colleagues studies. These findings, collected with genetic tools with cellular precision, strongly challenge the early anatomical framework of fear and anxiety and suggest that 1) the rat CeA plays important roles in both fear and anxiety and 2) the coarseness of lesion studies can overlook important and subtle aspects of brain regions' roles in specific phenotypes. Interestingly, it is now acknowledged that there are multiple subpopulations of neurons in many brain regions that antagonize each other's activity within a common circuit (Daniel and Rainnie, 2016). Although lesions studies have been important for much of the early progress on neuroanatomy and behavior, it is clear that this type of manipulation obfuscates many interesting and important features of brain function.

Despite not changing anxiety-like behaviors, lesions and inactivation studies in the CeA drastically affected fear behaviors (Davis, 1997; Liang et al., 1992a). A large body of literature shows the amygdala and all of its regions as essential to fear learning and expression (LeDoux, 2003, 2007; Sigurdsson et al., 2007). It was also established that CRF

in the CeA was important for fear learning, but not the expression of fear (Asok et al., 2018; Pitts and Takahashi, 2011; Pitts et al., 2009; Sanford et al., 2017). We determined that CeA^{CRF} neurons in rats were part of this process. Similar to mice (Sanford et al., 2017), chemogenetic inhibition of CeA^{CRF} neurons did not affect shock-induced freezing but prevented fear learning (Chapter 2). This result was further supported by data showing that inhibition of these neurons at later time points, either immediately after fear conditioning or before fear retrieval trials, had no effect on freezing (Chapter 2). Therefore, CeA^{CRF} neurons are critical to fear learning in rats, which is consistent with the large body of previous literature in both rats and mice. This result is not surprising, but strongly suggests and perhaps proves that these neurons are capable of mediating multiple negative emotional states. Therefore the anatomical model of Davis and colleagues was only partially correct. In addition, we now know that CRF neurons are important for generating both of these negative emotional states and should be the topic of future investigations into how pathological fear and anxiety are produced and regulated by the brain. It will be interesting in future studies to examine the role of these neurons and their projections to remote brain regions in regulating these emotional states. It will also be intriguining to study the role of these neurons in other negative emotions, such as those evoked by drug withdrawal and other forms of stress. Altogether, the data discussed so far prove that CeA^{CRF} neurons take on versatile roles in negative emotional states, a concept previously unidentified in previous studies.

Co-released transmitters

It has been long-known that neurons can release multiple neurotransmitters. This is perhaps most pronounced in neuropeptide neurons, where essentially all neurons that release

neuropeptides also release fast acting neurotransmitters such as glutamate or GABA (van den Pol, 2012). Most studies to date chose a gene that identifies a neuron based upon its released neurotransmitter, such as *Vgat* for GABA cells, *Vglut2* for glutamate cells, *Dat1/Slc6a3* for dopamine cells, and so on. Achieved with Cre driver mouse lines and Cre-dependent viral genetic tools, most experiments manipulate neurons and their axons and determine the impacts on behavior (Daigle et al., 2018; Harris et al., 2014; Madisen et al., 2015; Taniguchi et al., 2011). Recent studies have started using antagonists to determine if the transmitter of interest is truly mediating the observed effects, like in one study on oxytocin's effects in the VTA (Hung et al., 2017). However, the presence of other neurotransmitters with potential for release and influence on behavior or physiology often is overlooked. Since we determined that CeA^{CRF} neurons are GABAergic and co-express several other neuropeptides (Chapter 1) and manipulating these neurons had effects on fear and anxiety (Chapter 2), we sought out to determine which transmitters were responsible for the observed effects.

We found that GABA, CRF, dynorphin, and neurotensin from CeA^{CRF} neurons play distinct roles in fear and anxiety behaviors (Chapter 3). GABA, but not CRF, dynorphin, or neurotensin regulates baseline anxiety. When stimulated, CRF and dynorphin release is contributing to evoked anxiety behavior, but not neurotensin. When fear conditioned, CeA^{CRF} cells release CRF and dynorphin to promote learning, but appear to release neurotensin to regulate or dampen cued fear learning. This is one of the first studies to examine different signaling molecules released from a specific neuronal population in isolation. The observed effects are consistent with the literature such that CRF and dynorphin promote fear and anxiety (Asok et al., 2018; Crowley et al., 2016; Knoll et al., 2007; Knoll et al., 2011; McCall et al., 2015; Pitts et al., 2009; Regev et al., 2012; Sanford

et al., 2017) and neurotensin has minimal effects on anxiety (Laszlo et al., 2010) and dampens fear (Prus et al., 2014; Steele et al., 2017; Toda et al., 2014; Yamada et al., 2010). It is fascinating that specific neurons can release neurotransmitters that have opposing roles on behavior. This process could be to coordinate signaling downstream to properly gate the flow of information through specific circuitries. Indeed, there is recent evidence that neurotensin and dynorphin bidirectionally modulate inhibitory transmission in the oval BNST (Normandeau et al., 2018a). In this manner, these neurons could fine-tune behavioral outputs that are appropriate for a given environmental context or challenge. Future studies should determine how these different peptides, in isolation and in combination, influence physiology and plasticity in the extended amygdala and its projection targets. In addition, they should evaluate how a history of stress or aversive learning modifies how these peptides signal in these structures.

We chose to employ RNA interference techniques instead of pharmacology to understand which neuropeptides were important for CeA^{CRF} contributions to fear and anxiety. Although antagonists are extremely useful agents, it remains unclear whether the inhibited signal is truly coming from the manipulated neurons in question. For example, administering a kappa opioid receptor antagonist while stimulating CeA^{CRF} neurons could have an effect but since there may be other dynorphin neurons nearby, it is possible that indirect effects could lead to dynorphin release from other neuronal populations. In this case stimulating CeA^{CRF} neurons does recruit a dynorphin signal to drive behavior, but it may not be derived from the CeA^{CRF} neurons. shRNAs allows one to directly inhibit the release of a transmitter from a known population of cells. Since we used Cre-dependent shRNAs, it is almost guaranteed that we are preventing the signaling of different neuropeptides specifically from CeA^{CRF} neurons. Thus, our experimental design could be

considered 'cleaner' than pharmacology studies. Altogether, Chapter 3 of this dissertation demonstrates that CeA^{CRF} neurons release multiple transmitters to properly modulate fear and anxiety behaviors in rats, and highlights a complex neurological process that most likely common across many different neuronal populations and brain regions.

CeA^{CRF}→dlBNST circuit

Eventually the neuroanatomical framework developed by Davis and colleagues was expanded to incorporate CRF signaling (Davis et al., 2010). Using the fear-potentiated startle model, investigators were able to generate anxiety-like responses in rats. This was typically done with bright lighting in the test chamber, or the administration of CRF itself into the lateral ventricles (Liang et al., 1992b; Walker et al., 2009b). When CRF antagonists were administered into the ventricles or into the BNST, anxiety-like responses were abolished (Lee and Davis, 1997; Walker and Davis, 2008; Walker et al., 2009b), thus establishing a critical role for CRF acting at CRF1 receptors in anxiety. In agreement with these studies, CRF administration into the ventricles or the dlBNST in rats generates anxiety-like behaviors (Lee and Davis, 1997; Liang et al., 1992b; Sahuque et al., 2006; Swerdlow et al., 1986) that were reduced by CRF1 receptor antagonists injected into the BNST, but not into the CeA (Lee and Davis, 1997; Sahuque et al., 2006). Thus, the BNST, but not the CeA, appeared to orchestrate anxiety-like responses that are dependent on CRF.

At this point in time, there was little knowledge of specific neural circuits that could be mediating anxiety. However, it was known that many neurons of the CeA express CRF, and that a strong CRF pathway from the CeA to the BNST existed (Sakanaka et al., 1986); replicated in Chapter 1). Due to the anatomy and pharmacology data, Davis and colleagues proposed that a potential pro-anxiety circuit might be the CeA^{CRF} pathway to the BNST.

However, this intriguing hypothesis remained untested in the literature. Only recently with the ability to target genetically-defined populations of neurons has this pathway been able to be examined in isolation. One study reported that disconnecting the CeA from the BNST with contralateral lesions prevented stress-induced anxiety on the elevated plus maze (Cai et al., 2012). However, no pathway specific manipulations have been performed in the context of anxiety behavior. The experiments presented in Chapter 3 are the first examples of pathway and cell-type specific manipulations of the CeA^{CRF}→dlBNST circuit. Chemogenetic inhibition of this pathway, achieved with infection of CeA^{CRF} neurons with Cre-dependent hM4Di and targeted microinjections of CNO into the dlBNST, prevented stress-induced anxiety. Chemogenetic activation of these same axon terminals in the dlBNST generated an anxiety state to a similar to that of stress. These results are the first demonstration of this pathway's critical role in anxiety, proving the CRF pathway hypothesis proposed by Davis and colleagues as correct.

It is still unknown exactly how CeA^{CRF} inputs to the dlBNST affect local neurophysiology. Since CeA^{CRF} cells are GABAergic, there are most likely inhibitory synapses connecting CeA^{CRF} cells to dlBNST cells. However, there is evidence from studies performed in other brain structures that peptide release may be the preferential signaling mechanism. In mouse, CeA^{CRF} projections to the locus coeruleus do not form many inhibitory synapses, but high frequency stimulation with channelrhodopin2 elicited increases in spontaneous activity of postsynaptic neurons, indicating evoked neuropeptide release (McCall et al., 2015). It has been reported that CRF enhanced glutamate release in the dlBNST that is dependent on CRF1 receptors (Kash et al., 2008; Nobis et al., 2011; Silberman et al., 2013). In addition, dynorphin can inhibit incoming anxiolytic terminals from the BLA (Crowley et al., 2016) and neurotensin can modulate GABAergic

transmission in the oval BNST (Normandeau et al., 2018b). Therefore, CRF, and perhaps dynorphin and neurotensin release from CeA^{CRF} terminals could influence the excitatory/inhibitory balance in the dlBNST, leading to a net physiological effect that promotes anxiety. Considering CeA^{CRF} terminals mostly target the oval nucleus, an anxiogenic subregion (Kim et al., 2013) that houses most of the $dlBNST^{CRF}$ neurons (Chapter 1), this scenario is likely. It will be important for future studies to dissect the microcircuitry of the dlBNST and determine how CRF from the CeA modulates local circuit function as well as consequences downstream in remote brain regions to promote anxiety.

It is also interesting that CeA^{CRF} terminals cluster in the oval nucleus where $dlBNST^{CRF}$ neurons are. The final piece of data in this report shows $dlBNST^{CRF}$ neurons as essential to CeA^{CRF} neuron-induced anxiety. This was determined with a chemogenetic disconnection procedure (Figure 4.6) and a Caspase-mediated disconnection during immobilization stress (Figure 4.7). In both cases, the data suggest that CeA^{CRF} neurons promote anxiety with the help of $dlBNST^{CRF}$ neurons. This is a novel finding that implies a CRF-to-CRF "chaining" that promotes anxiety. However, since the experiments did not employ pathway-specific manipulations, it is possible that indirect circuit mechanisms lead to the dependence on $dlBNST^{CRF}$ neurons. As discussed in Chapter 4, CeA^{CRF} projections to the locus coeruleus or other brainstem regions could lead to feed-forward effects in the dlBNST. Indeed, neurons of the dlBNST respond to and become activated by norepinephrine (Nobis et al., 2011). Thus, it cannot be said for certain that CeA^{CRF} inputs directly activate $dlBNST^{CRF}$ neurons. It is likely the case that both mechanisms exist, but future studies will need to determine if and when each one occurs, and whether CeA^{CRF} terminals can directly influence the activity of $dlBNST^{CRF}$ neurons in brain slice.

The CRF-to-CRF cell chaining finding is similar to a recent study reporting that CeA somatostatin neurons promote anxiety by recruiting dlBNST somatostatin neurons (Ahrens et al., 2018). In that study, the authors found that dynorphin release was a major component linking the CeA to the dlBNST in its provocation of anxiety. Since a considerable portion of CeA^{CRF} neurons express somatostatin and dynorphin (Chapter 1), it is likely that CRF neurons are part of that story. This concept is also consistent with recent studies done in non-human primates. In models of anxiety in monkeys, brain imaging analysis consistently shows that anxious temperament and behaviors are associated with simultaneous activity in the CeA and BNST (Fox et al., 2018; Fox and Shackman, 2017; Shackman and Fox, 2016; Shackman et al., 2017). Furthermore, overexpression of CRF in the primate CeA generates anxious temperments (Kalin et al., 2016). Therefore, it is proposed that the CeA and BNST function as a coupled unit to properly regulate anxiety-like responses in several species, and that CRF is a critical signaling molecule. Altogether the findings presented here demonstrate the CeA^{CRF}→dlBNST pathway as an essential component of anxiety behaviors, and suggest that this circuit could be disrupted in human anxiety disorders. Future investigations should evaluate how this circuit adapts after stress exposure and is modified in neuropsychiatric disease.

CRF systems in health and disease

The original purpose of a brain system like CRF circuitry in the extended amygdala was for ensuring survival ability in a dangerous environment. Since animals need to learn about and avoid predation and other threats, brain circuits are dedicated to this process. The amygdala receives external and internal information from many sensory modalities and

must integrate these signals to help execute a required behavioral response. Strong connectivity with and similar genetics to the BNST imply that these structures are related and communicate with each other for important purposes. Based on the literature and the original data presented here, it might be the case the CeA transmits information related to the stress state of an animal to the BNST for an appropriate behavioral response. A simple model is that CeA informs the BNST of a threat or an environmental stressor and the BNST comes online to orchestrate an anxiety-like behavior. This is an unproven hypothesis, but the data here suggest that this could be true. Future experimentation that focuses on ethologically relevant stressors or threats and utilizes different combinations of cell-type specific manipulations could lead to a definitive answer. For now, it remains clear that the extended amygdala systems are critical to negative emotional states related to stress, fear, and anxiety.

Like any complex system, there are many opportunities for processes to go wrong. As outlined above, persistent fear and exaggerated anxiety are hallmarks of some of the most prevalent neuropsychiatric disorders in humans (Baxter et al., 2013). There is much preclinical evidence that the extended amygdala is involved in many symptoms of anxiety disorders, and more and more clinical data suggests this is true in humans (Fox and Shackman, 2017; Shackman and Fox, 2016). Dysregulated activity in the CeA or BNST, whether CRF neurons or not, could be a large contributing factor to anxiety disorders. Since the preclinical evidence for CRF is so striking, there is much interest in the CRF1 receptor as a clinical target (Sanders and Nemeroff, 2016; Zorrilla and Koob, 2004). Hence, several small molecule CRF1 receptor antagonists with good brain penetrance have been created and tested in clinical trials for effects on stress-induced craving in alcoholism and anxiety symptoms in PTSD (Dunlop et al., 2017; Kwako et al., 2015; Schwandt et al., 2016).

Unfortunately, each of these trials failed to show improvements of symptoms with the antagonists compared with placebo (Discussed in Pomrenze et al., 2017). It is unclear why this is, considering the effects in animals are so strong. But the data presented here may give some clues.

As discussed above, CeA^{CRF} neurons express and most likely release several neuropeptides all with strong effects on emotional behavior. It is not hard to predict that many of these neuropeptide systems interact and work together to evoke an emotion or a behavioral output. It has already been reported that CRF and dynorphin synergize in the amygdala to regulate anxiety behavior (Bruchas et al., 2009). In addition, CRF and neurotensin cooperate in the oval BNST to regulate synaptic transmission and stress-induced anxiety (Normandeau et al., 2018b). These examples show that neuropeptide signaling is interactive and complex, and may depend on the circuit architecture it is acting on. Therefore, inhibiting only one receptor from one of these systems may be insufficient for reversing psychiatric states in humans. Future studies should evaluate how these neuropeptide systems interact in the extended amygdala, and those results should inform a new wave of clinical trials in humans aimed at ameliorating symptoms of psychiatric disorders characterized by negative emotional states.

The data in this dissertation have helped refine old psychological models of fear and anxiety. In addition, they have validated an old hypothesis while incorporating new features. We now know that the CeA^{CRF}→dlBNST pathway is critically involved in anxiety behavior, and this process involves CRF neurons of the dlBNST and most likely other neuropeptide modulators. Many new questions and experiments can be generated from these data, but overall, they represent another step forward in understanding how a primitive, yet complex brain system contributes to adaptive and maladaptive emotional

states. The data presented here should help inform future preclinical studies on the neurobiology of fear and anxiety and set the stage for the development of more innovative therapeutic strategies for fear and anxiety-related disorders in humans.

REFERENCES

Ahrens, S., Wu, M.V., Furlan, A., Hwang, G.R., Paik, R., Li, H., Penzo, M.A., Tollkuhn, J., and Li, B. (2018). A central extended amygdala circuit that modulates anxiety. J Neurosci 38, 5567-5583.

Alon, T., Zhou, L., Perez, C.A., Garfield, A.S., Friedman, J.M., and Heisler, L.K. (2009). Transgenic mice expressing green fluorescent protein under the control of the corticotropin-releasing hormone promoter. Endocrinology 150, 5626-5632.

American Psychiatric Association. (2016). Anxiety disorders : DSM-5 selections (Arlington, VA: American Psychiatric Association Publishing).

American Psychiatric Association., and American Psychiatric Association. DSM-5 Task Force. (2013). Diagnostic and statistical manual of mental disorders : DSM-5, 5th edn (Washington, D.C.: American Psychiatric Association).

Anderson, D.J., and Adolphs, R. (2014). A framework for studying emotions across species. Cell 157, 187-200.

Anderson, R.I., and Becker, H.C. (2017). Role of the dynorphin/kappa opioid receptor system in the motivational effects of ethanol. Alcoholism: Clinical and Experimental Research.

Arborelius, L., Owens, M.J., Plotsky, P.M., and Nemeroff, C.B. (1999). The role of corticotropin-releasing factor in depression and anxiety disorders. Journal of Endocrinology 160, 1-12.

Asan, E., Yilmazer-Hanke, D.M., Eliava, M., Hantsch, M., Lesch, K.P.P., and Schmitt, A. (2005). The corticotropin-releasing factor (CRF)-system and monoaminergic afferents in the central amygdala: investigations in different mouse strains and comparison with the rat. Neuroscience 131, 953-967.

Asok, A., Draper, A., Hoffman, A.F., Schulkin, J., Lupica, C.R., and Rosen, J.B. (2018). Optogenetic silencing of a corticotropin-releasing factor pathway from the central amygdala to the bed nucleus of the stria terminalis disrupts sustained fear. Mol Psychiatry 23, 914-922.

Bailey, K.R., and Crawley, J.N. (2009). Anxiety-Related Behaviors in Mice. In Methods of Behavior Analysis in Neuroscience, nd, and J.J. Buccafusco, eds. (Boca Raton (FL)).

Bale, T.L., and Vale, W.W. (2004). CRF and CRF receptors: role in stress responsivity and other behaviors. Annual review of pharmacology and toxicology 44, 525-557.

Bauer, E.P., LeDoux, J.E., and Nader, K. (2001). Fear conditioning and LTP in the lateral amygdala are sensitive to the same stimulus contingencies. Nat Neurosci 4, 687-688.

Baxter, A.J., Scott, K.M., Vos, T., and Whiteford, H.A. (2013). Global prevalence of anxiety disorders: a systematic review and meta-regression. Psychological medicine 43, 897-910.

Berridge, C.W., and Dunn, A.J. (1987). A corticotropin-releasing factor antagonist reverses the stress-induced changes of exploratory behavior in mice. Horm Behav 21, 393-401.

Bimboim, H.C., and Doly, J. (1979). A rapid alkaline extraction procedure for screening recombinant plasmid DNA. Nucleic Acids Research 7, 1513-1523.

Binder, E.B., and Nemeroff, C.B. (2010). The CRF system, stress, depression and anxiety-insights from human genetic studies. Mol Psychiatry 15, 574-588.

Blanchard, R.J., Blanchard, D.C., Rodgers, J., and Weiss, S.M. (1990). The characterization and modelling of antipredator defensive behavior. Neurosci Biobehav Rev 14, 463-472.

Blank, T., Nijholt, I., Eckart, K., and Spiess, J. (2002). Priming of long-term potentiation in mouse hippocampus by corticotropin-releasing factor and acute stress: implications for hippocampus-dependent learning. J Neurosci 22, 3788-3794.

Botta, P., Demmou, L., Kasugai, Y., Markovic, M., Xu, C., Fadok, J.P., Lu, T., Poe, M.M., Xu, L., Cook, J.M., *et al*. (2015). Regulating anxiety with extrasynaptic inhibition. Nat Neurosci 18, 1493-1500.

Bourgeais, L., Gauriau, C., and Bernard, J.F. (2001). Projections from the nociceptive area of the central nucleus of the amygdala to the forebrain: a PHA-L study in the rat. The European journal of neuroscience 14, 229-255.

Brown, M.R., Fisher, L.A., Spiess, J., Rivier, C., Rivier, J., and Vale, W. (1982). Corticotropin-releasing factor: actions on the sympathetic nervous system and metabolism. Endocrinology 111, 928-931.

Bruchas, M.R., Land, B.B., Lemos, J.C., and Chavkin, C. (2009). CRF1-R activation of the dynorphin/kappa opioid system in the mouse basolateral amygdala mediates anxiety-like behavior. PLoS One 4, e8528.

Butler, P.D., Weiss, J.M., Stout, J.C., and Nemeroff, C.B. (1990). Corticotropin-releasing factor produces fear-enhancing and behavioral activating effects following infusion into the locus coeruleus. J Neurosci 10, 176-183.

Buynitsky, T., and Mostofsky, D.I. (2009). Restraint stress in biobehavioral research: Recent developments. Neurosci Biobehav Rev 33, 1089-1098.

Bystritsky, A. (2006). Treatment-resistant anxiety disorders. Mol Psychiatry 11, 805-814.

Cai, L., Bakalli, H., and Rinaman, L. (2012). Yohimbine anxiogenesis in the elevated plus maze is disrupted by bilaterally disconnecting the bed nucleus of the stria terminalis from the central nucleus of the amygdala. Neuroscience 223, 200-208.

Cassell, M.D., Freedman, L.J., and Shi, C. (1999). The intrinsic organization of the central extended amygdala. Annals of the New York Academy of Sciences 877, 217-241.

Cassell, M.D., and Gray, T.S. (1989). Morphology of peptide-immunoreactive neurons in the rat central nucleus of the amygdala. J Comp Neurol 281, 320-333.

Chen, C., Wilcoxen, K.M., Huang, C.Q., Xie, Y.F., McCarthy, J.R., Webb, T.R., Zhu, Y.F., Saunders, J., Liu, X.J., Chen, T.K., *et al.* (2004). Design of 2,5-dimethyl-3-(6-dimethyl-4-methylpyridin-3-yl)-7-dipropylaminopyrazolo[1,5-a]py rimidine (NBI 30775/R121919) and structure--activity relationships of a series of potent and orally active corticotropin-releasing factor receptor antagonists. J Med Chem 47, 4787-4798.

Chen, Y., Molet, J., Gunn, B.G., Ressler, K., and Baram, T.Z. (2015). Diversity of reporter expression patterns in transgenic mouse lines targeting corticotropin releasing hormone-expressing neurons. Endocrinology, en20151673.

Christianson, J.P., Ragole, T., Amat, J., Greenwood, B.N., Strong, P.V., Paul, E.D., Fleshner, M., Watkins, L.R., and Maier, S.F. (2010). 5-hydroxytryptamine 2C receptors in the basolateral amygdala are involved in the expression of anxiety after uncontrollable traumatic stress. Biol Psychiatry 67, 339-345.

Ciocchi, S., Herry, C., Grenier, F., Wolff, S.B., Letzkus, J.J., Vlachos, I., Ehrlich, I., Sprengel, R., Deisseroth, K., Stadler, M.B., *et al.* (2010). Encoding of conditioned fear in central amygdala inhibitory circuits. Nature 468, 277-282.

Clugnet, M.C., and LeDoux, J.E. (1990). Synaptic plasticity in fear conditioning circuits: induction of LTP in the lateral nucleus of the amygdala by stimulation of the medial geniculate body. J Neurosci 10, 2818-2824.

Cotta-de-Almeida, V., Schonhoff, S., Shibata, T., Leiter, A., and Snapper, S.B. (2003). A new method for rapidly generating gene-targeting vectors by engineering BACs through homologous recombination in bacteria. Genome Research 13, 2190-2194.

Crowley, N.A., Bloodgood, D.W., Hardaway, J.A., Kendra, A.M., McCall, J.G., Al-Hasani, R., McCall, N.M., Yu, W., Schools, Z.L., Krashes, M.J., *et al*. (2016). Dynorphin controls the gain of an amygdalar anxiety circuit. Cell Rep 14, 2774-2783.

Dabrowska, J., Hazra, R., Guo, J.D., Dewitt, S., and Rainnie, D.G. (2013a). Central CRF neurons are not created equal: phenotypic differences in CRF-containing neurons of the rat paraventricular hypothalamus and the bed nucleus of the stria terminalis. Front Neurosci 7, 156.

Dabrowska, J., Hazra, R., Guo, J.D., Li, C., Dewitt, S., Xu, J., Lombroso, P.J., and Rainnie, D.G. (2013b). Striatal-enriched protein tyrosine phosphatase-STEPs toward understanding chronic stress-induced activation of corticotrophin releasing factor neurons in the rat bed nucleus of the stria terminalis. Biol Psychiatry 74, 817-826.

Daigle, T.L., Madisen, L., Hage, T.A., Valley, M.T., Knoblich, U., Larsen, R.S., Takeno, M.M., Huang, L., Gu, H., Larsen, R., *et al*. (2018). A Suite of Transgenic Driver and Reporter Mouse Lines with Enhanced Brain-Cell-Type Targeting and Functionality. Cell 174, 465-480 e422.

Daniel, S.E., and Rainnie, D.G. (2016). Stress Modulation of Opposing Circuits in the Bed Nucleus of the Stria Terminalis. Neuropsychopharmacology 41, 103-125.

Davis, M. (1992). The role of the amygdala in fear and anxiety. Annu Rev Neurosci 15, 353-375.

Davis, M. (1997). Neurobiology of fear responses: the role of the amygdala. J Neuropsychiatry Clin Neurosci 9, 382-402.

Davis, M., Rainnie, D., and Cassell, M. (1994a). Neurotransmission in the rat amygdala related to fear and anxiety. Trends Neurosci 17, 208-214.

Davis, M., Rainnie, D., and Cassell, M. (1994b). Neurotransmission in the rat amygdala related to fear and anxiety. Trends in Neurosciences 17, 208-214.

Davis, M., and Shi, C. (2000). The amygdala. Curr Biol 10, R131.

Davis, M., Walker, D.L., Miles, L., and Grillon, C. (2010). Phasic vs sustained fear in rats and humans: role of the extended amygdala in fear vs anxiety. Neuropsychopharmacology 35, 105-135.

Day, H.E., Curran, E.J., Watson, S.J., Jr., and Akil, H. (1999). Distinct neurochemical populations in the rat central nucleus of the amygdala and bed nucleus of the stria terminalis: evidence for their selective activation by interleukin-1beta. J Comp Neurol 413, 113-128.

Dedic, N., Kuhne, C., Jakovcevski, M., Hartmann, J., Genewsky, A.J., Gomes, K.S., Anderzhanova, E., Pohlmann, M.L., Chang, S., Kolarz, A., *et al.* (2018). Chronic CRH depletion from GABAergic, long-range projection neurons in the extended amygdala reduces dopamine release and increases anxiety. Nat Neurosci 21, 803-807.

Deisseroth, K. (2014). Circuit dynamics of adaptive and maladaptive behaviour. Nature 505, 309-317.

Delaney, A.J., and Sah, P. (2001). Pathway-specific targeting of GABA(A) receptor subtypes to somatic and dendritic synapses in the central amygdala. J Neurophysiol 86, 717-723.

Dong, H.W., Petrovich, G.D., and Swanson, L.W. (2001). Topography of projections from amygdala to bed nuclei of the stria terminalis. Brain Res Brain Res Rev 38, 192-246.

Dunlop, B.W., Binder, E.B., Iosifescu, D., Mathew, S.J., Neylan, T.C., Pape, J.C., Carrillo-Roa, T., Green, C., Kinkead, B., Grigoriadis, D., *et al.* (2017). Corticotropin-Releasing Factor Receptor 1 Antagonism Is Ineffective for Women With Posttraumatic Stress Disorder. Biol Psychiatry 82, 866-874.

Fadok, J.P., Krabbe, S., Markovic, M., Courtin, J., Xu, C., Massi, L., Botta, P., Bylund, K., Muller, C., Kovacevic, A., *et al.* (2017). A competitive inhibitory circuit for selection of active and passive fear responses. Nature 542, 96-100.

Fadok, J.P., Markovic, M., Tovote, P., and Lüthi, A. (2018). New perspectives on central amygdala function. Current Opinion in Neurobiology 49, 141-147.

Fanselow, M.S., Kim, J.J., Young, S.L., Calcagnetti, D.J., DeCola, J.P., Helmstetter, F.J., and Landeira-Fernandez, J. (1991). Differential effects of selective opioid peptide antagonists on the acquisition of pavlovian fear conditioning. Peptides 12, 1033-1037.

Faul, F., Erdfelder, E., Lang, A.G., and Buchner, A. (2007). G*Power 3: a flexible statistical power analysis program for the social, behavioral, and biomedical sciences. Behav Res Methods 39, 175-191.

Fendt, M., Koch, M., and Schnitzler, H.U. (1997). Corticotropin-releasing factor in the caudal pontine reticular nucleus mediates the expression of fear-potentiated startle in the rat. Eur J Neurosci 9, 299-305.

Filipiak, W.E., and Saunders, T.L. (2006). Advances in transgenic rat production. Transgenic Res 15, 673-686.

Flandreau, E.I., Ressler, K.J., Owens, M.J., and Nemeroff, C.B. (2012). Chronic overexpression of corticotropin-releasing factor from the central amygdala produces HPA axis hyperactivity and behavioral anxiety associated with gene-expression changes in the hippocampus and paraventricular nucleus of the hypothalamus. Psychoneuroendocrinology 37, 27-38.

Fox, A.S., Oler, J.A., Birn, R.M., Shackman, A.J., Alexander, A.L., and Kalin, N.H. (2018). Functional Connectivity within the Primate Extended Amygdala Is Heritable and Associated with Early-Life Anxious Temperament. J Neurosci 38, 7611-7621.

Fox, A.S., and Shackman, A.J. (2017). The central extended amygdala in fear and anxiety: Closing the gap between mechanistic and neuroimaging research. Neurosci Lett.

Gafford, G., Jasnow, A.M., and Ressler, K.J. (2014). Grin1 receptor deletion within CRF neurons enhances fear memory. PLoS One 9, e111009.

Gafford, G.M., Guo, J.D., Flandreau, E.I., Hazra, R., Rainnie, D.G., and Ressler, K.J. (2012). Cell-type specific deletion of GABA(A)alpha1 in corticotropin-releasing factor-containing neurons enhances anxiety and disrupts fear extinction. Proc Natl Acad Sci U S A 109, 16330-16335.

Gallagher, J.P., Orozco-Cabal, L.F., Liu, J., and Shinnick-Gallagher, P. (2008). Synaptic physiology of central CRH system. Eur J Pharmacol 583, 215-225.

Gomez, J.L., Bonaventura, J., Lesniak, W., Mathews, W.B., Sysa-Shah, P., Rodriguez, L.A., Ellis, R.J., Richie, C.T., Harvey, B.K., Dannals, R.F., *et al*. (2017). Chemogenetics revealed: DREADD occupancy and activation via converted clozapine. Science 357, 503-507.

Gray, T.S., and Magnuson, D.J. (1987). Neuropeptide neuronal efferents from the bed nucleus of the stria terminalis and central amygdaloid nucleus to the dorsal vagal complex in the rat. J Comp Neurol 262, 365-374.

Gray, T.S., and Magnuson, D.J. (1992). Peptide immunoreactive neurons in the amygdala and the bed nucleus of the stria terminalis project to the midbrain central gray in the rat. Peptides 13, 451-460.

Griebel, G., and Holmes, A. (2013). 50 years of hurdles and hope in anxiolytic drug discovery. Nat Rev Drug Discov 12, 667-687.

Grieder, T.E., Herman, M.A., Contet, C., Tan, L.A., Vargas-Perez, H., Cohen, A., Chwalek, M., Maal-Bared, G., Freiling, J., Schlosburg, J.E., *et al*. (2014). VTA CRF neurons mediate the aversive effects of nicotine withdrawal and promote intake escalation. Nat Neurosci 17, 1751-1758.

Grupe, D.W., and Nitschke, J.B. (2013). Uncertainty and anticipation in anxiety: an integrated neurobiological and psychological perspective. Nat Rev Neurosci 14, 488-501.

Gungor, N.Z., and Paré, D. (2016). Functional heterogeneity in the bed nucleus of the stria terminalis. The Journal of Neuroscience 36, 8038-8049.

Harris, J.A., Hirokawa, K.E., Sorensen, S.A., Gu, H., Mills, M., Ng, L.L., Bohn, P., Mortrud, M., Ouellette, B., Kidney, J., *et al*. (2014). Anatomical characterization of Cre driver mice for neural circuit mapping and manipulation. Front Neural Circuits 8, 76.

Haubensak, W., Kunwar, P.S., Cai, H., Ciocchi, S., Wall, N.R., Ponnusamy, R., Biag, J., Dong, H.W., Deisseroth, K., Callaway, E.M., *et al*. (2010). Genetic dissection of an amygdala microcircuit that gates conditioned fear. Nature 468, 270-276.

Hazim, A.I., Ramanathan, S., Parthasarathy, S., Muzaimi, M., and Mansor, S.M. (2014). Anxiolytic-like effects of mitragynine in the open-field and elevated plus-maze tests in rats. J Physiol Sci 64, 161-169.

Heinrichs, S.C., Menzaghi, F., Merlo Pich, E., Britton, K.T., and Koob, G.F. (1995). The role of CRF in behavioral aspects of stress. Ann N Y Acad Sci 771, 92-104.

Heisler, L.K., Zhou, L., Bajwa, P., Hsu, J., and Tecott, L.H. (2007). Serotonin 5-HT(2C) receptors regulate anxiety-like behavior. Genes Brain Behav 6, 491-496.

Herman, M.A., Kallupi, M., Luu, G., Oleata, C.S., Heilig, M., Koob, G.F., Ciccocioppo, R., and Roberto, M. (2013). Enhanced GABAergic transmission in the central nucleus of the amygdala of genetically selected Marchigian Sardinian rats: alcohol and CRF effects. Neuropharmacology 67, 337-348.

Hikichi, T., Akiyoshi, J., Yamamoto, Y., Tsutsumi, T., Isogawa, K., and Nagayama, H. (2000). Suppression of conditioned fear by administration of CRF receptor antagonist CP-154,526. Pharmacopsychiatry 33, 189-193.

Hung, L.W., Neuner, S., Polepalli, J.S., Beier, K.T., Wright, M., Walsh, J.J., Lewis, E.M., Luo, L., Deisseroth, K., Dolen, G., and Malenka, R.C. (2017). Gating of social reward by oxytocin in the ventral tegmental area. Science 357, 1406-1411.

Insel, T.R. (2012). Next-generation treatments for mental disorders. Sci Transl Med 4, 155ps119.

Ji, G., Fu, Y., Adwanikar, H., and Neugebauer, V. (2013). Non-pain-related CRF1 activation in the amygdala facilitates synaptic transmission and pain responses. Mol Pain 9, 2.

Jones, C.E., and Monfils, M.H. (2016). Fight, Flight, or Freeze? The Answer May Depend on Your Sex. Trends Neurosci 39, 51-53.

Kaczmarczyk, S.J., and Green, J.E. (2001). A single vector containing modified cre recombinase and LOX recombination sequences for inducible tissue-specific amplification of gene expression. Nucleic Acids Research 29, e56-e56.

Kaczmarek, L., and Chaudhuri, A. (1997). Sensory regulation of immediate-early gene expression in mammalian visual cortex: implications for functional mapping and neural plasticity. Brain Res Brain Res Rev 23, 237-256.

Kalin, N.H., Fox, A.S., Kovner, R., Riedel, M.K., Fekete, E.M., Roseboom, P.H., Tromp do, P.M., Grabow, B.P., Olsen, M.E., Brodsky, E.K., *et al*. (2016). Overexpressing Corticotropin-Releasing Factor in the Primate Amygdala Increases Anxious Temperament and Alters Its Neural Circuit. Biol Psychiatry 80, 345-355.

Kash, T.L., Nobis, W.P., Matthews, R.T., and Winder, D.G. (2008). Dopamine enhances fast excitatory synaptic transmission in the extended amygdala by a CRF-R1-dependent process. J Neurosci 28, 13856-13865.

Kash, T.L., Pleil, K.E., Marcinkiewcz, C.A., Lowery-Gionta, E.G., Crowley, N., Mazzone, C., Sugam, J., Hardaway, J.A., and McElligott, Z.A. (2015). Neuropeptide regulation of signaling and behavior in the BNST. Mol Cells 38, 1-13.

Kash, T.L., and Winder, D.G. (2006). Neuropeptide Y and corticotropin-releasing factor bi-directionally modulate inhibitory synaptic transmission in the bed nucleus of the stria terminalis. Neuropharmacology 51, 1013-1022.

Keen-Rhinehart, E., Michopoulos, V., Toufexis, D.J., Martin, E.I., Nair, H., Ressler, K.J., Davis, M., Owens, M.J., Nemeroff, C.B., and Wilson, M.E. (2009). Continuous expression of corticotropin-releasing factor in the central nucleus of the amygdala emulates the dysregulation of the stress and reproductive axes. Mol Psychiatry 14, 37-50.

Kessler, R.C., Petukhova, M., Sampson, N.A., Zaslavsky, A.M., and Wittchen, H.U. (2012). Twelve-month and lifetime prevalence and lifetime morbid risk of anxiety and mood disorders in the United States. Int J Methods Psychiatr Res 21, 169-184.

Kim, J., Zhang, X., Muralidhar, S., LeBlanc, S.A., and Tonegawa, S. (2017). Basolateral to central amygdala neural circuits for appetitive behaviors. Neuron 93, 1464-1479.e1465.

Kim, S.Y., Adhikari, A., Lee, S.Y., Marshel, J.H., Kim, C.K., Mallory, C.S., Lo, M., Pak, S., Mattis, J., Lim, B.K., *et al*. (2013). Diverging neural pathways assemble a behavioural state from separable features in anxiety. Nature 496, 219-223.

Knoll, A.T., Meloni, E.G., Thomas, J.B., Carroll, F.I., and Carlezon, W.A., Jr. (2007). Anxiolytic-like effects of kappa-opioid receptor antagonists in models of unlearned and learned fear in rats. J Pharmacol Exp Ther 323, 838-845.

Knoll, A.T., Muschamp, J.W., Sillivan, S.E., Ferguson, D., Dietz, D.M., Meloni, E.G., Carroll, F.I., Nestler, E.J., Konradi, C., and Carlezon, W.A., Jr. (2011). Kappa opioid receptor signaling in the basolateral amygdala regulates conditioned fear and anxiety in rats. Biol Psychiatry 70, 425-433.

Koob, G.F. (1999). Corticotropin-releasing factor, norepinephrine, and stress. Biol Psychiatry 46, 1167-1180.

Koob, G.F. (2008). A Role for Brain Stress Systems in Addiction. Neuron 59, 11-34.

Koob, G.F. (2009). Brain stress systems in the amygdala and addiction. Brain Res 1293, 61-75.

Koob, G.F., Cole, B.J., Swerdlow, N.R., Le Moal, M., and Britton, K.T. (1990). Stress, performance, and arousal: focus on CRF. NIDA Res Monogr 97, 163-176.

Krashes, M.J., Koda, S., Ye, C., Rogan, S.C., Adams, A.C., Cusher, D.S., Maratos-Flier, E., Roth, B.L., and Lowell, B.B. (2011). Rapid, reversible activation of AgRP neurons drives feeding behavior in mice. J Clin Invest 121, 1424-1428.

Kravets, J.L., Reyes, B.A., Unterwald, E.M., and Van Bockstaele, E.J. (2015). Direct targeting of peptidergic amygdalar neurons by noradrenergic afferents: linking stress-integrative circuitry. Brain Struc Func 220, 541-558.

Kwako, L.E., Spagnolo, P.A., Schwandt, M.L., Thorsell, A., George, D.T., Momenan, R., Rio, D.E., Huestis, M., Anizan, S., Concheiro, M., *et al*. (2015). The corticotropin releasing hormone-1 (CRH1) receptor antagonist pexacerfont in alcohol dependence: a randomized controlled experimental medicine study. Neuropsychopharmacology 40, 1053-1063.

Laszlo, K., Toth, K., Kertes, E., Peczely, L., and Lenard, L. (2010). The role of neurotensin in positive reinforcement in the rat central nucleus of amygdala. Behav Brain Res 208, 430-435.

LeDoux, J. (2003). The emotional brain, fear, and the amygdala. Cell Mol Neurobiol 23, 727-738.

LeDoux, J. (2007). The amygdala. Curr Biol 17, R868-874.

LeDoux, J.E. (2000). Emotion circuits in the brain. Annu Rev Neurosci 23, 155-184.

LeDoux, J.E. (2014). Coming to terms with fear. Proc Natl Acad Sci U S A 111, 2871-2878.

LeDoux, J.E., and Brown, R. (2017). A higher-order theory of emotional consciousness. Proc Natl Acad Sci USA 114.

Lee, Y., and Davis, M. (1997). Role of the hippocampus, the bed nucleus of the stria terminalis, and the amygdala in the excitatory effect of corticotropin-releasing hormone on the acoustic startle reflex. Journal of Neuroscience 17, 6434-6446.

Lesscher, H.M., McMahon, T., Lasek, A.W., Chou, W.H., Connolly, J., Kharazia, V., and Messing, R.O. (2008). Amygdala protein kinase C epsilon regulates corticotropin-releasing factor and anxiety-like behavior. Genes Brain Behav 7, 323-333.

Li, C., Pleil, K.E., Stamatakis, A.M., Busan, S., Vong, L., Lowell, B.B., Stuber, G.D., and Kash, T.L. (2012). Presynaptic inhibition of gamma-aminobutyric acid release in the bed nucleus of the stria terminalis by kappa opioid receptor signaling. Biol Psychiatry 71, 725-732.

Li, H., Penzo, M.A., Taniguchi, H., Kopec, C.D., Huang, Z.J., and Li, B. (2013). Experience-dependent modification of a central amygdala fear circuit. Nat Neurosci 16, 332-339.

Liang, K.C., Melia, K.R., Campeau, S., Falls, W.A., Miserendino, M.J., and Davis, M. (1992a). Lesions of the central nucleus of the amygdala, but not the paraventricular nucleus of the hypothalamus, block the excitatory effects of corticotropin-releasing factor on the acoustic startle reflex. J Neurosci 12, 2313-2320.

Liang, K.C., Melia, K.R., Miserendino, M.J., Falls, W.A., Campeau, S., and Davis, M. (1992b). Corticotropin-releasing factor: long-lasting facilitation of the acoustic startle reflex. J Neurosci 12, 2303-2312.

Madisen, L., Garner, A.R., Shimaoka, D., Chuong, A.S., Klapoetke, N.C., Li, L., van der Bourg, A., Niino, Y., Egolf, L., Monetti, C., *et al*. (2015). Transgenic mice for intersectional targeting of neural sensors and effectors with high specificity and performance. Neuron 85, 942-958.

Mahler, S.V., Vazey, E.M., Beckley, J.T., Keistler, C.R., McGlinchey, E.M., Kaufling, J., Wilson, S.P., Deisseroth, K., Woodward, J.J., and Aston-Jones, G. (2014). Designer receptors show role for ventral pallidum input to ventral tegmental area in cocaine seeking. Nat Neurosci 17, 577-585.

Makino, S., Gold, P.W., and Schulkin, J. (1994). Effects of corticosterone on CRH mRNA and content in the bed nucleus of the stria terminalis; comparison with the effects in the central nucleus of the amygdala and the paraventricular nucleus of the hypothalamus. Brain research 657, 141-149.

Marchant, N.J., Densmore, V.S., and Osborne, P.B. (2007). Coexpression of prodynorphin and corticotrophin-releasing hormone in the rat central amygdala: evidence of two distinct endogenous opioid systems in the lateral division. J Comp Neurol 504, 702-715.

Marcinkiewcz, C.A., Mazzone, C.M., D'Agostino, G., Halladay, L.R., Hardaway, J.A., DiBerto, J.F., Navarro, M., Burnham, N., Cristiano, C., Dorrier, C.E., *et al*. (2016). Serotonin engages an anxiety and fear-promoting circuit in the extended amygdala. Nature 537, 97-101.

Maren, S. (2001). Neurobiology of Pavlovian fear conditioning. Annu Rev Neurosci 24, 897-931.

Maren, S., and Fanselow, M.S. (1996). The amygdala and fear conditioning: has the nut been cracked? Neuron 16, 237-240.

Martin, E.I., Ressler, K.J., Jasnow, A.M., Dabrowska, J., Hazra, R., Rainnie, D.G., Nemeroff, C.B., and Owens, M.J. (2010). A novel transgenic mouse for gene-targeting within cells that express corticotropin-releasing factor. Biol Psychiatry 67, 1212-1216.

McCall, J.G., Al-Hasani, R., Siuda, E.R., Hong, D.Y., Norris, A.J., Ford, C.P., and Bruchas, M.R. (2015). CRH engagement of the locus coeruleus noradrenergic system mediates stress-induced anxiety. Neuron 87, 605-620.

Merchenthaler, I. (1984). Corticotropin releasing factor (CRF)-like immunoreactivity in the rat central nervous system. Extrahypothalamic distribution. Peptides 5 Suppl 1, 53-69.

Moga, M.M., and Gray, T.S. (1985). Evidence for corticotropin-releasing factor, neurotensin, and somatostatin in the neural pathway from the central nucleus of the amygdala to the parabrachial nucleus. J Comp Neurol 241, 275-284.

Naylor, J.C., Li, Q., Kang-Park, M.H., Wilson, W.A., Kuhn, C., and Moore, S.D. (2010). Dopamine attenuates evoked inhibitory synaptic currents in central amygdala neurons. Eur J Neurosci 32, 1836-1842.

Nguyen, A.Q., Dela Cruz, J.A., Sun, Y., Holmes, T.C., and Xu, X. (2016). Genetic cell targeting uncovers specific neuronal types and distinct subregions in the bed nucleus of the stria terminalis. J Comp Neurol 524, 2379-2399.

Nobis, W.P., Kash, T.L., Silberman, Y., and Winder, D.G. (2011). beta-Adrenergic receptors enhance excitatory transmission in the bed nucleus of the stria terminalis through a corticotrophin-releasing factor receptor-dependent and cocaine-regulated mechanism. Biol Psychiatry 69, 1083-1090.

Normandeau, C.P., Torruella Suarez, M.L., Sarret, P., McElligott, Z.A., and Dumont, E.C. (2018a). Neurotensin and dynorphin Bi-Directionally modulate CeA inhibition of oval BNST neurons in male mice. Neuropharmacology 143, 113-121.

Normandeau, C.P., Ventura-Silva, A.P., Hawken, E.R., Angelis, S., Sjaarda, C., Liu, X., Pego, J.M., and Dumont, E.C. (2018b). A Key Role for Neurotensin in Chronic-Stress-Induced Anxiety-Like Behavior in Rats. Neuropsychopharmacology 43, 285-293.

Olschowka, J.A., O'Donohue, T.L., Mueller, G.P., and Jacobowitz, D.M. (1982). Hypothalamic and extrahypothalamic distribution of CRF-like immunoreactive neurons in the rat brain. Neuroendocrinology 35, 305-308.

Osoegawa, K., Zhu, B., Shu, C.L., Ren, T., Cao, Q., Vessere, G.M., Lutz, M.M., Jensen-Seaman, M.I., Zhao, S., and de Jong, P.J. (2004). BAC resources for the rat genome project. Genome Res 14, 780-785.

Panksepp, J. (2011). Cross-species affective neuroscience decoding of the primal affective experiences of humans and related animals. PLoS One 6, e21236.

Pare, W.P., and Glavin, G.B. (1986). Restraint stress in biomedical research: a review. Neurosci Biobehav Rev 10, 339-370.

Penzo, M.A., Robert, V., Tucciarone, J., De Bundel, D., Wang, M., Van Aelst, L., Darvas, M., Parada, L.F., Palmiter, R.D., He, M., *et al*. (2015). The paraventricular thalamus controls a central amygdala fear circuit. Nature 519, 455-459.

Petrovich, G.D., and Swanson, L.W. (1997). Projections from the lateral part of the central amygdalar nucleus to the postulated fear conditioning circuit. Brain Res 763, 247-254.

Phelix, C.F., and Paull, W.K. (1990). Demonstration of distinct corticotropin releasing factor--containing neuron populations in the bed nucleus of the stria terminalis. A light and electron microscopic immunocytochemical study in the rat. Histochemistry 94, 345-364.

Pitts, M.W., and Takahashi, L.K. (2011). The central amygdala nucleus via corticotropin-releasing factor is necessary for time-limited consolidation processing but not storage of contextual fear memory. Neurobiol Learn Mem 95, 86-91.

Pitts, M.W., Todorovic, C., Blank, T., and Takahashi, L.K. (2009). The central nucleus of the amygdala and corticotropin-releasing factor: insights into contextual fear memory. J Neurosci 29, 7379-7388.

Pleil, K.E., Rinker, J.A., Lowery-Gionta, E.G., Mazzone, C.M., McCall, N.M., Kendra, A.M., Olson, D.P., Lowell, B.B., Grant, K.A., Thiele, T.E., and Kash, T.L. (2015). NPY signaling inhibits extended amygdala CRF neurons to suppress binge alcohol drinking. Nat Neurosci 18, 545-552.

Pliota, P., Bohm, V., Grossl, F., Griessner, J., Valenti, O., Kraitsy, K., Kaczanowska, J., Pasieka, M., Lendl, T., Deussing, J.M., and Haubensak, W. (2018). Stress peptides sensitize fear circuitry to promote passive coping. Mol Psychiatry.

Pomrenze, M.B., Fetterly, T.L., Winder, D.G., and Messing, R.O. (2017). The Corticotropin Releasing Factor Receptor 1 in Alcohol Use Disorder: Still a Valid Drug Target? Alcohol Clin Exp Res 41, 1986-1999.

Pomrenze, M.B., Millan, E.Z., Hopf, F.W., Keiflin, R., Maiya, R., Blasio, A., Dadgar, J., Kharazia, V., De Guglielmo, G., Crawford, E., *et al*. (2015). A transgenic rat for investigating the anatomy and function of corticotrophin releasing factor circuits. Front Neurosci 9, 487.

Potter, E., Sutton, S., Donaldson, C., Chen, R., Perrin, M., Lewis, K., Sawchenko, P.E., and Vale, W. (1994). Distribution of corticotropin-releasing factor receptor mRNA expression in the rat brain and pituitary. Proc Natl Acad Sci U S A 91, 8777-8781.

Prus, A.J., Hillhouse, T.M., and LaCrosse, A.L. (2014). Acute, but not repeated, administration of the neurotensin NTS1 receptor agonist PD149163 decreases conditioned footshock-induced ultrasonic vocalizations in rats. Prog Neuropsychopharmacol Biol Psychiatry 49, 78-84.

Regev, L., Tsoory, M., Gil, S., and Chen, A. (2012). Site-specific genetic manipulation of amygdala corticotropin-releasing factor reveals its imperative role in mediating behavioral response to challenge. Biological Psychiatry 71, 317-326.

Reyes, B.A., Carvalho, A.F., Vakharia, K., and Van Bockstaele, E.J. (2011). Amygdalar peptidergic circuits regulating noradrenergic locus coeruleus neurons: linking limbic and arousal centers. Exp Neurol 230, 96-105.

Rivier, C., and Vale, W. (1983). Modulation of stress-induced ACTH release by corticotropin-releasing factor, catecholamines and vasopressin. Nature 305, 325-327.

Roth, B.L. (2016). DREADDs for Neuroscientists. Neuron 89, 683-694.

Sahuque, L.L., Kullberg, E.F., McGeehan, A.J., Kinder, J.R., Hicks, M.P., Blanton, M.G., Janak, P.H., and Olive, M.F. (2006). Anxiogenic and aversive effects of corticotropin-releasing factor (CRF) in the bed nucleus of the stria terminalis in the rat: role of CRF receptor subtypes. Psychopharmacology (Berl) 186, 122-132.

Sakanaka, M., Shibasaki, T., and Lederis, K. (1986). Distribution and efferent projections of corticotropin-releasing factor-like immunoreactivity in the rat amygdaloid complex. Brain research 382, 213-238.

Sanders, J., and Nemeroff, C. (2016). The CRF System as a Therapeutic Target for Neuropsychiatric Disorders. Trends in Pharmacological Sciences 37, 1045-1054.

Sanford, C.A., Soden, M.E., Baird, M.A., Miller, S.M., Schulkin, J., Palmiter, R.D., Clark, M., and Zweifel, L.S. (2017). A central amygdala CRF circuit facilitates learning about weak threats. Neuron 93, 164-178.

Schindelin, J., Arganda-Carreras, I., Frise, E., Kaynig, V., Longair, M., Pietzsch, T., Preibisch, S., Rueden, C., Saalfeld, S., Schmid, B., *et al*. (2012). Fiji: an open-source platform for biological-image analysis. Nat Meth 9, 676-682.

Schmidt, H.D., and Duman, R.S. (2010). Peripheral BDNF produces antidepressant-like effects in cellular and behavioral models. Neuropsychopharmacology 35, 2378-2391.

Schwaber, J.S., Kapp, B.S., Higgins, G.A., and Rapp, P.R. (1982). Amygdaloid and basal forebrain direct connections with the nucleus of the solitary tract and the dorsal motor nucleus. J Neurosci 2, 1424-1438.

Schwandt, M.L., Cortes, C.R., Kwako, L.E., George, D.T., Momenan, R., Sinha, R., Grigoriadis, D.E., Pich, E., Leggio, L., and Heilig, M. (2016). The CRF1 Antagonist Verucerfont in Anxious Alcohol-Dependent Women: Translation of Neuroendocrine, But not of Anti-Craving Effects. Neuropsychopharmacology.

Seif, T., Chang, S.J., Simms, J.A., Gibb, S.L., Dadgar, J., Chen, B.T., Harvey, B.K., Ron, D., Messing, R.O., Bonci, A., and Hopf, F.W. (2013). Cortical activation of accumbens hyperpolarization-active NMDARs mediates aversion-resistant alcohol intake. Nat Neurosci 16, 1094-1100.

Shackman, A.J., and Fox, A.S. (2016). Contributions of the central extended amygdala to fear and anxiety. The Journal of Neuroscience 36, 8050-8063.

Shackman, A.J., Fox, A.S., Oler, J.A., Shelton, S.E., Oakes, T.R., Davidson, R.J., and Kalin, N.H. (2017). Heightened extended amygdala metabolism following threat characterizes the early phenotypic risk to develop anxiety-related psychopathology. Mol Psychiatry 22, 724-732.

Shalev, U., Erb, S., and Shaham, Y. (2010). Role of CRF and other neuropeptides in stress-induced reinstatement of drug seeking. Brain Res 1314, 15-28.

Sigurdsson, T., Doyere, V., Cain, C.K., and LeDoux, J.E. (2007). Long-term potentiation in the amygdala: a cellular mechanism of fear learning and memory. Neuropharmacology 52, 215-227.

Silberman, Y., Matthews, R.T., and Winder, D.G. (2013). A corticotropin releasing factor pathway for ethanol regulation of the ventral tegmental area in the bed nucleus of the stria terminalis. J Neurosci 33, 950-960.

Silberman, Y., and Winder, D.G. (2013). Corticotropin releasing factor and catecholamines enhance glutamatergic neurotransmission in the lateral subdivision of the central amygdala. Neuropharmacology 70, 316-323.

Smith, R.J., and Aston-Jones, G. (2008). Noradrenergic transmission in the extended amygdala: role in increased drug-seeking and relapse during protracted drug abstinence. Brain Struct Funct 213, 43-61.

Spiess, J., Rivier, J., Rivier, C., and Vale, W. (1981). Primary structure of corticotropin-releasing factor from ovine hypothalamus. Proc Natl Acad Sci U S A 78, 6517-6521.

Staley, K.J., and Proctor, W.R. (1999). Modulation of mammalian dendritic GABA(A) receptor function by the kinetics of Cl- and HCO3- transport. J Physiol 519 Pt 3, 693-712.

Steele, F.F., 3rd, Whitehouse, S.C., Aday, J.S., and Prus, A.J. (2017). Neurotensin NTS1 and NTS2 receptor agonists produce anxiolytic-like effects in the 22-kHz ultrasonic vocalization model in rats. Brain Res 1658, 31-35.

Sternson, S.M., and Roth, B.L. (2014). Chemogenetic tools to interrogate brain functions. Annu Rev Neurosci 37, 387-407.

Stuber, G.D., Sparta, D.R., Stamatakis, A.M., van Leeuwen, W.A., Hardjoprajitno, J.E., Cho, S., Tye, K.M., Kempadoo, K.A., Zhang, F., Deisseroth, K., and Bonci, A. (2011). Excitatory transmission from the amygdala to nucleus accumbens facilitates reward seeking. Nature 475, 377-380.

Sun, N., and Cassell, M.D. (1993). Intrinsic GABAergic neurons in the rat central extended amygdala. J Comp Neurol 330, 381-404.

Swanson, L.W., and Simmons, D.M. (1989). Differential steroid hormone and neural influences on peptide mRNA levels in CRH cells of the paraventricular nucleus: a hybridization histochemical study in the rat. The Journal of comparative neurology 285, 413-435.

Swerdlow, N.R., Geyer, M.A., Vale, W.W., and Koob, G.F. (1986). Corticotropin-releasing factor potentiates acoustic startle in rats: blockade by chlordiazepoxide. Psychopharmacology 88, 147-152.

Takahashi, L.K. (2001). Role of CRF(1) and CRF(2) receptors in fear and anxiety. Neurosci Biobehav Rev 25, 627-636.

Taniguchi, H., He, M., Wu, P., Kim, S., Paik, R., Sugino, K., Kvitsiani, D., Fu, Y., Lu, J., Lin, Y., *et al*. (2011). A resource of Cre driver lines for genetic targeting of GABAergic neurons in cerebral cortex. Neuron 71, 995-1013.

Toda, H., Boku, S., Nakagawa, S., Inoue, T., Kato, A., Takamura, N., Song, N., Nibuya, M., Koyama, T., and Kusumi, I. (2014). Maternal separation enhances conditioned fear and decreases the mRNA levels of the neurotensin receptor 1 gene with hypermethylation of this gene in the rat amygdala. PLoS One 9, e97421.

Tovote, P., Esposito, M.S., Botta, P., Chaudun, F., Fadok, J.P., Markovic, M., Wolff, S.B., Ramakrishnan, C., Fenno, L., Deisseroth, K., *et al*. (2016). Midbrain circuits for defensive behaviour. Nature 534, 206-212.

Tovote, P., Fadok, J.P., and Luthi, A. (2015). Neuronal circuits for fear and anxiety. Nat Rev Neurosci 16, 317-331.

Treit, D., and Fundytus, M. (1988). Thigmotaxis as a test for anxiolytic activity in rats. Pharmacol Biochem Behav 31, 959-962.

Van Bockstaele, E.J., Colago, E.E., and Valentino, R.J. (1998). Amygdaloid corticotropin-releasing factor targets locus coeruleus dendrites: substrate for the co-ordination of emotional and cognitive limbs of the stress response. Journal of neuroendocrinology 10, 743-757.

van den Pol, A.N. (2012). Neuropeptide transmission in brain circuits. Neuron 76, 98-115.

van der Kooy, D., Koda, L.Y., McGinty, J.F., Gerfen, C.R., and Bloom, F.E. (1984). The organization of projections from the cortex, amygdala, and hypothalamus to the nucleus of the solitary tract in rat. J Comp Neurol 224, 1-24.

Van Pett, K., Viau, V., Bittencourt, J.C., Chan, R.K., Li, H.Y., Arias, C., Prins, G.S., Perrin, M., Vale, W., and Sawchenko, P.E. (2000). Distribution of mRNAs encoding CRF receptors in brain and pituitary of rat and mouse. The Journal of Comparative Neurology 428, 191-212.

Veening, J.G., Swanson, L.W., and Sawchenko, P.E. (1984). The organization of projections from the central nucleus of the amygdala to brainstem sites involved in central autonomic regulation: a combined retrograde transport-immunohistochemical study. Brain Res 303, 337-357.

Veinante, P., and Freund-Mercier, M.J. (1998). Intrinsic and extrinsic connections of the rat central extended amygdala: an in vivo electrophysiological study of the central amygdaloid nucleus. Brain Res 794, 188-198.

Veinante, P., Stoeckel, M.E., and Freund-Mercier, M.J. (1997). GABA- and peptide-immunoreactivities co-localize in the rat central extended amygdala. Neuroreport 8, 2985-2989.

Walker, D., Yang, Y., Ratti, E., Corsi, M., Trist, D., and Davis, M. (2009a). Differential effects of the CRF-R1 antagonist GSK876008 on fear-potentiated, light- and CRF-enhanced startle suggest preferential involvement in sustained vs phasic threat responses. Neuropsychopharmacology 34, 1533-1542.

Walker, D.L., and Davis, M. (1997a). Anxiogenic effects of high illumination levels assessed with the acoustic startle response in rats. Biological Psychiatry 42, 461-471.

Walker, D.L., and Davis, M. (1997b). Double dissociation between the involvement of the bed nucleus of teh stria terminalis and the central nucleus of the amygdala in startle increases produced by conditioned versus unconditioned fear. Journal of Neuroscience 17, 9375-9383.

Walker, D.L., and Davis, M. (2008). Role of the extended amygdala in short-duration versus sustained fear: a tribute to Dr. Lennart Heimer. Brain Struct Funct 213, 29-42.

Walker, D.L., Miles, L.A., and Davis, M. (2009b). Selective participation of the bed nucleus of the stria terminalis and CRF in sustained anxiety-like versus phasic fear-like responses. Prog Neuropsychopharmacol Biol Psychiatry 33, 1291-1308.

Walker, D.L., Toufexis, D.J., and Davis, M. (2003). Role of the bed nucleus of the stria terminalis versus the amygdala in fear, stress, and anxiety. Eur J Pharmacol 463, 199-216.

Wamsteeker Cusulin, J.I., Fuzesi, T., Watts, A.G., and Bains, J.S. (2013). Characterization of corticotropin-releasing hormone neurons in the paraventricular nucleus of the hypothalamus of Crh-IRES-Cre mutant mice. PLoS One 8, e64943.

Wang, L., Goebel-Stengel, M., Stengel, A., Wu, S.V., Ohning, G., and Tache, Y. (2011). Comparison of CRF-immunoreactive neurons distribution in mouse and rat brains and selective induction of Fos in rat hypothalamic CRF neurons by abdominal surgery. Brain Res 1415, 34-46.

Wang, X.F., Liu, J.J., Xia, J., Liu, J., Mirabella, V., and Pang, Z.P. (2015). Endogenous glucagon-like peptide-1 suppresses high-fat food intake by reducing synaptic drive onto mesolimbic dopamine neurons. Cell Rep 12, 726-733.

Yamada, D., Wada, E., Amano, T., Wada, K., and Sekiguchi, M. (2010). Lack of neurotensin type 1 receptor facilitates contextual fear memory depending on the memory strength. Pharmacol Biochem Behav 96, 363-369.

Yang, C.F., Chiang, M.C., Gray, D.C., Prabhakaran, M., Alvarado, M., Juntti, S.A., Unger, E.K., Wells, J.A., and Shah, N.M. (2013). Sexually dimorphic neurons in the ventromedial hypothalamus govern mating in both sexes and aggression in males. Cell 153, 896-909.

Yizhar, O., Fenno, L.E., Davidson, T.J., Mogri, M., and Deisseroth, K. (2011). Optogenetics in neural systems. Neuron 71, 9-34.

Yu, X., Ye, Z., Houston, C.M., Zecharia, A.Y., Ma, Y., Zhang, Z., Uygun, D.S., Parker, S., Vyssotski, A.L., Yustos, R., *et al*. (2015). Wakefulness is governed by GABA and histamine cotransmission. Neuron 87, 164-178.

Zahm, D.S., Jensen, S.L., Williams, E.S., and Martin, J.R., 3rd (1999). Direct comparison of projections from the central amygdaloid region and nucleus accumbens shell. Eur J Neurosci 11, 1119-1126.

Zhang, F., Gradinaru, V., Adamantidis, A.R., Durand, R., Airan, R.D., de Lecea, L., and Deisseroth, K. (2010). Optogenetic interrogation of neural circuits: technology for probing mammalian brain structures. Nat Protoc 5, 439-456.

Zhao-Shea, R., DeGroot, S.R., Liu, L., Vallaster, M., Pang, X., Su, Q., Gao, G., Rando, O.J., Martin, G.E., George, O., *et al*. (2015). Increased CRF signalling in a ventral tegmental area-interpeduncular nucleus-medial habenula circuit induces anxiety during nicotine withdrawal. Nat Commun 6, 6770.

Zorrilla, E.P., and Koob, G.F. (2004). The therapeutic potential of CRF1 antagonists for anxiety. Expert Opin Investig Drugs 13, 799-828.